Meso- and Micro-scale Modelling in China: Wind atlas analysis for 12 meteorological stations in NE China (Dongbei)

Mortensen, Niels Gylling; Yang, Z.; Hansen, Jens Carsten; Rathmann, Ole Steen; Kelly, Mark C.

Publication date:
2010

Document Version
Publisher's PDF, also known as Version of record

Meso- and Micro-scale Modelling in China: Wind atlas analysis for 12 meteorological stations in NE China (Dongbei)

Risø-I-Report

Niels G. Mortensen, Yang Zhenbin, Jens Carsten Hansen,
Ole Rathmann and Mark Kelly
Risø-I-3072(EN)
June 2010

Risø DTU
National Laboratory for Sustainable Energy

Author: Niels G. Mortensen, Yang Zhenbin, Jens Carsten Hansen, Ole Rathmann and Mark Kelly
Title: Meso- and Micro-scale Modelling in China: Wind atlas analysis for 12 meteorological stations in NE China (Dongbei)
Division: Wind Energy

Abstract (max. 2000 char.):
As part of the "Meso-Scale and Micro-Scale Modelling in China" project, also known as the CMA component of the Sino-Danish Wind Energy Development Programme (WED), microscale modelling and analyses have been carried out for 12 meteorological stations in NE China.
Wind speed and direction data from the twelve 70-m masts have been analysed using the Wind Atlas Analysis and Application Program (WAsP 10). The wind-climatological inputs are the observed wind climates derived from the WAsP Climate Analyst. Topographical inputs are elevation maps constructed from SRTM 3 data and roughness length maps constructed from Google Earth satellite imagery. The maps have been compared to Chinese topographical maps and adjusted accordingly. Summaries are given of the data measured at the 12 masts for the reference period 2009.
The main result of the microscale modelling is an observational wind atlas for NE China which can be used for verification of the mesoscale modelling. In addition, the microscale modelling itself has been verified by comparing observed and modelled vertical wind profiles at the 12 sites. WAsP generally works well in Dongbei, even in its default set-up, though forested hilly and complex sites are less well modelled. Modelling of the wind profiles can be improved by using project-specific wind atlas heights and also sometimes by changing the heat flux parameters of WAsP. The southernmost sites seem to be slightly more unstable on average than the default settings in WAsP; the northern and most elevated sites seem somewhat more stable.
The sensitivity of the WAsP modelling to 11 different input parameters has been investigated and it is found that the modelling is rather robust to changes in input data and parameters, when using the 70-m level anemometer as predictor. Site-specific air density (power curve) and calibrated anemometers are confirmed to be prerequisites for reliable predictions; project-specific wind atlas heights are highly recommended.

Risø-I-3072(EN)
June 2010

Contract no.:
n/a

Groups own reg. no.:
1170040-01

Sponsorship:
Danida

Cover:

Pages: 71
Tables: 13
References: 23
Information Service Department
Risø National Laboratory for Sustainable Energy
Technical University of Denmark
P.O. Box 49
DK-4000 Roskilde
Denmark
Telephone +45 4677 4005
bibl@risoe.dtu.dk
Fax +45 4677 4013
www.risoe.dtu.dk

Contents

Summary

As part of the “Meso-Scale and Micro-Scale Modelling in China” project, also known as the CMA component of the Sino-Danish Wind Energy Development Programme (WED), microscale modelling and analyses have been carried out for 12 meteorological stations in NE China, four in each of the three provinces of Dongbei.

Wind speed and direction data from the twelve 70-m masts have been analysed using the Wind Atlas Analysis and Application Program (WAsP 10). The wind-climatological inputs are the observed wind climates derived from the WAsP Climate Analyst. Topographical inputs are elevation maps constructed from SRTM 3 data and roughness length maps constructed from Google Earth satellite imagery. The maps have been compared to Chinese topographical maps and adjusted accordingly. Summaries are given of the data measured at the 12 masts for the reference period 2009.

The main result of the microscale modelling is an observational wind atlas for NE China which can be used for verification of the mesoscale modelling. In addition, the microscale modelling itself has been verified by comparing observed and modelled vertical wind profiles at the 12 sites. WAsP generally works well in Dongbei, even in its default set-up, though forested hilly and complex sites are less well modelled. Modelling of the wind profiles can be improved by using project-specific wind atlas heights and also sometimes by changing the heat flux parameters of WAsP. The southernmost sites seem to be slightly more unstable on average than the default settings in WAsP; the northern and most elevated sites seem somewhat more stable.

The sensitivity of the WAsP modelling to 11 different input parameters has been investigated and it is found that the modelling is rather robust to changes in input data and parameters, when using the 70-m level anemometer as predictor. Site-specific air density (power curve) and calibrated anemometers are confirmed to be prerequisites for reliable predictions; project-specific wind atlas heights are highly recommended. The heat flux parameters of WAsP can be used to tweak the modelled wind profiles, but high-quality wind profile measurements are required in order to verify this.

1 Introduction

In 1997, China Meteorological Administration (CMA) and Risø National Laboratory for Sustainable Energy at the Technical University of Denmark (Risø DTU) entered into an agreement with the overall objective of assessing the wind resources of the three provinces of Liaoning, Jilin and Heilongjiang in NE China (Dongbei), see Figure 1.

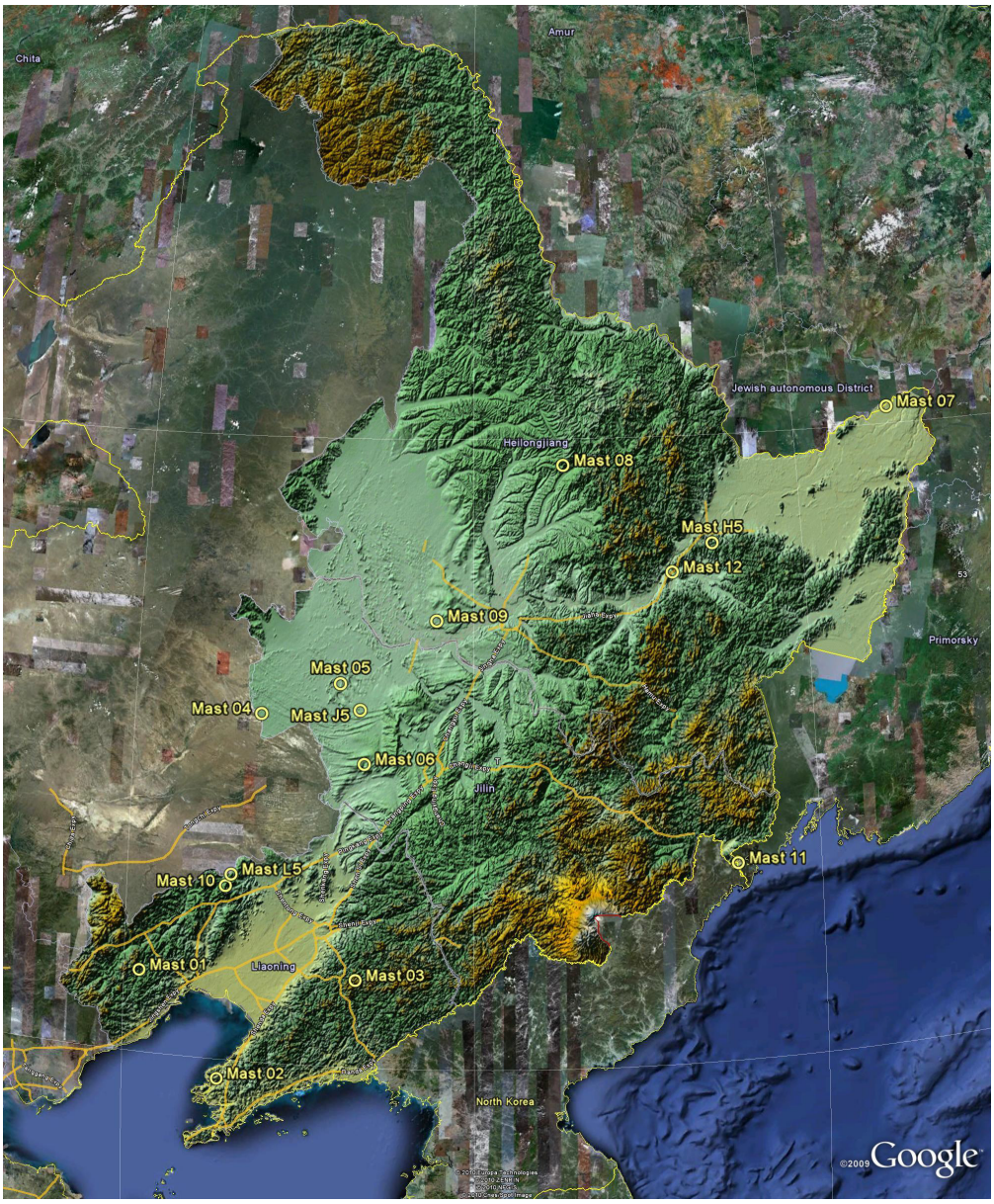

Figure 1. Overview map of Dongbei showing the location of the 15 meteorological masts referred to in the text (Image © 2010 Europa Technologies, NFGIS, ZENRIN, US Dept. of State Geographer and Google Inc.).

NE China (Dongbei) covers an area of almost 800,000 km^2 – spanning 15° of latitude and longitude – with elevations from 0 to 2744 meters above sea level. In order to assess the wind resources of such a diverse geographical region – including provision of reliable data for physical planning (national, regional or local), wind farm siting, project development, wind farm layout design and micrositing of wind turbines – the project has

adopted the framework of the wind atlas methodology developed at Risø DTU (Frank *et al.*, 2001; Badger *et al*., 2006; Hansen *et al*., 2007). Figure 2 is a schematic presentation of this framework.

Mesoscale	**Pre-processing** Wind classes Terrain elevation Terrain roughness Input specifications Model setup	**Modelling** Mesoscale model; e.g. KAMM, WRF, MC2, MM5 or similar.	**Post-processing** Predicted wind climate Regional wind climate Predicted wind resource for selected terrain site coordinates	**Numerical WA** Mesoscale maps Database of results WAsP *.LIB files Uncertainties Parameters
Measurements	**Met. stations** Siting Design Construction Installation Operation	**Wind data** Data collection Quality control Wind database Wind statistics Observed wind climate	**Verification** Meso- and microscale results vs. measured data Adjust model and model parameters to fit data Satellite imagery (offshore sites only)	**Applications** Best practices Courses and training Microscale flow model Wind farm wake model ⇒ **Wind farm AEP**
Microscale	**Pre-processing** Wind speed distributions Wind direction distribution Terrain elevation Terrain roughness Sheltering obstacles	**Modelling** Microscale model: Linearised, e.g. WAsP, MS-Micro or similar. Non-linear, e.g. CFD (Computational Fluid Dynamics).	**Post-processing** Regional wind climate Predicted wind climate Predicted wind resource for selected terrain site coordinates	**Observational WA** Microscale maps Database of results WAsP *.LIB files Uncertainties Parameters © 2006-08 Risoe DTU

Figure 2. Overview of state-of-the-art wind atlas methodologies – this graphic further describes the design and contents of the "Meso-scale and Micro-scale Modelling in China" project (reprinted from Hansen et al., 2007).

The project "Mesoscale and microscale modelling in China" – also known as Component A of the Sino-Danish Wind Energy Development Programme (WED) – has been implemented in four sub-projects: 1) mesoscale modelling, 2) measurements, 3) micro-scale modelling and 4) guidelines for application; each associated with extensive capacity building and R&D. The contents of and relations between these four different projects in Component A are shown in schematic form in Figure 2 and the methodology is described further by e.g. Hansen *et al*. (2007) and Mortensen *et al*. (2008).

The present report is thus concerned mainly with the 'green part' of Figure 2, microscale modelling, and constitutes one of the main outputs of this project. Other outputs are given in electronic form as WAsP workspace files (Mortensen *et al*., 2009). Results from the other projects are reported separately.

1.1 Microscale modelling

The overall purpose of the microscale modelling activities is three-fold, cf. Figure 2:

- Verification of the mesoscale modelling at the met. station sites
- Verification of the microscale modelling at the met. station sites
- Establishment of an observational wind atlas for Dongbei

The verification activities also include study of modelling sensitivities and uncertainties, and possible adaptations of the methodology and models to Dongbei.

The main input to the microscale modelling is long-term observed wind climates from a number of meteorological stations. In Component A, 12 dedicated meteorological masts have been erected; four 70-m masts in each of the three provinces of Dongbei, see Figure

1. In addition to the purposes mentioned above, these masts serve as reference stations for wind resource calculations at wind farm sites in the vicinity of the masts, and as test beds for comparison of wind sensors and mounting arrangements. For the latter purpose, the masts have been instrumented doubly: on one side with state-of-the-art wind sensors and hardware specified according to international standards and on the other side with standard equipment commonly used in China. This comprehensive instrumentation at four levels on each mast provides a unique data set for investigation of the uncertainties associated with wind measurements using different sensors and systems, mounting of sensors and microscale modelling of the wind profiles.

At the time of writing, more than one-years-worth of data is available from the 12 stations, nine of which have been instrumented doubly. The year 2009 has been selected as the reference one-year period for the wind atlas analyses. Table 1 provides a summary of some weather observations at the stations which are relevant for wind power.

Table 1. Summary of weather observations at the 12 meteorological stations: Data-collecting period, absolute minimum air temperature (T_{min}), absolute maximum air temperature (T_{max}), mean air temperature (T_{mean}), mean barometric pressure (B), elevation above mean sea level (z), mean air density (ρ).

Province Mast ID	**Period**	T_{min} [°C]	T_{max} [°C]	T_{mean} [°C]	B [hPa]	z [m]	ρ [kg m^{-3}]
Liaoning							
Mast 01	2009	-18.2	38.8	9.9	972.2	351	1.197
Mast 02	2009	-18.8	32.2	9.7	998.7	130	1.230
Mast 03	2009	-27.1	27.4	3.1	896.9	1030	1.131
Mast L5*	2009	-22.4	41.8	8.0	n/a	315	1.210
Jilin							
Mast 04	2009	-27.7	35.6	6.4	993.5	170	1.238
Mast 05	2009	-31.7	33.3	5.5	996.7	139	1.246
Mast 06*	2009	-33.0	35.0	5.7	n/a	187	1.237
Mast J5*	2009	-32.2	34.9	5.9	n/a	160	1.240
Heilongjiang							
Mast 07	2009	-34.8	30.6	2.0	1006.3	40	1.274
Mast 08	2009	-36.7	30.3	1.3	972.5	327	1.235
Mast 09	2009	-35.6	33.2	4.0	995.1	149	1.251
Mast H5*	2009	-25.0	34.2	3.5	n/a	312	1.229

* Temperature measured inside the CMA data logger enclosure. Air density estimated since barometric pressure is not available. H5 data are given for the one-year period 2008-11-01 to 2009-11-01.

Table 2 provides a summary of the wind observations at the stations for the 70-m level of the masts. The masts M01 to M09 feature double instrumentation of cup anemometers and wind vanes, one set of CMA instruments and one set of Risø DTU instruments. Masts L5, J5 and H5 feature CMA instrumentation only. Data from mast MH5 are given for the one-year period 2008-11-01 to 2009-11-01. Data from mast MJ5 are given for 30 metres a.g.l. since the 50- and 70-m levels are not complete for 2009. The statistics from mast M06 are based on a combination of Risø DTU and CMA measurements in order to get one full year of data.

Some statistics for all four levels of each mast are given in the Appendices.

Table 2. Summary of wind observations 70 (30) meters above ground level at the meteorological stations: Data-collecting period, data recovery rate (R), Weibull A- and k-parameters, Weibull-derived mean wind speed (U) and power density (E), and the direction (D_U) and magnitude ($|U|$) of the mean wind vector.

Province Mast ID	**Year**	***R*** [%]	***A*** [ms^{-1}]	***k***	***U*** [ms^{-1}]	***E*** [Wm^{-2}]	D_U [deg]	$\|U\|$ [ms^{-1}]
Liaoning								
Mast 01	2009	100.0	5.9	2.10	5.22	156	250	1.16
Mast 02	2009	100.0	8.8	1.96	7.78	566	002	0.34
Mast 03	2009	91.1	8.3	2.11	7.49	406	225	2.30
Mast L5*	2009	100.0	8.3	2.18	7.42	426	270	2.78
Jilin								
Mast 04	2009	100.0	8.0	2.22	7.07	376	283	2.05
Mast 05	2009	100.0	7.9	2.18	7.03	378	259	1.80
Mast 06	2009	100.0	7.5	2.17	6.69	323	241	2.35
Mast J5*	2009	100.0	(5.8)	(1.88)	(5.18)	(176)	(249)	(1.64)
Heilongjiang								
Mast 07	2009	100.0	7.5	2.30	6.66	319	247	2.07
Mast 08	2009	100.0	5.2	1.99	4.65	120	157	0.37
Mast 09	2009	100.0	7.3	2.49	6.48	268	302	1.18
Mast H5*	2009	100.0	7.7	2.23	6.81	344	204	3.21

* Masts L5, J5 and H5 feature CMA instrumentation only. H5 data are given for the one-year period 2008-11-01 to 2009-11-01. J5 data are given for 30 metres a.g.l. M06 combines Risø DTU and CMA measurements in order to get one full year of data.

After pre-processing, the wind measurements are used as input to a microscale model which is able to model the influence of the nearby terrain on the measurements. Employing detailed descriptions of terrain elevation, land-use and the occurrence of sheltering obstacles around each meteorological station, the observed wind climate is transformed into what would have been measured at the location of the station if the surroundings were completely flat and uniform with a certain roughness, and the wind measurements had been taken at certain standard heights. Through this transformation procedure, the observed wind climate is freed from the influence of local topography to become regionally representative. These generalised wind climates, as well as other results of the microscale modelling, are given in Chapter 3.

The microscale model used for the analysis is the Wind Atlas Analysis and Application Program (WAsP); a brief description of the model is given in Chapter 4. A more general introduction to the wind atlas methodology is given by Troen and Petersen (1989).

How to set up and run the WAsP model is described by Mortensen *et al*. (2009) and the current best practices for WAsP-related work is given in the Appendices.

2 Wind atlas analyses

This chapter describes the analyses carried out in the microscale modelling project.

2.1 Meteorological stations and masts

The 12 sites were selected not only to cover the three provinces of Dongbei, but also to represent different types of terrain and climatology. A main objective has been to provide reliable data for verification of the mesoscale and microscale modelling. The locations of the meteorological stations are shown in Figure 1.

The design and characteristics of the 70-m masts and Risø DTU instrumentation are described by Lindelöw-Marsden and Enevoldsen (2010). Photos taken during the site inspection trip (Mortensen *et al*., 2010) serve to verify that actual installations are done according to these master designs. The alignment of the wind direction vanes during the installation was done using a compass; the wind directions recorded in the data logger are therefore referenced to magnetic north and they have been transformed accordingly (Mortensen *et al*., 2010) as part of the present analysis.

2.2 Topographical inputs

For a general impression of the setting, the terrain surrounding each mast is shown in panoramic photographs taken during the site inspection trip (Mortensen *et al*., 2010).

2.2.1 Elevation maps

Elevation maps for each site were constructed from Shuttle Radar Topography Mission (SRTM) 3 arc-second data, using Surfer 9. The maps cover 20×20 km^2, with 20- or 10-m height contours; but are detailed with 5-m contours in an area of 2×2 km^2 close to the station. Overview maps are shown for each station in the descriptions in Chapter 3; the maps used for the flow modelling are given in the WAsP workspaces. The maps have been verified against other elevation information – especially close to the masts.

2.2.2 Land-use map

During a site inspection trip (Mortensen *et al*., 2010) the land-use around each station was compared to print-outs of Google Earth imagery and sector-wise photos were taken of characteristic land-use types. Roughness maps were constructed from this information using satellite imagery (Google Earth). These preliminary maps have been compared to Chinese topographical maps, where such maps were available.

2.3 Wind-climatological inputs

Observed wind climates, i.e. the wind rose and wind speed distribution, are constructed using the WAsP Climate Analyst, version 1.1. Figure 48 in the Appendix shows the status of the meteorological measurements conducted with Risø DTU equipment at the time of writing; Figure 49 the status of the CMA measurements. The measurements and data bases are described in detail by Lindelöw-Marsden and Enevoldsen (2010).

2.4 Other resources

In addition to the present report, the following information, data and files are available:

- Site inspection report (Mortensen *et al*., 2010)
- Photographs from the site inspection trip (Mortensen *et al*., 2010)

- WAsP-compatible elevation and roughness maps for each station
- WAsP Climate Analyst projects for each station
- WAsP workspaces for each station

Other Component A project reports provide additional information and descriptions (Badger *et al*., 2010; Lindelöw-Marsden and Enevoldsen, 2010; Hansen *et al*., 2010).

2.5 Station-specific notes

The sections below contain some site-specific information.

2.5.1 Mast 01: Chaoyang, Heiniuyingzixiang

No CMA data are available for this station, so only Risø data are used to calculate the observed wind climate (OWC). Risø boom direction is roughly perpendicular to the prevailing winds.

2.5.2 Mast 02: Wafangdian, Fuzhoucheng, Xiaopengcun

Only about 5 months of CMA data are available for 2009, so only Risø data used to calculate the OWC. This station is one of the case studies in the application report (Hansen *et al*., 2010).

2.5.3 Mast 03: Benxi, Dongyingfang, Xiaosipingcun

Data recovery rates for the Risø DTU wind sensors are low (91%, 92%, 97% and 92%), but no substitution possible because CMA equipment is not working in the same periods.

2.5.4 Mast L5: Fuxin, Pingandi

No Risø DTU data are available for this station, so only CMA data used for the OWC.

2.5.5 Mast 04: Jianshecun, Tongyu, Baicheng

Both Risø and CMA data are available for 2009. The effect of data substitution can thus be tested at this site, see section 2.7.

2.5.6 Mast 05: Chuizi, Qian'an, Songyuan

Only about 6 months of CMA data are available for 2009, so only Risø data used to calculate the OWC. This station is one of the case studies in the application report (Hansen *et al*., 2010).

2.5.7 Mast 06: Tuanshan,Bolichengzi, Gongzhuling, Siping

Only about 6 months of Risø data are available for 2009, so Risø and CMA wind measurements combined in order to get one full year of data.

2.5.8 Mast J5: Songyuan, Qlanguo, Chaganhuacun

No Risø DTU data are available for this station, so only CMA data used for the OWC. Only 10 and 30 m data are available for 2009, so the main OWC is based on 30-m data.

2.5.9 Mast 07: Tongjiang, Bachaxiang

Only about 10 months of CMA data are available for 2009, so only Risø data used to calculate the OWC

2.5.10 Mast 08: Suiling, Koumenzi

Only about 10 months of CMA data are available for 2009, so only Risø data used to calculate the OWC

2.5.11 Mast 09: Zhaozhou, Tianzhutang

Only about 7 months of CMA data are available for 2009, so only Risø data used to calculate the OWC

2.5.12 Mast H5: Jiamusi, Tuanjiexishan

No Risø DTU data are available for this station, so only CMA data used for the OWC. H5 data are available for the 1-year period from 2008-11-01 to 2009-11-01 only. This station is one of the case studies in the application report (Hansen *et al*., 2010).

2.6 Estimating site air density

An estimate of the site air density must be made at any wind turbine or wind farm site in order to calculate a realistic wind power density and annual energy production (AEP). Air density can be calculated from measurements of atmospheric pressure and ambient air temperature at the site:

$$\rho = \frac{B \times 100}{R \times (T + 273.15)} \qquad (1)$$

where ρ is air density (kg m^{-3}), B is atmospheric pressure (hPa), R is the gas constant for dry air (287.05 J kg^{-1} K^{-1}) and T is air temperature (°C).

Measurements of atmospheric pressure and air temperature have been made every 10 minutes during 2009 using the Risø DTU instrumentation at masts M01-M09, see Table 3. However, due to malfunction of the system, the series is not complete for mast M06.

Table 3. Summary for the year 2009 of air-density-related observations at the twelve meteorological stations: mean air temperature (T_{mean}), mean atmospheric pressure (B), elevation above mean sea level (z), measured mean air density (ρ_m), WAsP-derived mean air density (ρ_W), predicted mean air density (ρ_p) and final mean air density (ρ). Values in brackets are average panel temperatures minus one degree.

Province Mast ID	T_{mean} [°C]	B [hPa]	z [m]	ρ_m [kg m^{-3}]	ρ_W [kg m^{-3}]	ρ_p [kg m^{-3}]	ρ [kg m^{-3}]
Liaoning							
Mast 01	9.9	972.2	351	1.1968	1.196	1.1978	1.197
Mast 02	9.7	998.7	130	1.2302	1.229	1.2296	1.230
Mast 03	3.1	896.9	1030	1.1312	1.127	1.1313	1.131
Mast L5	(8.0)	—	315	—	1.209	1.2103	1.210
Jilin							
Mast 04	6.4	993.5	170	1.2382	1.237	1.2373	1.238
Mast 05	5.5	996.7	139	1.2460	1.245	1.2450	1.246
Mast 06	(5.7)	—	187	—	1.237	1.2373	1.237
Mast J5	(5.9)	—	160	—	1.240	1.2402	1.240
Heilongjiang							
Mast 07	2.0	1006.3	40	1.2742	1.277	1.2759	1.274
Mast 08	1.3	972.5	327	1.2345	1.235	1.2354	1.235
Mast 09	4.0	995.1	149	1.2509	1.250	1.2498	1.251
Mast H5*	(3.5)	—	312	—	1.228	1.2286	1.229

* H5 data are given for the one-year period 2008-11-01 to 2009-11-01.

Measurements of air temperature have not been made at masts ML5, MJ5 and MH5. However, the CMA system measures a 'panel temperature' inside the CMA data logger enclosure. This panel temperature follows the ambient air temperature closely, but is offset because of the lack of ventilation. At mast M04, where one year of concurrent measurements from the two systems are available, the mean panel temperature is about 1 degree higher than the mean air temperature when averaged over the year. We therefore estimate the annual average air temperature at masts M06, ML5, MJ5 and MH5 from the average panel temperature by subtracting 1 degree from this value.

Measurements of atmospheric pressure are not carried out at masts ML5, MJ5 and MH5. At these sites, we use the Air Density Calculator of WAsP to estimate the air density from the site elevation and annual average air temperature at the site. This estimate is given in the ρ_W-column in Table 3.

A comparison of measured and WAsP-derived mean air densities is shown in Figure 3.

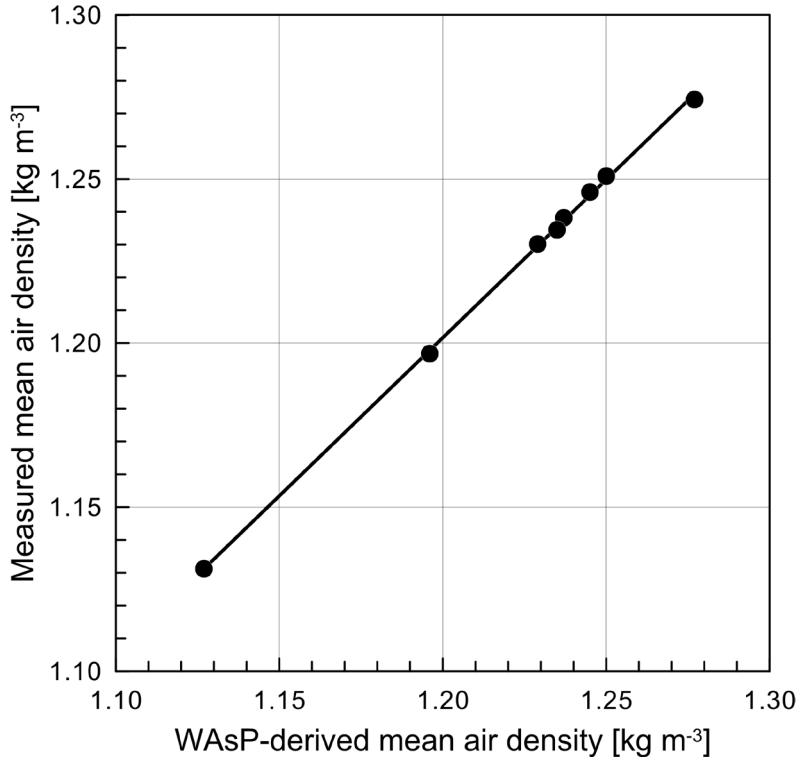

Figure 3. Measured and WAsP-derived mean air densities for eight stations in Dongbei.

Finally, we use the regression line in Figure 3 to calculate the air density at masts M06, ML5, MJ5 and MH5; this estimate is given in the ρ_p-column in Table 3. The air density used as basis for the WAsP calculations is given the right-most column of Table 3.

2.7 Sensitivity analysis and uncertainties

Sensitivity analysis (SA) is the study of how the variation (uncertainty) in the output of a mathematical model can be apportioned, qualitatively or quantitatively, to different sources of variation in the input of the model (Wikipedia, 2010). In other words, it is the process of systematically changing the input data and parameters in the WAsP modelling in order to determine the effects of such changes on the output, which in this case the estimated annual energy production (AEP) of a wind turbine or a wind farm. Sensitivity analysis thus investigates the robustness and uncertainty of the microscale modelling.

The factors investigated and the questions asked in the present analysis are:

1. **Cup anemometer calibration**. What is the consequence for the AEP prediction of a 1% error in the cup anemometer calibration?
2. **Cup anemometer height**. What is the consequence for the AEP prediction of a 1% error in the cup anemometer height above ground level?
3. **Wind atlas heights**. What is the consequence for the AEP prediction of using the standard heights in the WAsP generalised wind climate rather than project-adapted heights?
4. **Wind direction offset**. What is the consequence for the AEP prediction of a 10 degree offset error in the wind direction? This corresponds to e.g. not taking the magnetic declination in Dongbei into account.
5. **Air density**. What is the consequence for the AEP prediction of a 2.5% error in the air density? This corresponds to choosing the wrong performance table in the WAsP wind turbine generator.
6. **Neutral stability**. What is the consequence for the AEP prediction of assuming neutral atmospheric stability conditions rather than WAsP default settings?
7. **Heat flux offset value**. What is the consequence for the AEP prediction of a change of 10 Wm^{-2} in the offset heat flux value?
8. **Background roughness length z_0**. What is the consequence for the AEP prediction of making the background roughness length smaller by a factor of two?
9. **Background roughness length z_0**. What is the consequence for the AEP prediction of making the background roughness length larger by a factor of two?
10. **Position of mast**. What is the consequence for the AEP prediction of a 10 metre error in the horizontal position of the meteorological mast? This corresponds to the typical uncertainty of a handheld GPS system.
11. **Elevation map source and detail**. What is the consequence for the AEP prediction of using a map derived from SRTM 3 data only?

The reference case, to which we compare, is a WAsP modelling setup with default parameters – except for the wind atlas heights which have been adapted to the design of the measurement masts. The wind atlas heights are thus 10, 30, 50, 70 and 100 m above ground level in this baseline scenario. The predictor OWC on the mast is the 70-m level.

Sensitivity analyses have been performed for the three stations which are used for the case studies in the application report: M02, M05 and MH5 (Hansen *et al.*, 2010). These three stations represent very different climatological, topographical and geographical conditions:

- M02: Hilly coastal site in Liaoning
- M05: Flat inland site in Jilin
- MH5: Complex (steep slopes) inland site in Heilongjiang

The sensitivity analysis is carried out by changing the inputs in turn, redo the calculation, and record the change in the calculation of the power production (AEP) from a wind turbine located at the site of the meteorological mast.

2.7.1 Sensitivity analysis for M02, Wafangdian

Table 4 lists the results of a sensitivity analysis for mast M02, Wafangdian.

Table 4. Sensitivity analysis for mast M02, Wafangdian. The AEP prediction is made for a single wind turbine and for three different tower heights: 75, 100 and 125 m.

Parameter	Input change	Output change (AEP)		
		75 m	100 m	125 m
U calibration (1%)	0.01	1.8%	1.7%	1.5%
Anemometer height (1%)	-0.01	0.4%	0.4%	0.4%
Adapted atlas heights	standard	1.4%	0.0%	2.5%
Direction offset (10°)	10	1.7%	1.2%	0.9%
Air density (2.5%)	-0.024	-1.9%	-1.8%	-1.7%
Neutral stability	neutral	-1.6%	-7.1%	-10.5%
Heat flux (10 Wm^{-2})	10 Wm^{-2}	0.2%	1.1%	1.7%
BG roughness (half)	half of 5 cm	0.4%	0.7%	0.6%
BG roughness (double)	double of 5 cm	0.0%	-0.7%	-1.0%
Position of mast (10 m)	±10 m	0.1%	0.1%	0.1%
Elevation detail (SRTM)	SRTM 3	-0.2%	-0.7%	-1.0%

The same results are shown graphically in Figure 4.

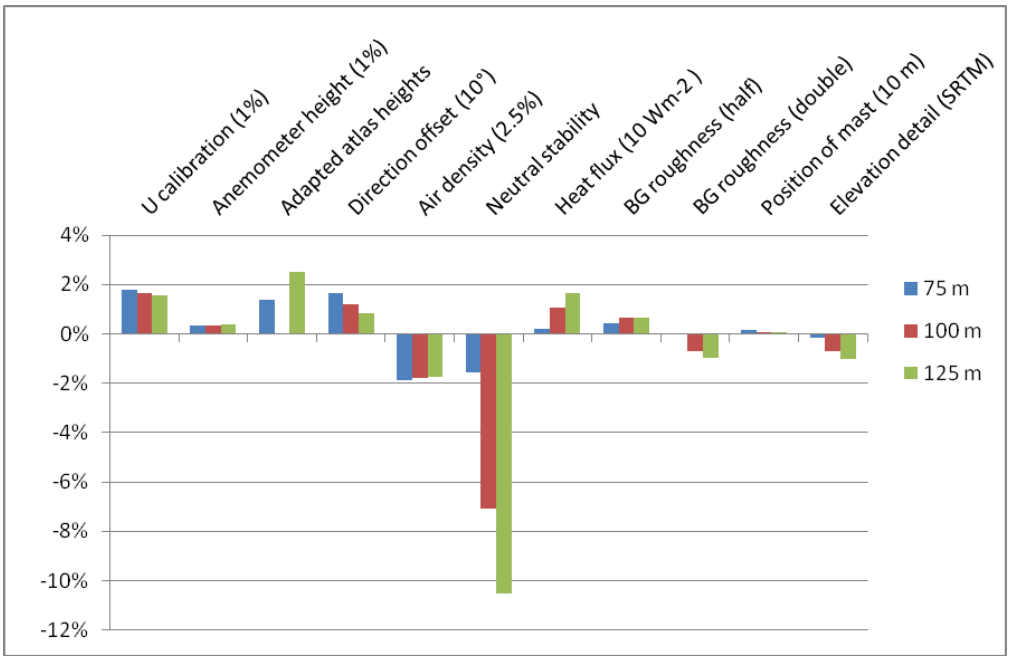

Figure 4. Sensitivity analysis for mast M02, Wafangdian. The AEP prediction is made for a single wind turbine and for three different tower heights: 75, 100 and 125 m.

2.7.2 Sensitivity analysis for M05, Chuizi

Table 5 lists the results of a sensitivity analysis for mast M05, Chuizi.

Table 5. Sensitivity analysis for mast M05, Chuizi. The AEP prediction is made for a single wind turbine and for three different tower heights: 75, 100 and 125 m.

Parameter	Input change	Output change (AEP)		
		75 m	100 m	125 m
U calibration (1%)	0.01	2.1%	1.9%	1.7%
Anemometer height (1%)	-0.01	0.5%	0.4%	0.4%
Adapted atlas heights	standard	1.7%	0.0%	3.3%
Direction offset (10°)	10	0.4%	0.4%	0.4%
Air density (2.5%)	-0.024	-2.1%	-1.9%	-1.8%
Neutral stability	neutral	-1.8%	-7.9%	-11.5%
Heat flux (10 Wm^{-2})	10 Wm^{-2}	0.3%	1.2%	1.8%
BG roughness (half)	half of 5 cm	-0.1%	0.0%	0.1%
BG roughness (double)	double of 5 cm	0.1%	-0.3%	-0.2%
Position of mast (10 m)	±10 m	0.1%	0.0%	0.0%
Elevation detail (SRTM)	SRTM 3	0.1%	0.2%	0.3%

The same results are shown graphically in Figure 5.

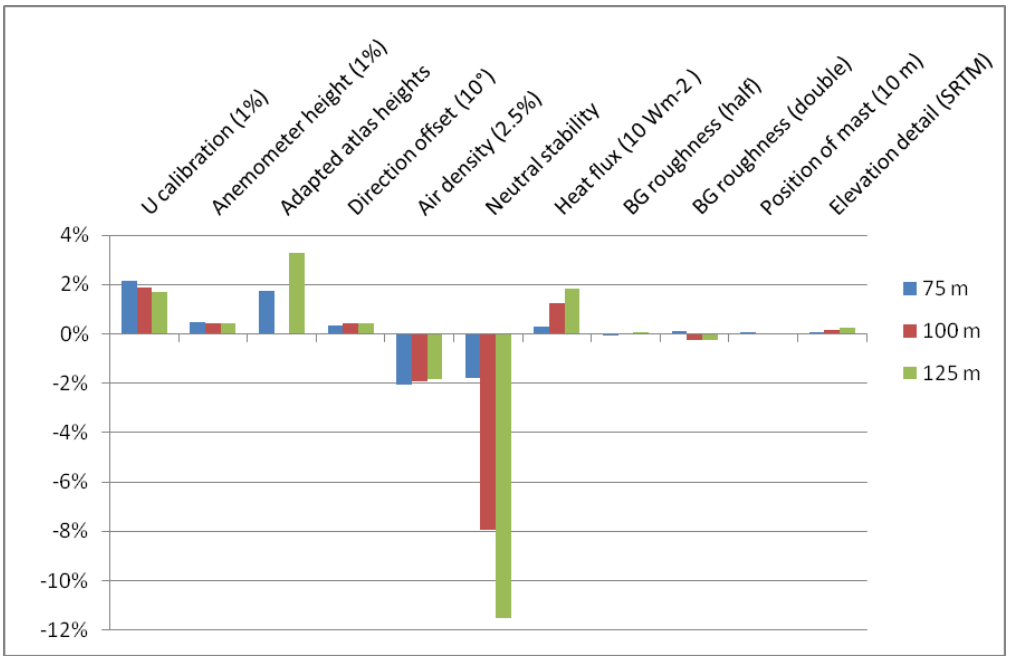

Figure 5. Sensitivity analysis for mast M05, Chuizi. The AEP prediction is made for a single wind turbine and for three different tower heights: 75, 100 and 125 m.

2.7.3 Sensitivity analysis for MH5, Jiamusi

Table 6 lists the results of a sensitivity analysis for mast MH5, Jiamusi.

Table 6. Sensitivity analysis for mast MH5, Jiamusi. The AEP prediction is made for a single wind turbine and for three different tower heights: 75, 100 and 125 m.

Parameter	Input change	Output change (AEP)		
		75 m	100 m	125 m
U calibration (1%)	0.01	2.2%	2.1%	2.0%
Anemometer height (1%)	-0.01	0.3%	0.3%	0.3%
Adapted atlas heights	standard	1.1%	0.0%	4.1%
Direction offset (10°)	10	0.2%	0.2%	0.2%
Air density (2.5%)	-0.024	-2.1%	-2.1%	-2.1%
Neutral stability	neutral	-1.3%	-6.2%	-9.4%
Heat flux (10 Wm^{-2})	10 Wm^{-2}	0.3%	1.2%	1.8%
BG roughness (half)	half of 20 cm	0.4%	0.6%	-0.1%
BG roughness (double)	double 20 cm	-0.7%	-1.5%	-1.7%
Position of mast (10 m)	±10 m	0.4%	0.2%	0.1%
Elevation detail (SRTM)	SRTM 3	0.0%	0.0%	0.0%

The same results are shown graphically in Figure 6.

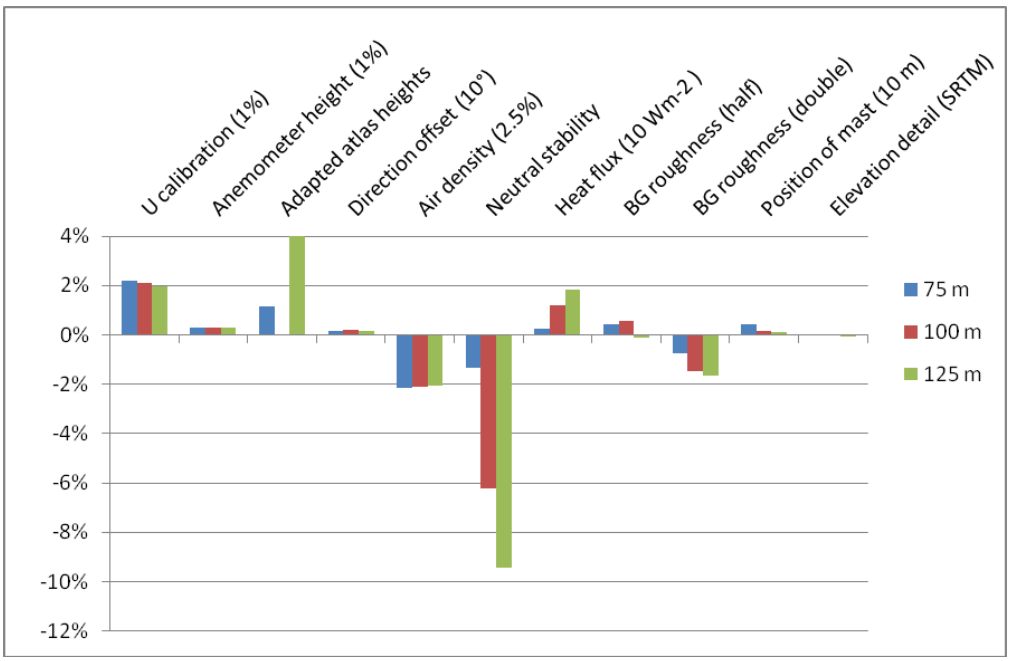

Figure 6. Sensitivity analysis for mast MH5, Jiamusi. The AEP prediction is made for a single wind turbine and for three different tower heights: 75, 100 and 125 m.

Assuming neutral stability conditions at these three masts would lead to the largest changes in the predicted AEP; however, this case is shown for reference and comparison purposes only and does not influence the WAsP modelling directly. Changing the offset heat flux value over land by 10 Wm^{-2} also changes the predictions significantly; this parameter is thus a way of tweaking the wind profile to better match the measured mean wind speeds.

Not surprisingly, changes in the cup anemometer calibration and air density setting have direct and significant impacts on the AEP predictions. Less obvious, the predictions may also be quite sensitive to adaptation of the wind atlas standard heights to the project (anemometer and/or wind turbine heights) and in some cases to an offset of 10 degrees in the wind directions.

The remaining parameter and data changes have less than 1% impact on the predictions for any of the prediction heights in this particular case. Nevertheless, the numbers show the importance of providing accurate input parameters for the flow modelling.

2.7.4 Uncertainty estimates

It is common practice to apply the equation for an independent stochastic process to combine the uncertainties from 1…*n* sources:

$$\left(\frac{\Delta P}{P}\right)^2_{\text{total}} = \left(\frac{\Delta P}{P}\right)^2_1 + \left(\frac{\Delta P}{P}\right)^2_2 + \ldots + \left(\frac{\Delta P}{P}\right)^2_n \qquad (2)$$

Assuming that the distribution of AEP estimates is Gaussian it is further possible to get the exceedance statistics. If we apply this approach (2) to the sensitivity analyses given above, and assume that the input changes are representative of typical uncertainties, we can calculate the overall or combined uncertainty of the AEP predictions, see Table 7.

Table 7. Uncertainty estimates for three stations and three wind turbine tower heights.

Province	**Mast**	**75 m**	**100 m**	**125 m**
		[%]	[%]	[%]
Liaoning	Mast 02	3.0	2.8	3.9
Jilin	Mast 05	3.0	2.5	4.3
Heilongjiang	Mast H5	2.9	3.1	5.3

Here, we have of course only considered some of the important factors in the uncertainty assessment regarding *measurements* (cup anemometer calibration, anemometer height above ground level, direction offset and air density calculation) and *WAsP modelling* (wind atlas heights, heat flux, background roughness length, position of mast and elevation detail).

Equally important factors in an AEP calculation for a wind farm could be the *long-term wind climate* (e.g. MCP techniques), *microscale modelling* (horizontal extrapolation from met. mast to wind turbine sites), *wind turbine characteristics* (power and thrust curves), *wind farm characteristics* (turbine positions, wake modelling, large-scale effects), *availability issues* (electrical losses etc.) and the *human factor*.

2.7.5 Measurement biases

In addition to the uncertainties described above, some measurement conditions also give rise to biases in the predictions (Lindelöw-Marsden and Enevoldsen, 2010). One such issue is the shadowing effect of the lattice mast on the cup anemometer. This effect is investigated on mast M04 where data from both Risø DTU and CMA cup anemometers are available for the entire year of 2009.

The observed wind climate at mast M04 is shown in Figure 20; the directions of the Risø and CMA cup anemometer booms are 163° and 223°, respectively. Using only the Risø cup data to calculate the mean wind climate and AEP for 2009 leads to the 'Risø' values in Table 8; substituting CMA cup data for the Risø cup data in the sector 323°-003° (343°±20°) leads to the 'Risø + CMA' values below.

Table 8. Measurement and prediction bias caused by tower shadow effects at mast M04.

Mast M04	***h***	***A***	***k***	***U***	***E***	***AEP***
Data set	[m]	[ms^{-1}]		[ms^{-1}]	[Wm^{-2}]	[$GWhy^{-1}$]
Risø cup only	70	8.0	2.24	7.07	376	7.594
Risø + CMA	70	8.1	2.28	7.20	391	7.881
Ratio	—	—	—	0.982	0.962	0.964

The effect of the tower shadow for the 70-m level at mast M04 on the annual mean wind speed, power density and AEP are decreases of 1.8%, 3.8% and 3.6%, respectively. Similar biases are likely to occur at the other masts, but the data recovery rates do not allow for proper data substitution.

3 Observed and Regional Wind Climates

In this chapter, the topographical and climatological data for the meteorological stations used in the study are presented in tables and graphs. For each station, the tables give the calculated regionally representative wind climatology – the generalised wind climate – obtained from the station data by applying the Wind Atlas analysis, together with a summary of the raw data – the observed wind climate – and the measuring conditions. Each station summary is printed on a pair of facing pages containing

- station description and elevation map
- observed wind climate at 70 metres above ground level
- observed and modelled wind speed profiles
- calculated regionally representative Weibull parameters
- calculated regional mean wind speeds and power densities

The presentation of the data is explained in more detail in the following sections.

3.1 The station description

The station description comprises the geographical location and a station elevation map. The ruggedness index (RIX) is given for the met. station site in the map caption.

3.1.1 Geographical coordinates

The longitude and latitude of each station are given in decimal degrees referred to the horizontal datum World Geodetic System 1984 (WGS84). The position has been determined using a Garmin eTrex GPS (Global Positioning System) receiver. Three readings were taken (corresponding approximately to the three legs of the mast) and subsequently averaged to find the position of the mast, see Table 9. The position has been verified by plotting the position on a topographical map or satellite image.

3.1.2 Elevation

The elevation of the station is given in metres above mean sea level (m a.s.l.) referred to the vertical datum WGS84 Earth Gravitational Model (EGM96). In practice, the elevations of the mast positions were determined by the WAsP flow model (Mortensen *et al*., 2009) from 5-m height contour elevation maps derived from Shuttle Radar Topography Mission (SRTM) 3 arc-second data. The elevation has been verified by comparing to ordinary Chinese topographical maps.

3.1.3 Grid coordinates

The Cartesian grid coordinates consist of the Universal Transverse Mercator (UTM) Easting (E) and Northing (N) in full metres. The number of the UTM zone (Z), to which these coordinates refer, is also given. The horizontal datum is the World Geodetic System 1984 (WGS84).

3.1.4 Station topographical map

The topographical map shows the terrain elevations in a 20×20-km^2 area around the station – with the station approximately in the middle of the map. The height contour interval is 10 or 20 metres. The contour lines used in the orographic flow model may be

much more detailed (1-, 2- or 5-m contours close to the station). Some areas of different roughness length may be indicated as well, in particular land, sea and lake areas.

The elevation information was obtained from version 2.1 (the 'finished' version) of the Shuttle Radar Topography Mission (SRTM) data set. Additional information was obtained from printed Chinese topographical maps. Information on land use and thereby roughness length of the terrain surface was obtained from satellite imagery (e.g. Google Earth), topographical maps and from field visits to the sites.

3.2 Observed wind climate

The observed wind climate comprises the distributions of the wind measurements at 70 m a.g.l. in the form of a wind rose and a histogram. The observed and modelled mean wind profiles at the station are also shown. The data period reported is the year 2009.

3.2.1 Wind rose and histogram

The wind rose shows the distribution of wind directions in the processed time-series. Wind direction is divided in twelve 30°-sectors; the angular axis is given in degrees from 0° to 360° clockwise, the units on the radius axis is per cent.

The histogram shows the total distribution of observed wind speeds (bar graph) in the processed time-series. A Weibull distribution function has been fitted to the data and is shown with a grey dashed line. Also shown (with a blue dashed line) is the emergent distribution, i.e. the distribution that emerges by adding together the sector-wise Weibull distributions. The units on the x-axis is [ms^{-1}], on the y-axis [% per ms^{-1}].

3.2.2 Wind speed profiles

This graph shows the measured and Weibull-derived mean wind speeds at 10, 30, 50 and 70 metres above ground level (a.g.l.); these values are shown using black and blue dots, respectively. WAsP-modelled wind profiles are shown with full lines, using the 70-m level as the predictor OWC. The modelled wind profile using default parameter values is shown in blue and a neutral profile is shown in green for reference. At some sites, an adapted wind profile is shown in red, the adaptation value(s) are given in the caption.

The adaption consists of changing the mean heat flux value over land in the WAsP project configuration. The main purpose of this has been to illustrate this option and to minimise the difference between measured and modelled wind profiles. The adapted heat flux value may not be entirely realistic and the shape of the modelled wind profiles may also be changed by changing the roughness length of the terrain surface. The roughness maps and heat flux values proposed here may therefore change in future analyses.

3.3 Generalised wind climate

The Wind Atlas table give the estimated (calculated) omni-directional Weibull *A*- and *k*-parameters, the mean wind speed and the mean wind power density for each of 5 heights and 5 roughness length classes. Wind speed and power density were calculated using the Weibull parameters of the Wind Atlas tables. The Weibull *A*-parameters and the mean wind speeds are given in [ms^{-1}]; the mean power density in [Wm^{-2}].

Note that the five roughness classes correspond to uniform surfaces with a roughness length of 0 (0.0002) m, 0.03 m, 0.10 m, 0.40 m and 1.50 m, respectively. Compared to the European Wind Atlas (Troen and Petersen, 1989), an extra class with z_0 = 1.50 m is used here, because of the occurrence of forests at some of the sites.

3.4 Station statistics and climatologies

The station statistics and climatologies given below were compiled and modelled in 2010 – using data collected from the one-year period January to December 2009. The wind atlas data were calculated using the available information at the time of writing and the results may change in subsequent analyses and editions. The 12 stations included in the report are listed in Table 9 below and their locations are shown on the sketch map in Chapter 1. This map further shows the elevations of Dongbei, derived from the Shuttle Radar Topography Mission data set SRTM30, which contains spot heights of node points in grids with 30 arc-second resolutions (926 metres or less). More summaries of the wind measurements are given in the Appendix.

Table 9. Mast coordinates and elevations. The datum used is WGS 84; elevations are determined by the WAsP flow model from SRTM3 maps with 5-m height contours.

Province	**Longitude**	**Latitude**	**Elevation**	**Easting**	**Northing**	**UTM**
Mast ID	[°E]	[°N]	[m a.s.l.]	[m]	[m]	zone
Liaoning						
01	120.27608	41.10905	342	271280	4554439	51
02	121.65722	39.73201	134	384932	4398875	51
03	123.99825	41.16924	1017	583740	4558025	51
L5	121.83645	42.46533	315	404342	4702100	51
Jilin						
04	122.27773	44.52714	168	442608	4930678	51
05	123.65746	44.94102	136	551871	4976609	51
06	124.10508	43.94166	185	588686	4865987	51
J5	124.01715	44.61596	155	580701	4940793	51
Heilongjiang						
07	133.87547	48.21450	40	416464	5340753	53
08	127.64503	47.66755	327	398278	5280240	52
09	125.34413	45.74241	147	215611	5071930	52
H5*	130.33285	46.64002	312	602009	5166025	52

* The position of Mast H5 has not been independently verified and is therefore considered preliminary.

The elevations of the mast positions were determined by the WAsP flow model (Mortensen *et al.*, 2009) from 5-m height contour elevation maps derived from Shuttle Radar Topography Mission (SRTM) 3 arc-second data.

3.5 Chaoyang, Heiniuyingzixiang (M01)

M01	120.27608°E	41.10905°N	342 m	E 271280 m	N 4554439 m	UTM 51

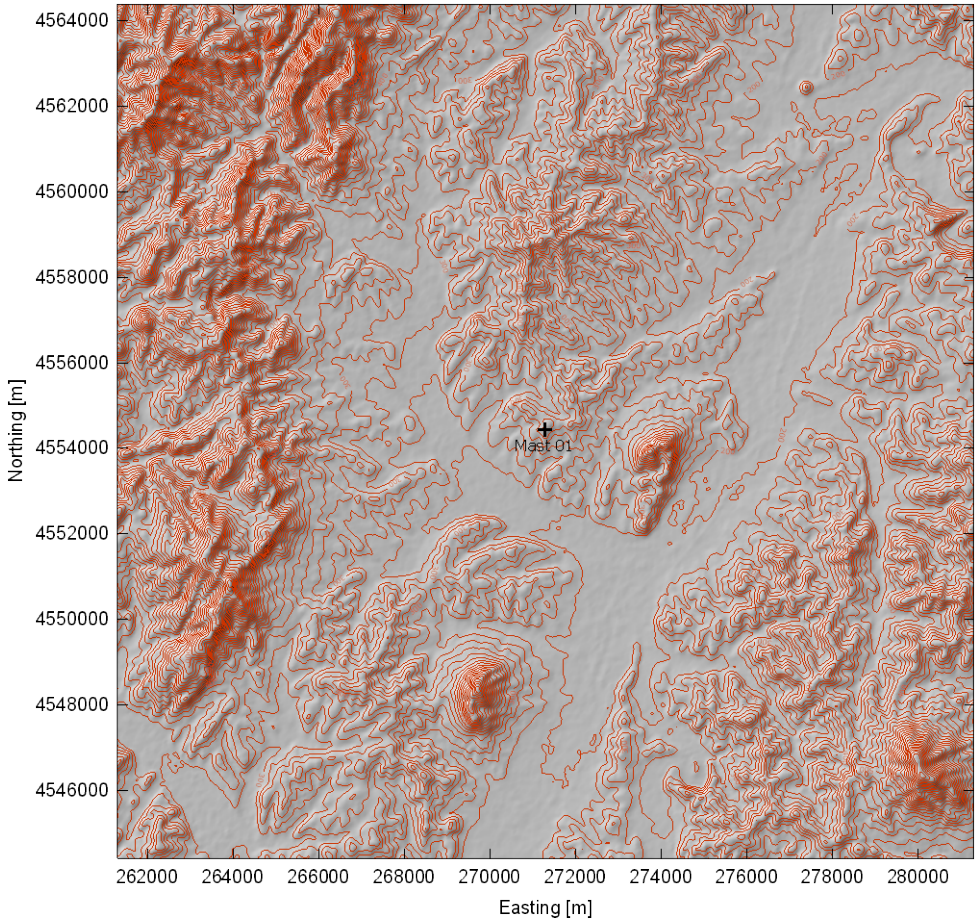

Figure 7. Elevation map from SRTM3 data, covering 20×20 km^2, with 20-m contours. The ruggedness index for the site is 0%.

3.5.1 Observed wind climate

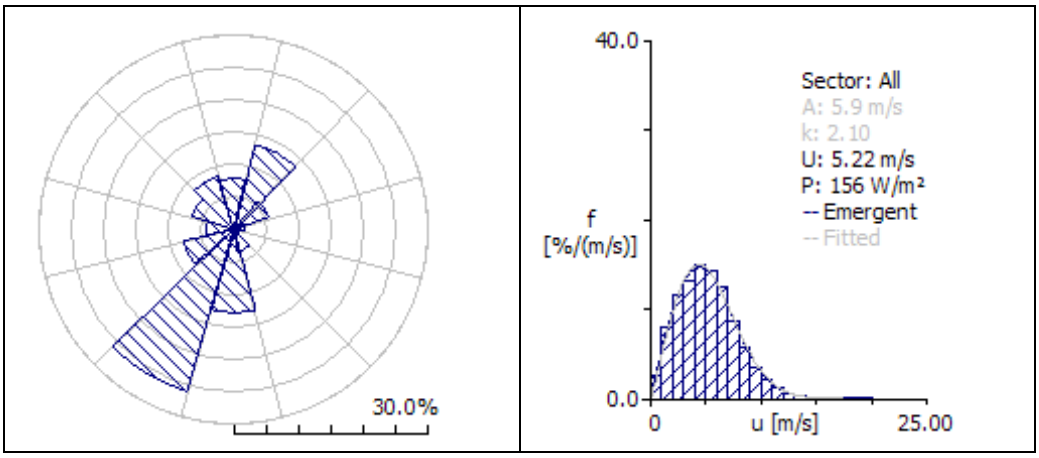

Figure 8. Wind rose and total wind speed distribution for Chaoyang at 70 m a.g.l. The number of observations is 52560 and the recovery rate for 2009 is 100%.

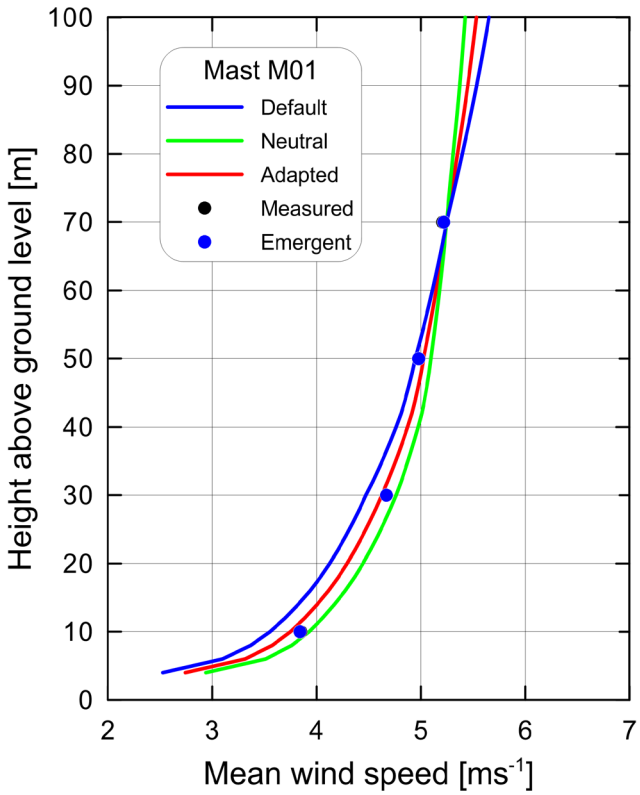

Figure 9. Measured and WAsP-modelled wind profiles for Chaoyang. The adapted wind profile corresponds to a mean heat flux over land of -10 Wm^{-2} (default -40 Wm^{-2}).

3.5.2 Generalised wind climate

Height	Parameter	0.00 m	0.03 m	0.10 m	0.40 m	1.50 m
10.0 m	Weibull A [m/s]	5.4	3.8	3.3	2.6	1.7
	Weibull k	1.90	1.63	1.63	1.63	1.61
	Mean speed [m/s]	4.82	3.39	2.96	2.33	1.55
	Power density [W/m²]	133	56	37	18	5
30.0 m	Weibull A [m/s]	6.0	4.7	4.3	3.6	2.8
	Weibull k	1.95	1.79	1.78	1.75	1.71
	Mean speed [m/s]	5.30	4.21	3.81	3.23	2.52
	Power density [W/m²]	172	95	71	44	22
50.0 m	Weibull A [m/s]	6.2	5.3	4.8	4.2	3.4
	Weibull k	1.95	1.95	1.92	1.87	1.81
	Mean speed [m/s]	5.51	4.70	4.29	3.71	3.02
	Power density [W/m²]	194	120	93	62	35
70.0 m	Weibull A [m/s]	6.4	5.7	5.3	4.6	3.8
	Weibull k	1.90	2.10	2.06	1.99	1.91
	Mean speed [m/s]	5.65	5.08	4.66	4.08	3.38
	Power density [W/m²]	214	141	111	77	46
100.0 m	Weibull A [m/s]	6.5	6.3	5.8	5.1	4.3
	Weibull k	1.83	2.07	2.08	2.09	2.05
	Mean speed [m/s]	5.80	5.58	5.13	4.51	3.80
	Power density [W/m²]	241	189	146	99	61

Non-default parameters values: Air density [kg/m^3]: 1.18 (default is 1.225) Standard height #2 [m]: 30.00 (default is 25.00) Standard height #4 [m]: 70.00 (default is 100.00) Standard height #5 [m]: 100.00 (default is 200.00).

3.6 Wafangdian, Fuzhoucheng, Xiaopengcun (M02)

M02	121.65722°E	39.73201°N	134 m	E 384932 m	N 4398875 m	UTM 51

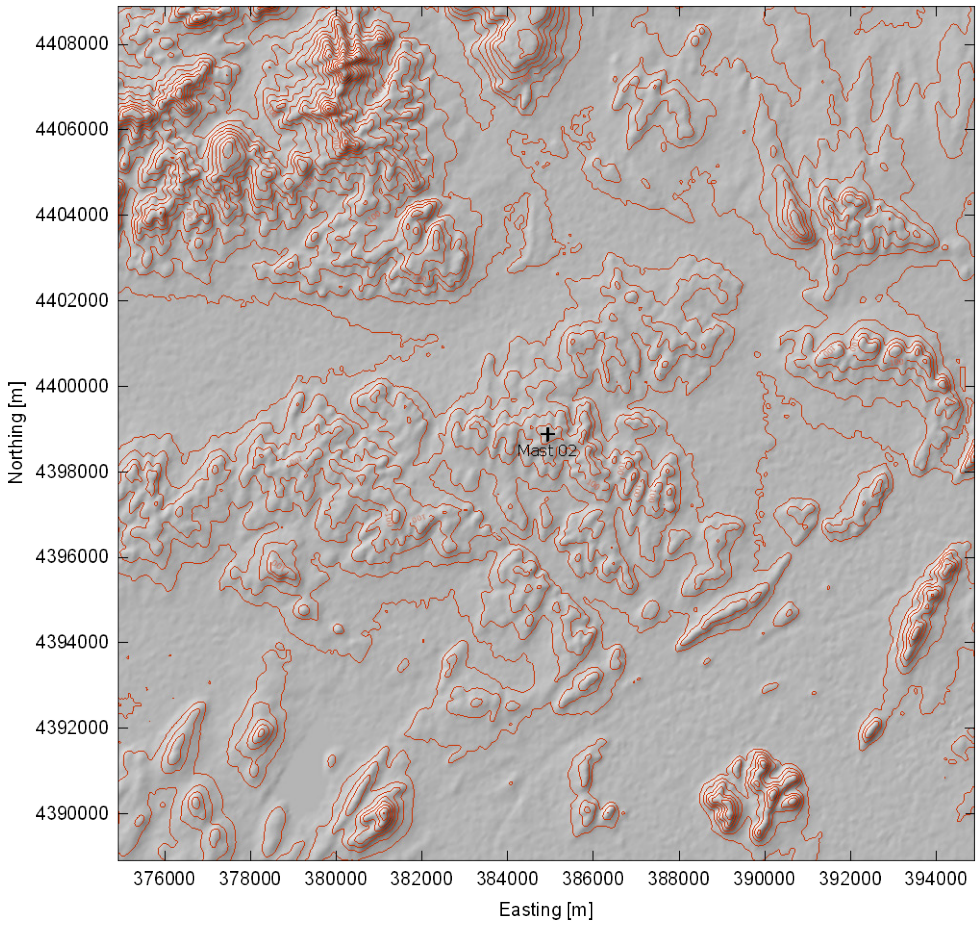

Figure 10. Elevation map from SRTM3 data, covering 20×20 km^2, with 20-m contours. The ruggedness index for the site is 1.5%.

3.6.1 Observed wind climate

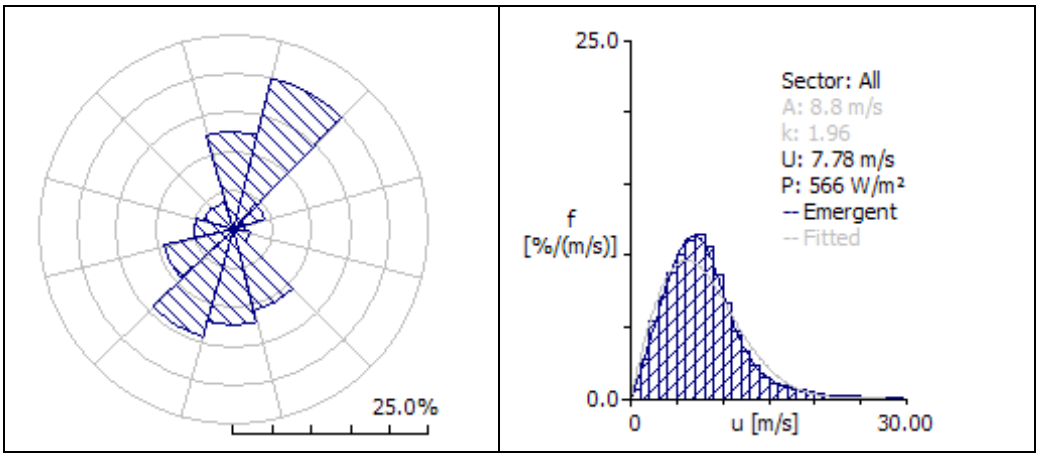

Figure 11. Wind rose and wind speed distribution for Wafangdian at 70 m a.g.l. The number of observations is 52557 and the recovery rate for 2009 is 100%.

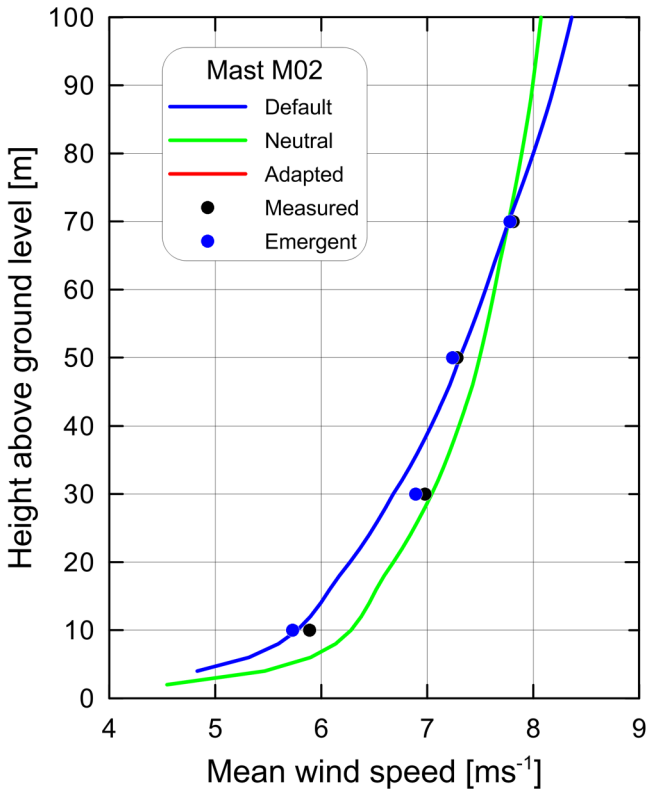

Figure 12. Measured and WAsP-modelled wind profiles for Wafangdian. No adapted wind profile is shown for this station.

3.6.2 Generalised wind climate

Height	Parameter	0.00 m	0.03 m	0.10 m	0.40 m	1.50 m
10.0 m	Weibull A [m/s]	8.0	5.6	4.9	3.8	2.6
	Weibull k	1.86	1.65	1.65	1.66	1.67
	Mean speed [m/s]	7.09	5.00	4.36	3.43	2.29
	Power density [W/m²]	456	186	122	59	17
30.0 m	Weibull A [m/s]	8.8	6.9	6.2	5.3	4.1
	Weibull k	1.88	1.76	1.76	1.76	1.76
	Mean speed [m/s]	7.80	6.15	5.56	4.72	3.69
	Power density [W/m²]	597	316	234	143	69
50.0 m	Weibull A [m/s]	9.1	7.7	7.0	6.1	4.9
	Weibull k	1.90	1.88	1.86	1.84	1.83
	Mean speed [m/s]	8.12	6.81	6.22	5.39	4.40
	Power density [W/m²]	669	398	307	202	111
70.0 m	Weibull A [m/s]	9.4	8.2	7.6	6.6	5.5
	Weibull k	1.87	2.00	1.96	1.93	1.90
	Mean speed [m/s]	8.32	7.31	6.71	5.88	4.90
	Power density [W/m²]	732	463	365	250	147
100.0 m	Weibull A [m/s]	9.6	9.0	8.3	7.3	6.2
	Weibull k	1.83	2.06	2.05	2.03	2.00
	Mean speed [m/s]	8.53	7.94	7.32	6.46	5.48
	Power density [W/m²]	807	577	453	314	194

Non-default parameters values: Air density [kg/m^3]: 1.24 (default is 1.225) Standard height #2 [m]: 30.00 (default is 25.00) Standard height #4 [m]: 70.00 (default is 100.00) Standard height #5 [m]: 100.00 (default is 200.00).

3.7 Benxi, Dongyingfang, Xiaosipingcun (M03)

M03	123.99825°E	41.16924°N	1017 m	E 583740 m	N 4558025 m	UTM 51

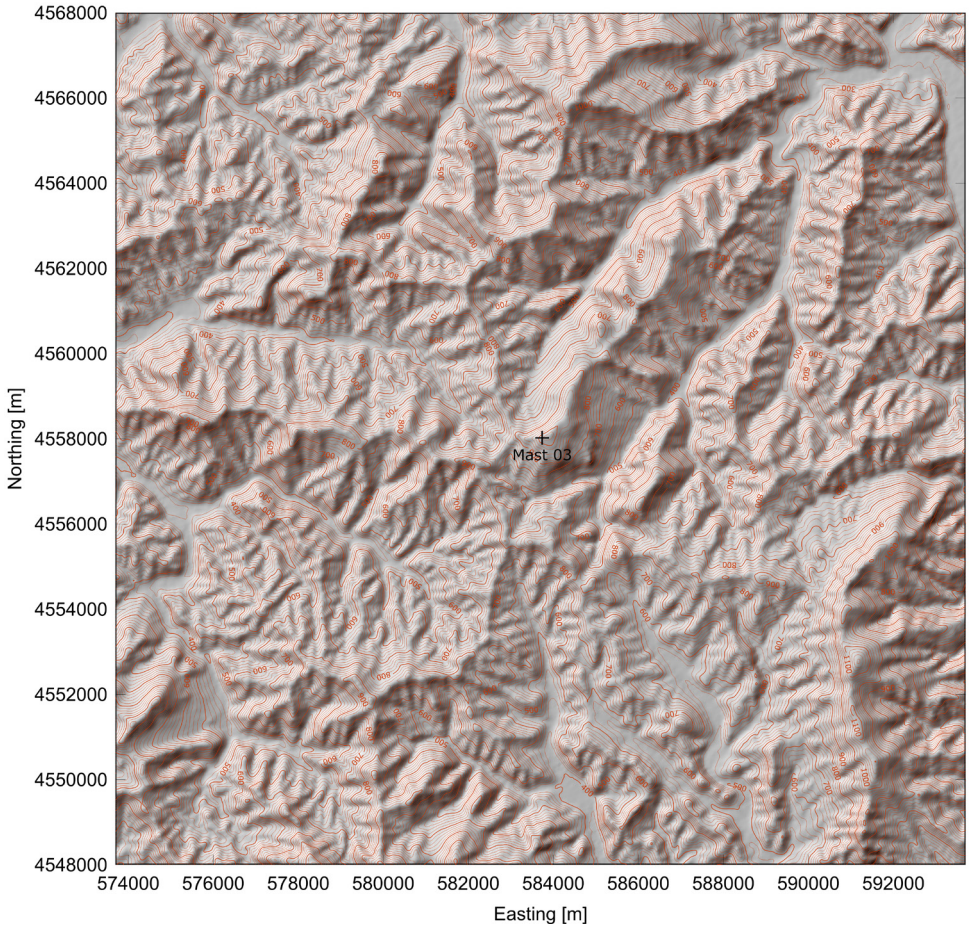

Figure 13. Elevation map from SRTM3 data, covering 20×20 km^2, with 20-m contours. The ruggedness index for the site is 31.3%.

3.7.1 Observed wind climate

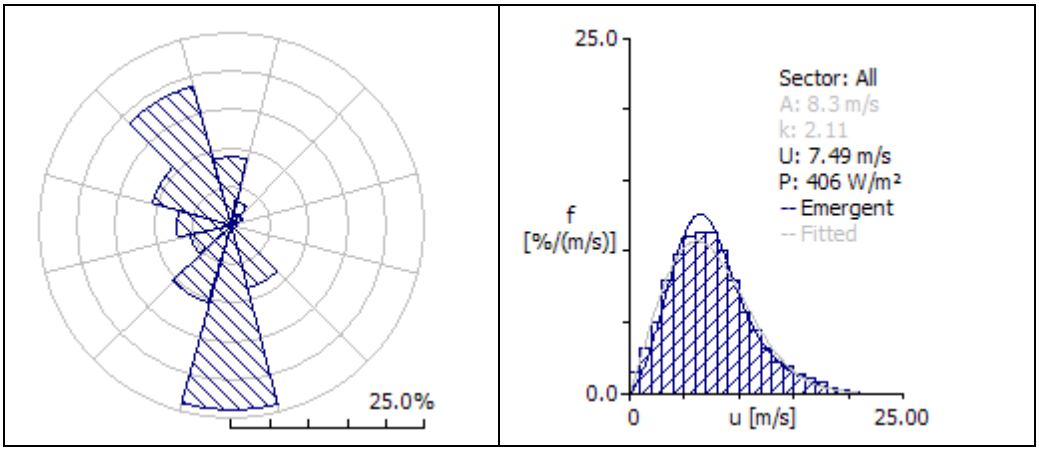

Figure 14. Wind rose and wind speed distribution for Benxi at 70 m a.g.l. The number of observations is 47894 and the recovery rate for 2009 is 91%.

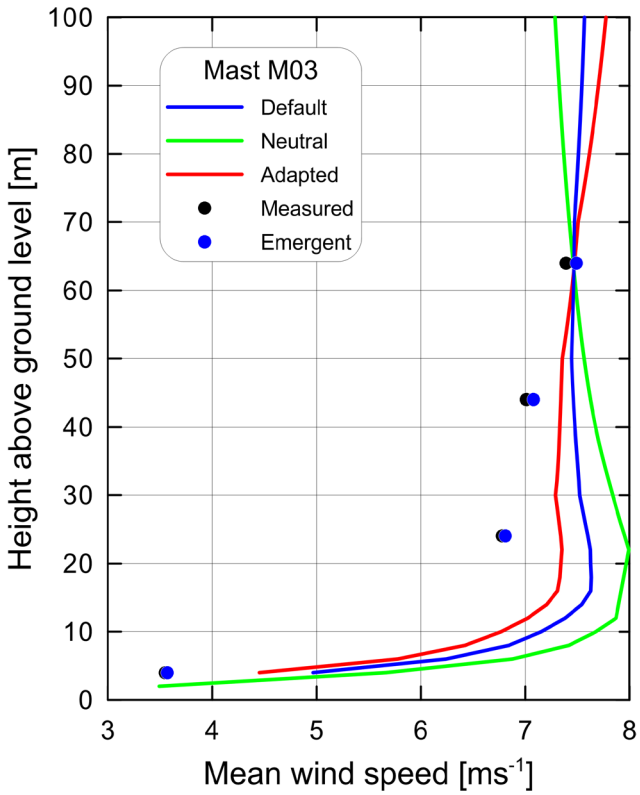

Figure 15. Measured and WAsP-modelled wind profiles for Benxi. The adapted wind profile corresponds to a mean heat flux over land of -80 Wm^{-2} (default -40 Wm^{-2}).

3.7.2 Generalised wind climate

Height	Parameter	0.00 m	0.03 m	0.10 m	0.40 m	1.50 m
10.0 m	Weibull A [m/s]	6.4	4.2	3.7	2.9	1.9
	Weibull k	2.19	1.79	1.79	1.79	1.78
	Mean speed [m/s]	5.67	3.76	3.28	2.58	1.72
	Power density [W/m²]	179	64	42	21	6
30.0 m	Weibull A [m/s]	7.0	5.4	4.9	4.1	3.2
	Weibull k	2.24	2.02	2.00	1.97	1.93
	Mean speed [m/s]	6.23	4.82	4.34	3.67	2.85
	Power density [W/m²]	233	119	87	54	26
50.0 m	Weibull A [m/s]	7.3	6.2	5.6	4.9	3.9
	Weibull k	2.24	2.24	2.19	2.14	2.07
	Mean speed [m/s]	6.49	5.51	5.00	4.31	3.48
	Power density [W/m²]	263	161	123	80	44
70.0 m	Weibull A [m/s]	7.5	6.9	6.3	5.4	4.5
	Weibull k	2.19	2.45	2.38	2.30	2.20
	Mean speed [m/s]	6.65	6.10	5.54	4.81	3.96
	Power density [W/m²]	289	203	156	105	61
100.0 m	Weibull A [m/s]	7.7	7.8	7.0	6.1	5.1
	Weibull k	2.12	2.48	2.47	2.46	2.40
	Mean speed [m/s]	6.82	6.88	6.25	5.45	4.55
	Power density [W/m²]	321	290	218	145	86

Non-default parameters values: Air density [kg/m^3]: 1.12 (default is 1.225) Standard height #2 [m]: 30.00 (default is 25.00) Standard height #4 [m]: 70.00 (default is 100.00) Standard height #5 [m]: 100.00 (default is 200.00).

3.8 Fuxin, Pingandi (ML5)

ML5	121.83645°E	42.46533°N	315 m	E 404342 m	N 4702100 m	UTM 51

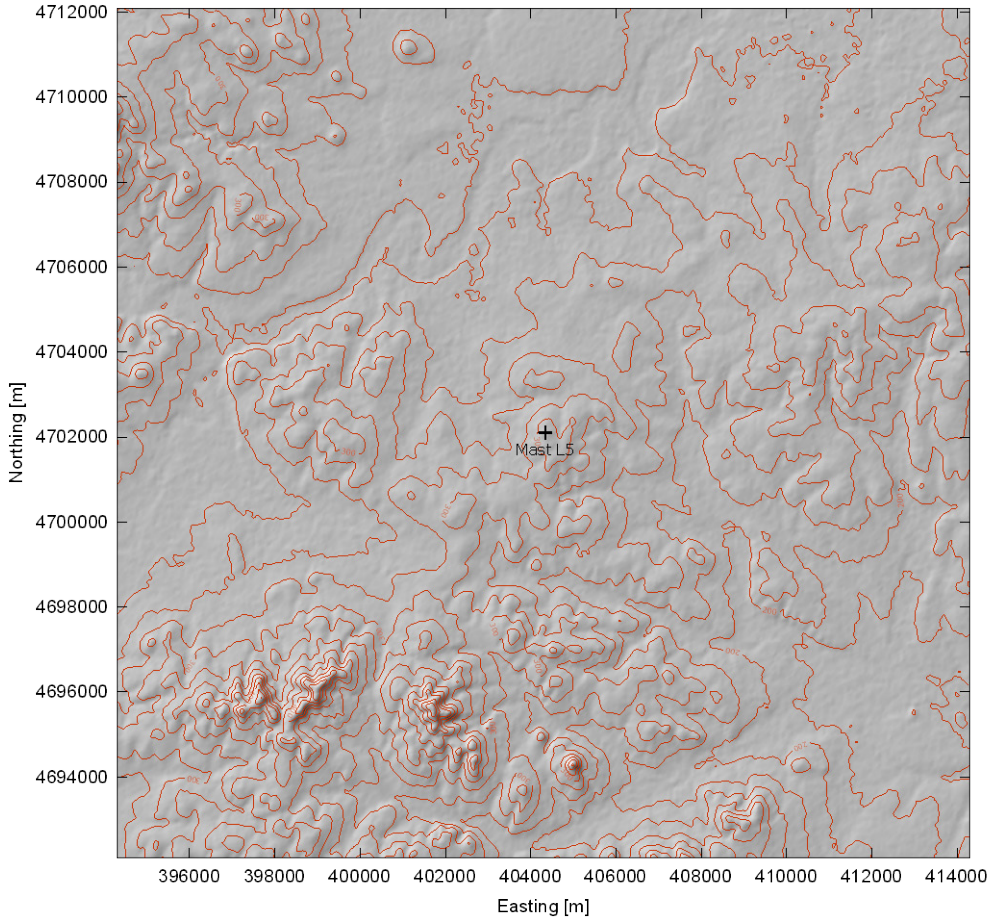

Figure 16. Elevation map from SRTM3 data, covering 20×20 km^2, with 20-m contours. The ruggedness index for the site is 0%.

3.8.1 Observed wind climate

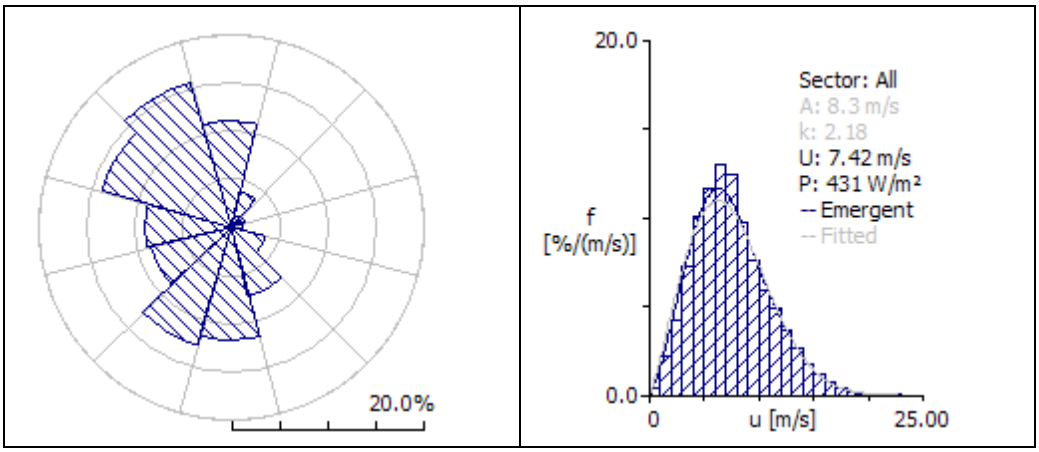

Figure 17. Wind rose and wind speed distribution for Pingandi at 70 m a.g.l. The number of observations is 52560 and the recovery rate is 100%.

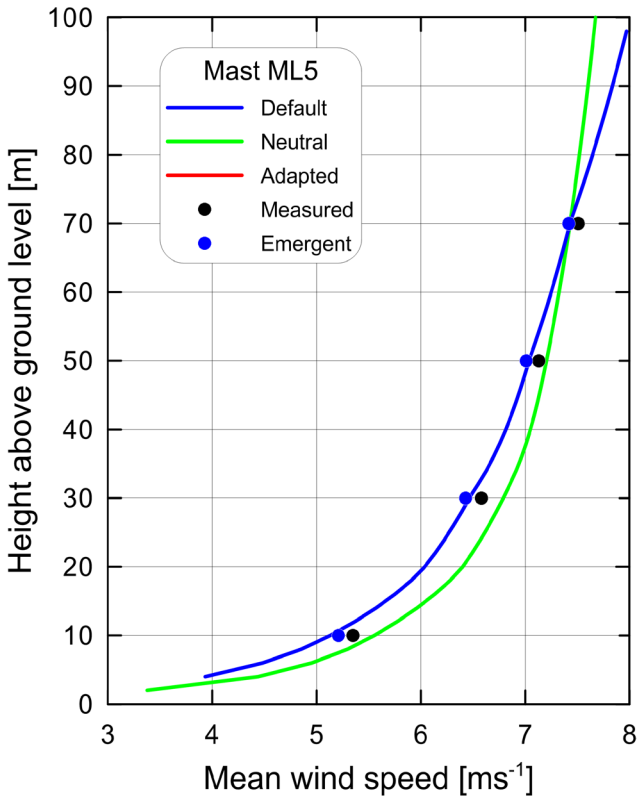

Figure 18. Measured and WAsP-modelled wind profiles for Pingandi. No adapted wind profile is shown for this station.

3.8.2 Generalised wind climate

Height	Parameter	0.00 m	0.03 m	0.10 m	0.40 m	1.50 m
10.0 m	Weibull A [m/s]	8.3	5.9	5.1	4.0	2.7
	Weibull k	2.08	1.83	1.85	1.86	1.85
	Mean speed [m/s]	7.39	5.22	4.55	3.58	2.38
	Power density [W/m²]	448	180	118	57	17
30.0 m	Weibull A [m/s]	9.2	7.3	6.6	5.6	4.3
	Weibull k	2.12	1.99	1.99	1.97	1.96
	Mean speed [m/s]	8.12	6.43	5.82	4.93	3.85
	Power density [W/m²]	584	310	229	140	67
50.0 m	Weibull A [m/s]	9.5	8.0	7.4	6.4	5.2
	Weibull k	2.13	2.13	2.12	2.09	2.05
	Mean speed [m/s]	8.45	7.13	6.52	5.64	4.60
	Power density [W/m²]	655	393	303	199	109
70.0 m	Weibull A [m/s]	9.8	8.7	8.0	7.0	5.8
	Weibull k	2.09	2.28	2.24	2.19	2.14
	Mean speed [m/s]	8.66	7.67	7.05	6.17	5.12
	Power density [W/m²]	719	462	363	248	146
100.0 m	Weibull A [m/s]	10.0	9.4	8.7	7.7	6.5
	Weibull k	2.03	2.29	2.31	2.32	2.28
	Mean speed [m/s]	8.88	8.35	7.69	6.79	5.74
	Power density [W/m²]	797	596	461	316	194

Non-default parameters values: Air density [kg/m^3]: 1.21 (default is 1.225) Standard height #2 [m]: 30.00 (default is 25.00) Standard height #4 [m]: 70.00 (default is 100.00) Standard height #5 [m]: 100.00 (default is 200.00).

3.9 Jianshecun, Tongyu, Baicheng (M04)

M04	122.27773°E	44.52714°N	168 m	E 442608 m	N 4930678 m	UTM 51

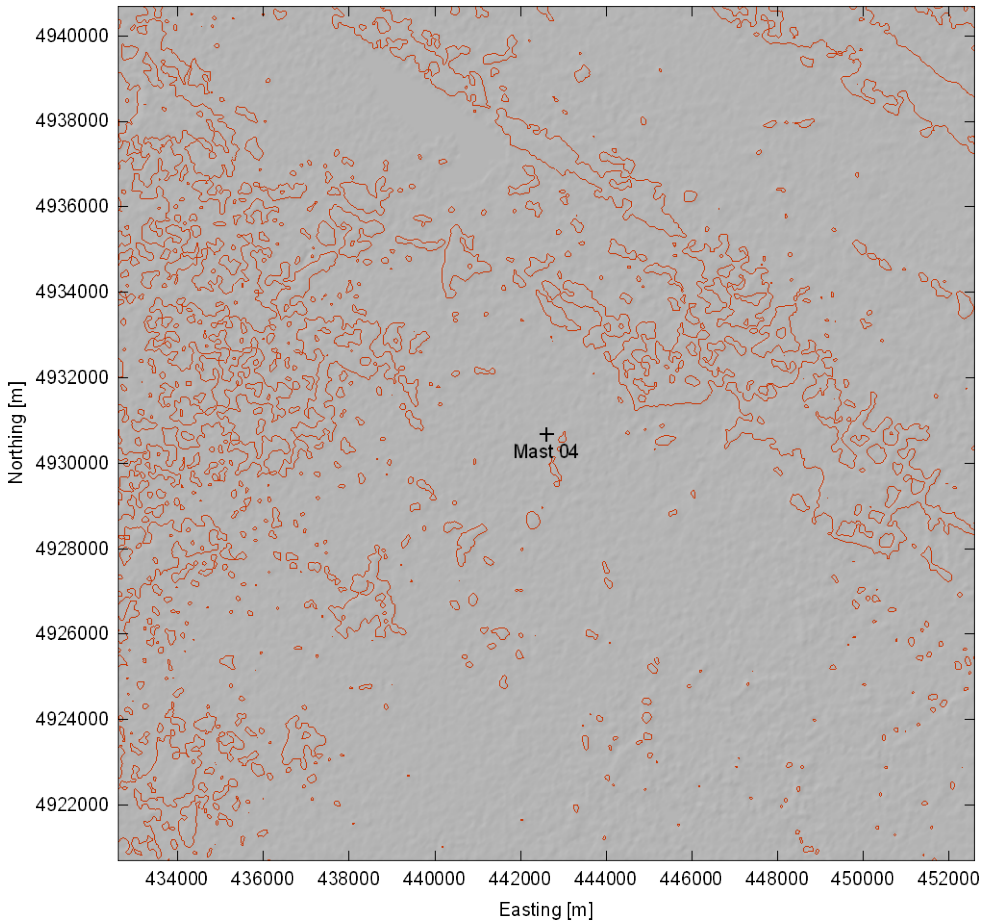

Figure 19. Elevation map from SRTM3 data, covering 20×20 km^2, with 10-m contours. The ruggedness index for the site is 0%.

3.9.1 Observed wind climate

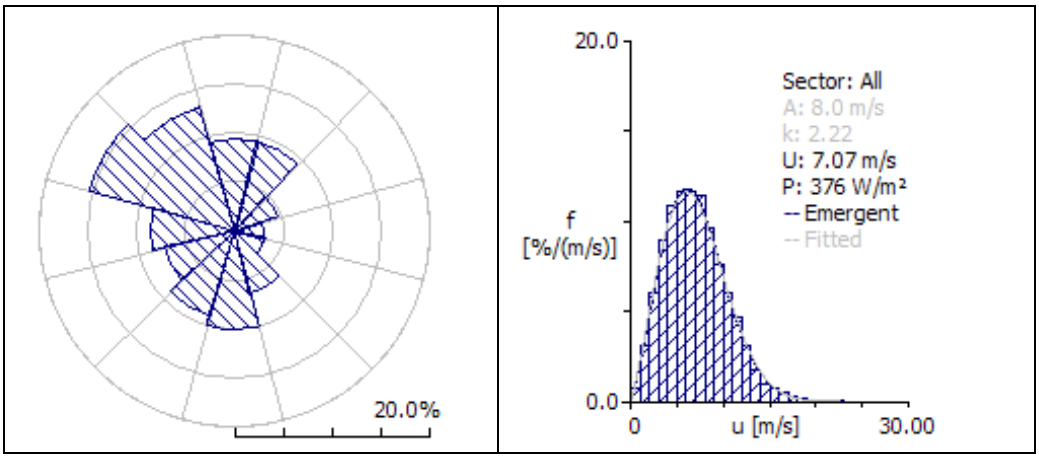

Figure 20. Wind rose and wind speed distribution for Jianshecun at 70 m a.g.l. The number of observations is 52560 and the recovery rate is 100%.

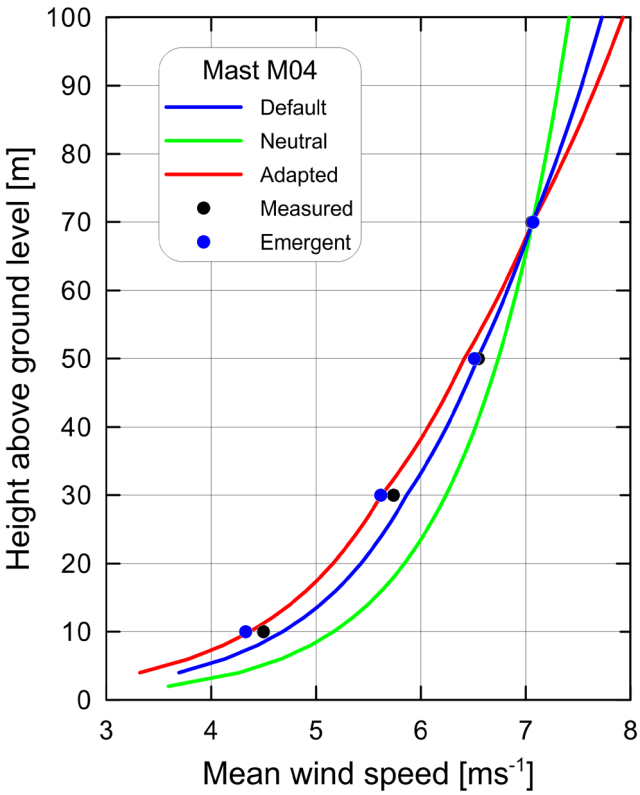

Figure 21. Measured and WAsP-modelled wind profiles for Jianshecun. The adapted wind profile corresponds to a mean heat flux over land of -80 Wm^{-2} (default -40 Wm^{-2}).

3.9.2 Generalised wind climate

Height	Parameter	0.00 m	0.03 m	0.10 m	0.40 m	1.50 m
10.0 m	Weibull A [m/s]	7.9	5.5	4.8	3.8	2.5
	Weibull k	2.05	1.78	1.79	1.79	1.79
	Mean speed [m/s]	7.01	4.94	4.31	3.39	2.25
	Power density [W/m²]	399	161	106	52	15
30.0 m	Weibull A [m/s]	8.7	6.9	6.2	5.3	4.1
	Weibull k	2.09	1.94	1.94	1.92	1.89
	Mean speed [m/s]	7.71	6.10	5.52	4.68	3.65
	Power density [W/m²]	519	277	206	127	61
50.0 m	Weibull A [m/s]	9.1	7.7	7.0	6.1	4.9
	Weibull k	2.10	2.10	2.08	2.04	1.99
	Mean speed [m/s]	8.02	6.78	6.19	5.36	4.36
	Power density [W/m²]	583	352	271	179	99
70.0 m	Weibull A [m/s]	9.3	8.3	7.6	6.6	5.5
	Weibull k	2.05	2.26	2.22	2.15	2.09
	Mean speed [m/s]	8.22	7.31	6.71	5.87	4.87
	Power density [W/m²]	642	415	325	223	131
100.0 m	Weibull A [m/s]	9.5	9.0	8.3	7.3	6.2
	Weibull k	1.99	2.25	2.27	2.28	2.23
	Mean speed [m/s]	8.43	7.99	7.35	6.47	5.46
	Power density [W/m²]	714	542	418	285	174

Non-default parameters values: Air density [kg/m^3]: 1.24 (default is 1.225) Standard height #2 [m]: 30.00 (default is 25.00) Standard height #4 [m]: 70.00 (default is 100.00) Standard height #5 [m]: 100.00 (default is 200.00).

3.10 Chuizi, Qian'an, Songyuan (M05)

M05	123.65746°E	44.94102°N	136 m	E 551871 m	N 4976609 m	UTM 51

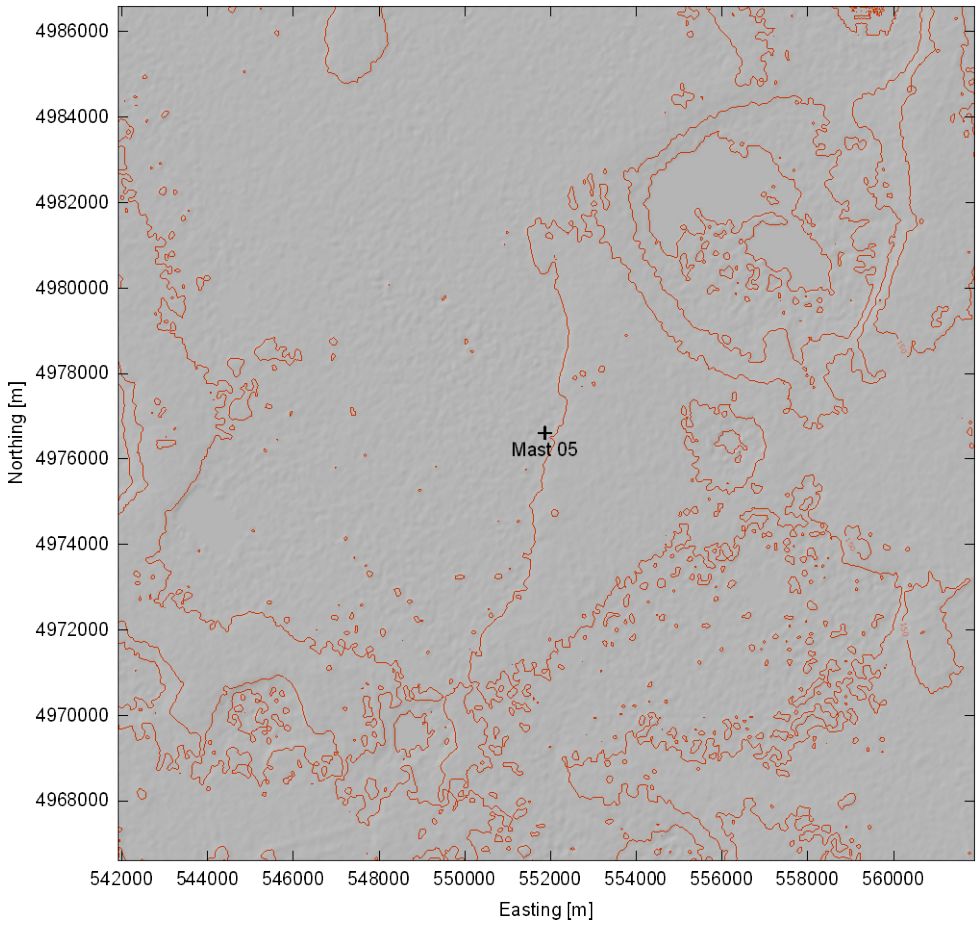

Figure 22. Elevation map from SRTM3 data, covering 20×20 km^2, with 10-m contours. The ruggedness index for the site is 0%.

3.10.1 Observed wind climate

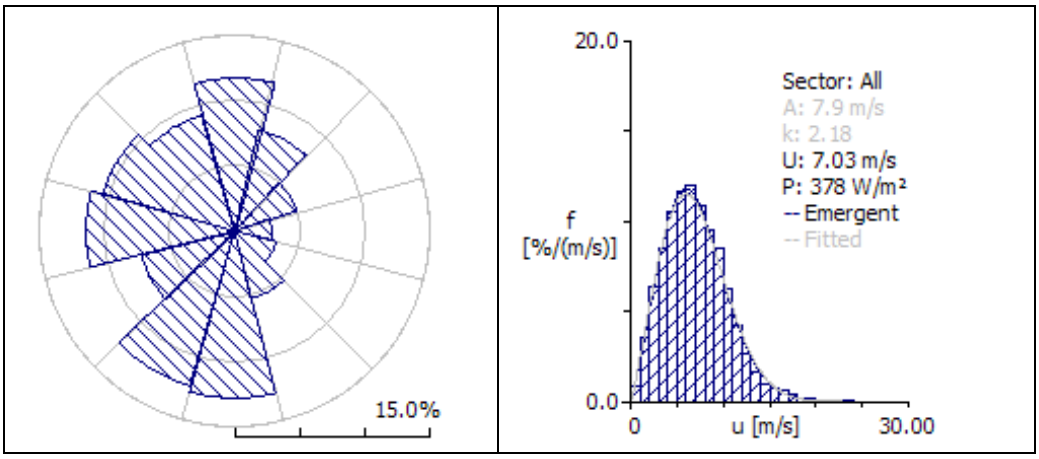

Figure 23. Wind rose and wind speed distribution for Chuizi at 70 m a.g.l. The number of observations is 52560 and the recovery rate is 100%.

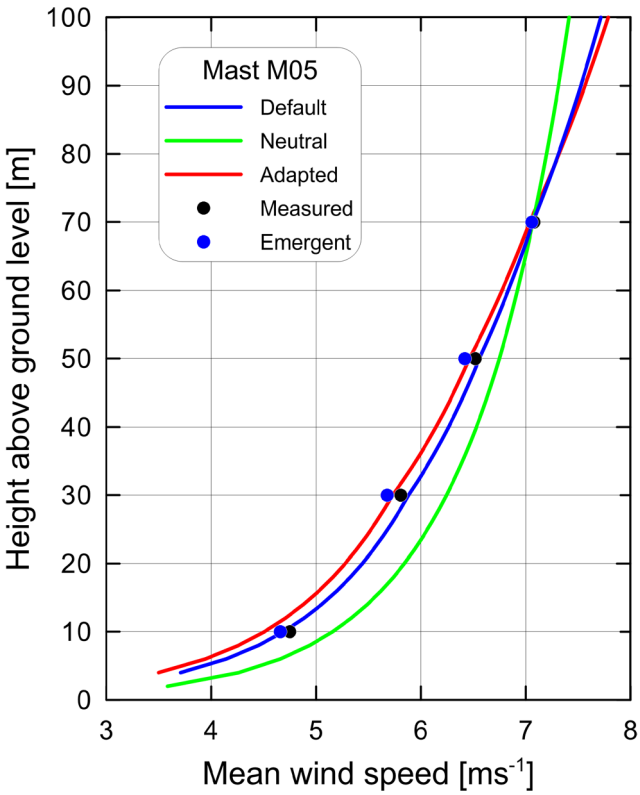

Figure 24. Measured and WAsP-modelled wind profiles for Chuizi. The adapted wind profile corresponds to a mean heat flux over land of -60 Wm^{-2} (default -40 Wm^{-2}).

3.10.2 Generalised wind climate

Height	Parameter	0.00 m	0.03 m	0.10 m	0.40 m	1.50 m
10.0 m	Weibull A [m/s]	7.9	5.5	4.8	3.8	2.5
	Weibull k	1.99	1.74	1.74	1.74	1.75
	Mean speed [m/s]	6.97	4.92	4.29	3.37	2.24
	Power density [W/m²]	402	164	108	53	16
30.0 m	Weibull A [m/s]	8.6	6.8	6.2	5.2	4.1
	Weibull k	2.03	1.89	1.88	1.87	1.85
	Mean speed [m/s]	7.66	6.07	5.49	4.65	3.63
	Power density [W/m²]	523	281	209	128	62
50.0 m	Weibull A [m/s]	9.0	7.6	6.9	6.0	4.9
	Weibull k	2.04	2.04	2.02	1.98	1.95
	Mean speed [m/s]	7.97	6.74	6.16	5.33	4.34
	Power density [W/m²]	587	355	274	181	99
70.0 m	Weibull A [m/s]	9.2	8.2	7.5	6.6	5.5
	Weibull k	1.99	2.20	2.15	2.09	2.04
	Mean speed [m/s]	8.17	7.27	6.67	5.83	4.85
	Power density [W/m²]	647	417	328	225	132
100.0 m	Weibull A [m/s]	9.4	9.0	8.2	7.3	6.1
	Weibull k	1.93	2.19	2.21	2.21	2.19
	Mean speed [m/s]	8.37	7.94	7.30	6.43	5.44
	Power density [W/m²]	720	544	420	287	175

Non-default parameters values: Air density [kg/m^3]: 1.24 (default is 1.225) Standard height #2 [m]: 30.00 (default is 25.00) Standard height #4 [m]: 70.00 (default is 100.00) Standard height #5 [m]: 100.00 (default is 200.00).

3.11 Tuanshan,Bolichengzi, Gongzhuling, Siping (M06)

M06	124.10508°E	43.94166°N	185 m	E 588686 m	N 4865987 m	UTM 51

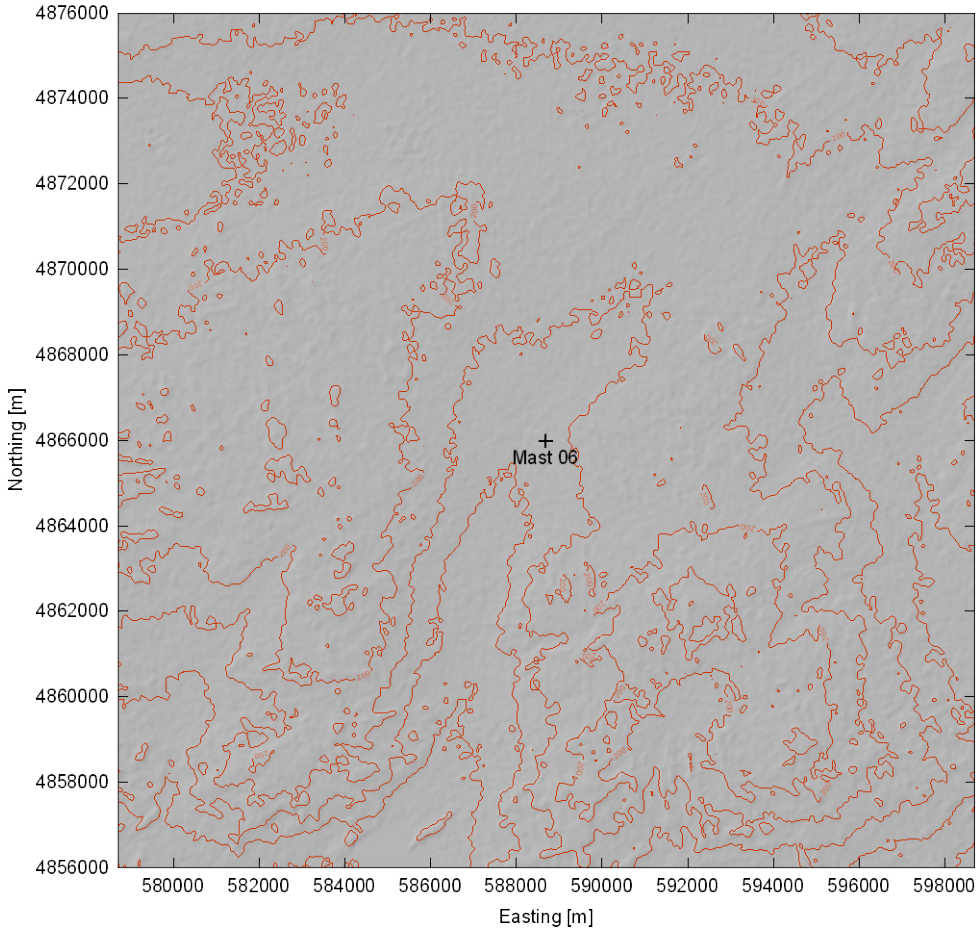

Figure 25. Elevation map from SRTM3 data, covering 20×20 km^2, with 10-m contours. The ruggedness index for the site is 0%.

3.11.1 Observed wind climate

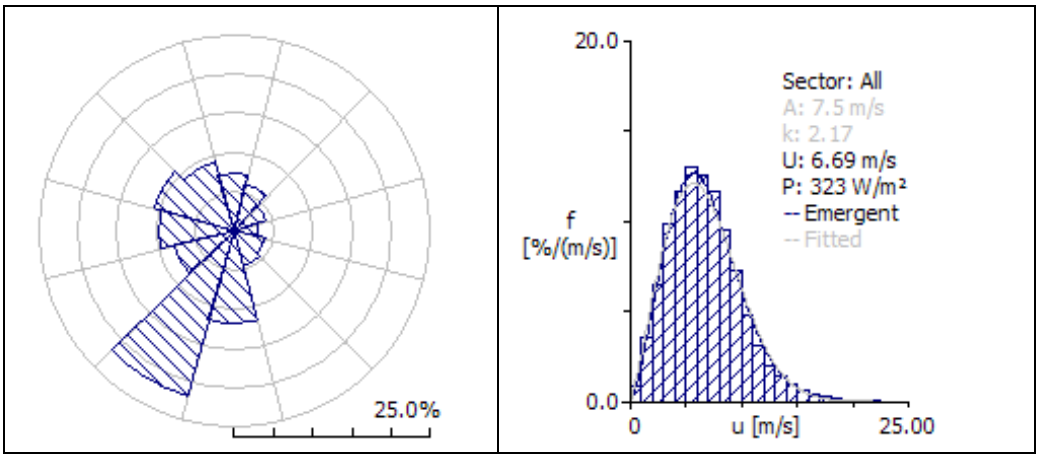

Figure 26. Wind rose and wind speed distribution for Tuanshan at 70 m a.g.l. The number of observations is 52560 and the recovery rate is 100%. Data from Risø DTU measurements (Jul-Dec 2009) and CMA measurements (Jan-Jun 2009).

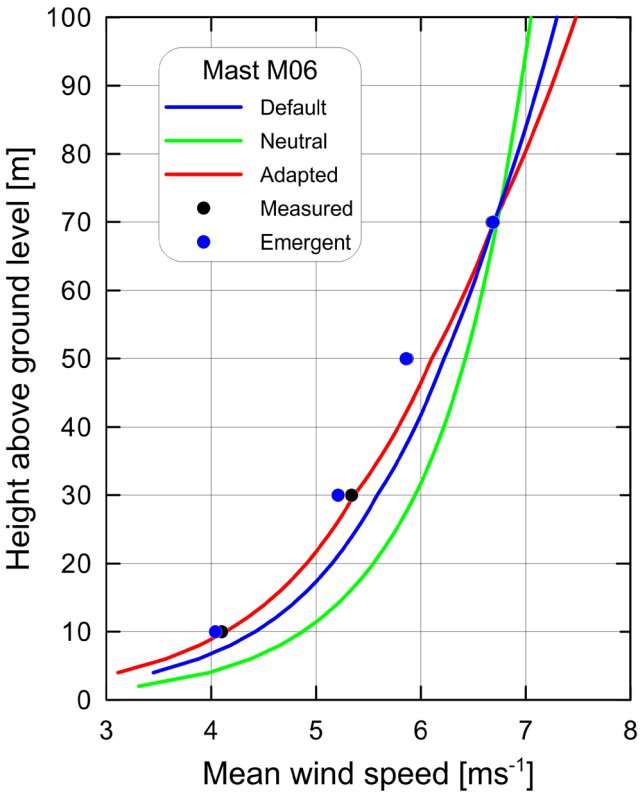

Figure 27. Measured and WAsP-modelled wind profiles for Tuanshan. The adapted wind profile corresponds to a mean heat flux over land of -80 Wm^{-2} (default -40 Wm^{-2}).

3.11.2 Generalised wind climate

Height	Parameter	0.00 m	0.03 m	0.10 m	0.40 m	1.50 m
10.0 m	Weibull A [m/s]	7.7	5.1	4.5	3.5	2.3
	Weibull k	2.02	1.66	1.67	1.67	1.66
	Mean speed [m/s]	6.86	4.58	3.99	3.13	2.09
	Power density [W/m²]	378	141	92	45	13
30.0 m	Weibull A [m/s]	8.5	6.6	5.9	5.0	3.9
	Weibull k	2.06	1.87	1.85	1.83	1.80
	Mean speed [m/s]	7.54	5.82	5.25	4.43	3.45
	Power density [W/m²]	492	251	186	113	54
50.0 m	Weibull A [m/s]	8.9	7.5	6.8	5.8	4.7
	Weibull k	2.08	2.07	2.03	1.98	1.93
	Mean speed [m/s]	7.85	6.62	6.01	5.18	4.19
	Power density [W/m²]	552	332	254	166	91
70.0 m	Weibull A [m/s]	9.1	8.2	7.5	6.5	5.4
	Weibull k	2.03	2.28	2.21	2.13	2.05
	Mean speed [m/s]	8.05	7.29	6.64	5.76	4.75
	Power density [W/m²]	609	408	315	213	124
100.0 m	Weibull A [m/s]	9.3	9.2	8.4	7.3	6.1
	Weibull k	1.96	2.33	2.33	2.31	2.24
	Mean speed [m/s]	8.25	8.18	7.45	6.49	5.43
	Power density [W/m²]	677	565	427	285	171

Non-default parameters values: Air density [kg/m^3]: 1.24 (default is 1.225) Standard height #2 [m]: 30.00 (default is 25.00) Standard height #4 [m]: 70.00 (default is 100.00) Standard height #5 [m]: 100.00 (default is 200.00).

3.12 Songyuan, Qlanguo, Chaganhuacun (MJ5)

MJ5	124.01715°E	44.61596°N	155 m	E 580701 m	N 4940793 m	UTM 51

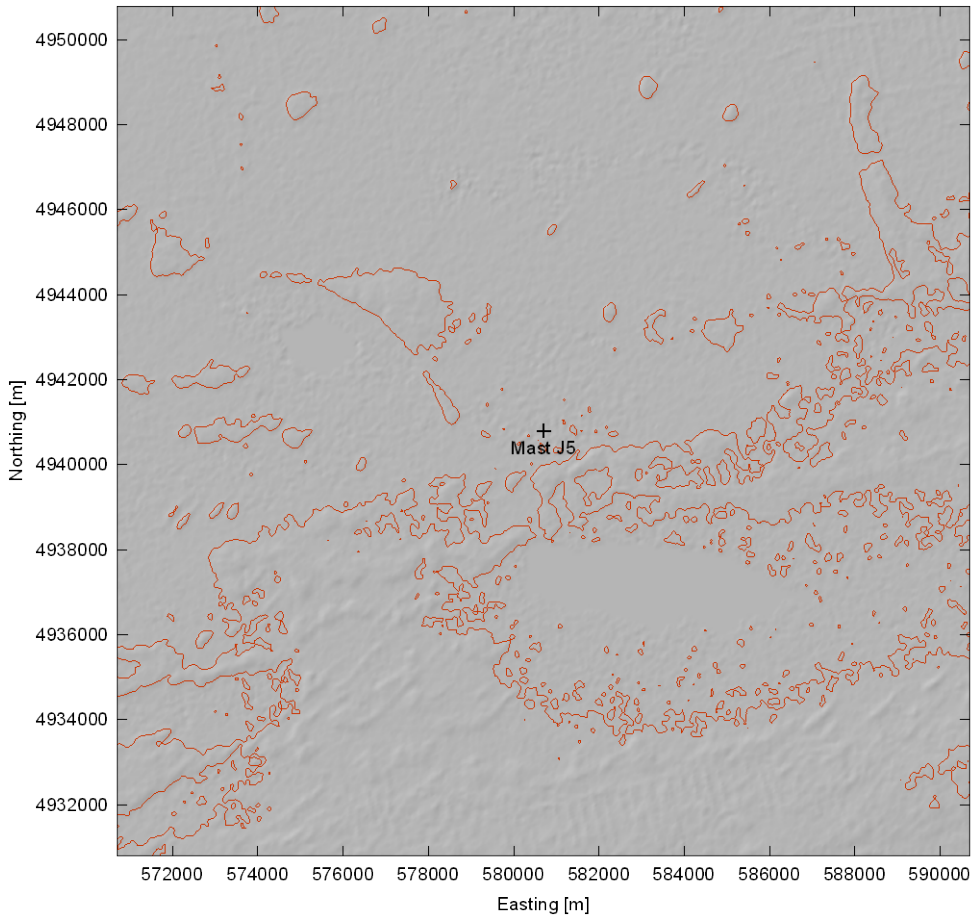

Figure 28. Elevation map from SRTM3 data, covering 20×20 km^2, with 20-m contours. The ruggedness index for the site is 0%.

3.12.1 Observed wind climate

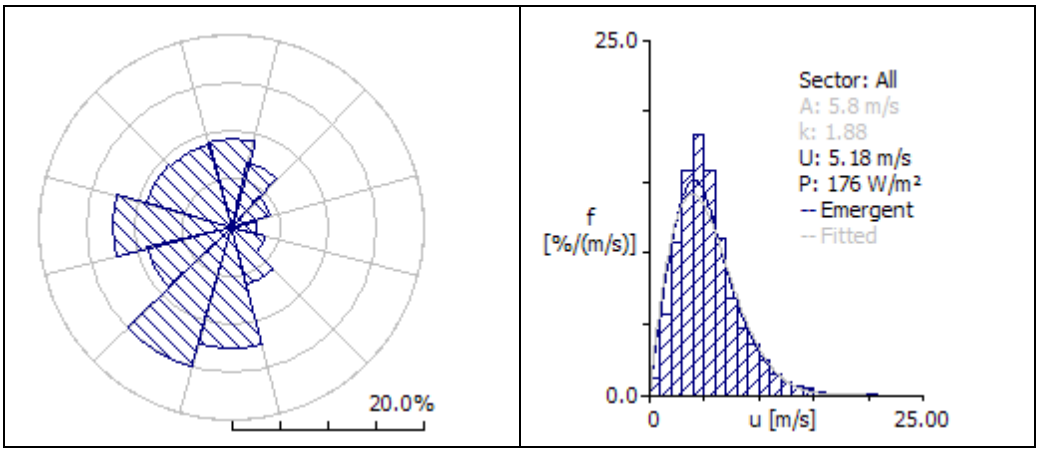

Figure 29. Wind rose and wind speed distribution for Songyuan at 30 m a.g.l. The number of observations is 52560 and the recovery rate is 100%.

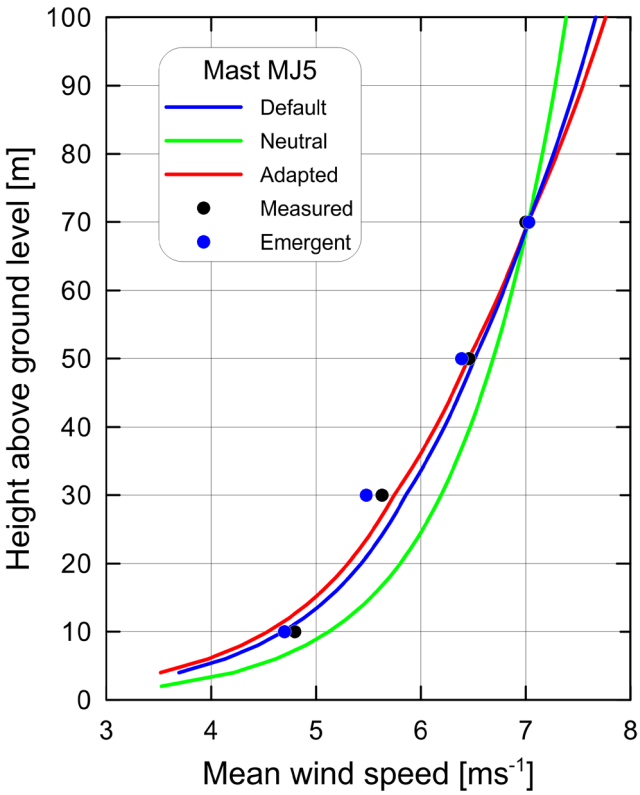

Figure 30. Measured and WAsP-modelled wind profiles for Songyuan. The adapted wind profile corresponds to a mean heat flux over land of -60 Wm^{-2}. Data for 8 months only.

3.12.2 Generalised wind climate

Height	Parameter	0.00 m	0.03 m	0.10 m	0.40 m	1.50 m
10.0 m	Weibull A [m/s]	7.2	5.1	4.4	3.5	2.3
	Weibull k	1.99	1.74	1.75	1.75	1.79
	Mean speed [m/s]	6.37	4.52	3.93	3.09	2.08
	Power density [W/m²]	307	127	84	41	12
30.0 m	Weibull A [m/s]	7.9	6.3	5.7	4.8	3.8
	Weibull k	2.04	1.91	1.89	1.88	1.90
	Mean speed [m/s]	7.00	5.59	5.05	4.28	3.37
	Power density [W/m²]	399	217	162	99	48
50.0 m	Weibull A [m/s]	8.2	7.0	6.4	5.5	4.5
	Weibull k	2.04	2.07	2.03	2.00	2.00
	Mean speed [m/s]	7.29	6.22	5.67	4.91	4.03
	Power density [W/m²]	449	276	213	141	77
70.0 m	Weibull A [m/s]	8.4	7.6	6.9	6.1	5.1
	Weibull k	2.00	2.22	2.17	2.12	2.10
	Mean speed [m/s]	7.47	6.72	6.15	5.38	4.51
	Power density [W/m²]	495	326	255	175	103
100.0 m	Weibull A [m/s]	8.6	8.3	7.6	6.7	5.7
	Weibull k	1.93	2.21	2.22	2.24	2.26
	Mean speed [m/s]	7.66	7.35	6.75	5.95	5.06
	Power density [W/m²]	552	429	331	225	137

Non-default parameters values: Air density [kg/m^3]: 1.24 (default is 1.225) Standard height #2 [m]: 30.00 (default is 25.00) Standard height #4 [m]: 70.00 (default is 100.00) Standard height #5 [m]: 100.00 (default is 200.00).

3.13 Tongjiang, Bachaxiang (M07)

M07	133.87547°E	48.21450°N	40 m	E 416464 m	N 5340753 m	UTM 53

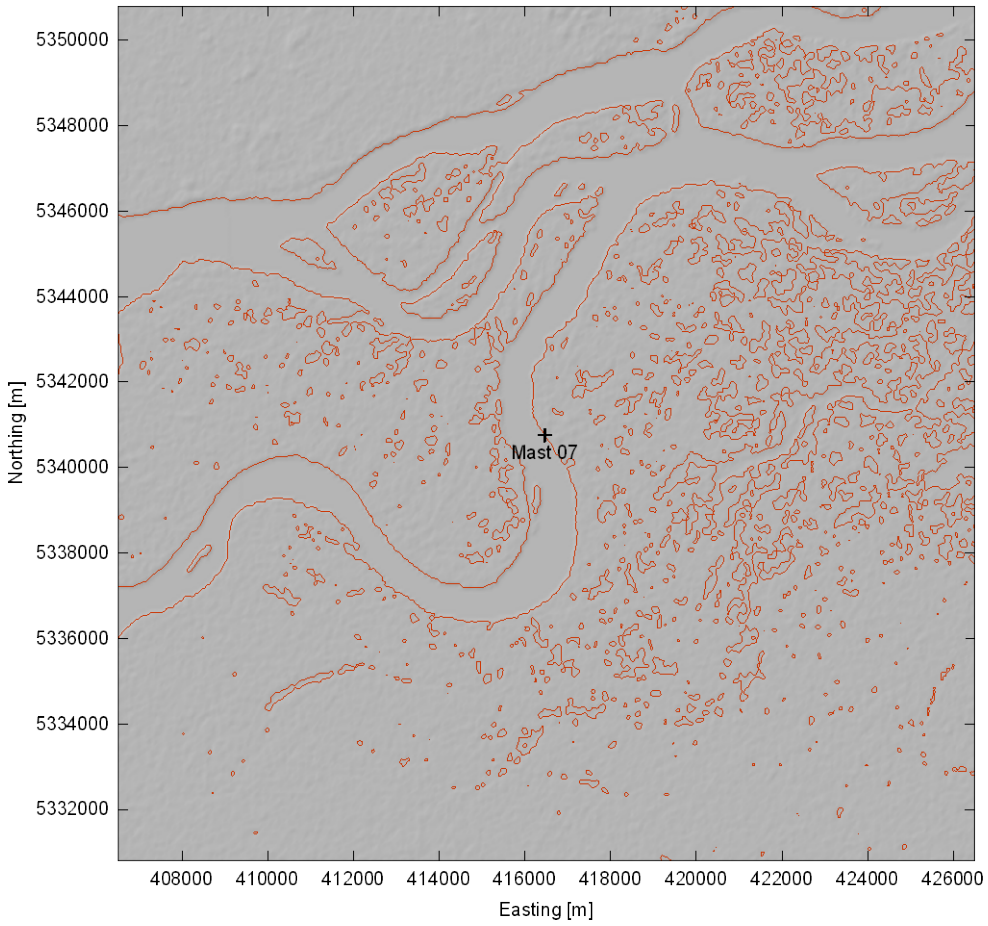

Figure 31. Elevation map from SRTM3 data, covering 20×20 km^2, with 20-m contours. The ruggedness index for the site is 0%.

3.13.1 Observed wind climate

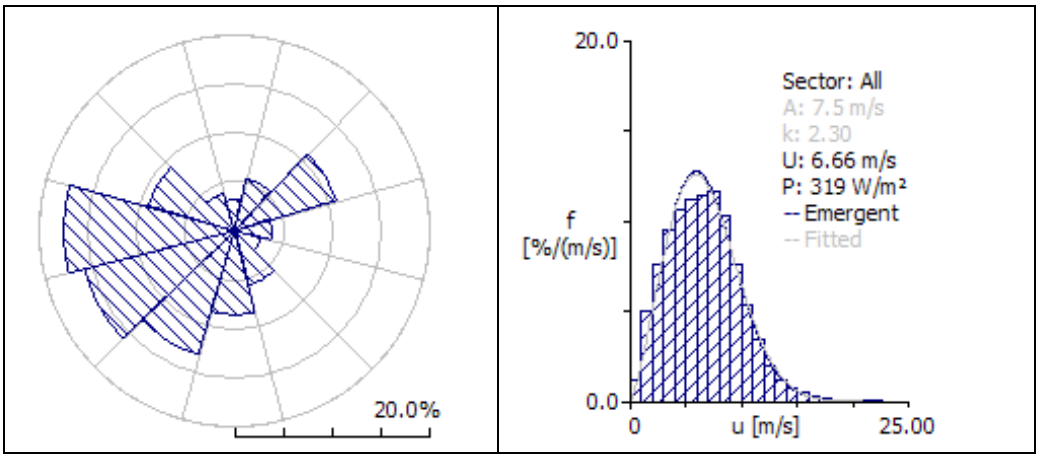

Figure 32. Wind rose and wind speed distribution for Tongjiang at 70 m a.g.l. The number of observations is 52560 and the recovery rate is 100%.

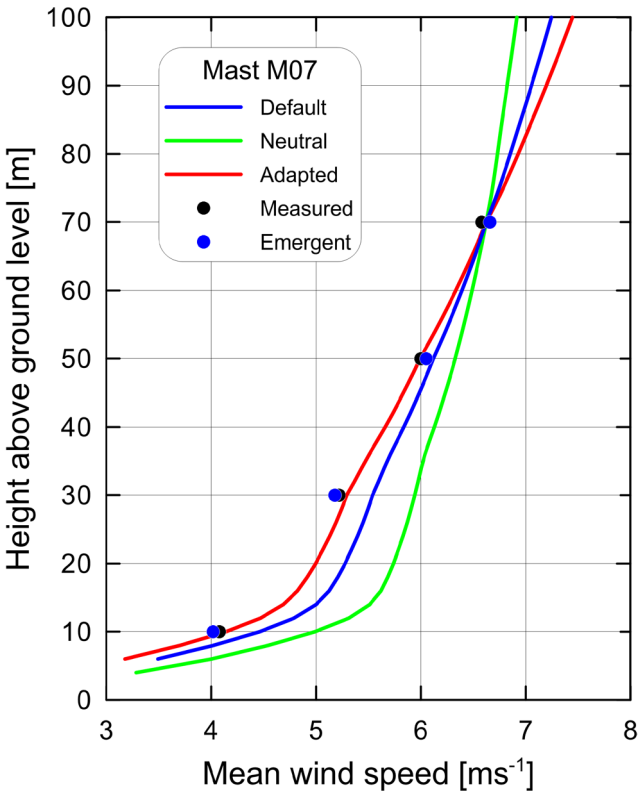

Figure 33. Measured and WAsP-modelled wind profiles for Tongjiang. The adapted wind profile corresponds to a mean heat flux over land of -80 Wm^{-2} (default -40 Wm^{-2}).

3.13.2 Generalised wind climate

Height	Parameter	0.00 m	0.03 m	0.10 m	0.40 m	1.50 m
10.0 m	Weibull A [m/s]	7.0	4.9	4.3	3.3	2.2
	Weibull k	2.03	1.76	1.76	1.75	1.74
	Mean speed [m/s]	6.18	4.36	3.80	2.98	1.99
	Power density [W/m²]	283	115	77	37	11
30.0 m	Weibull A [m/s]	7.7	6.1	5.5	4.6	3.6
	Weibull k	2.07	1.92	1.90	1.87	1.85
	Mean speed [m/s]	6.79	5.40	4.87	4.13	3.22
	Power density [W/m²]	368	199	148	91	44
50.0 m	Weibull A [m/s]	8.0	6.8	6.2	5.3	4.4
	Weibull k	2.08	2.08	2.04	1.99	1.95
	Mean speed [m/s]	7.07	6.01	5.48	4.74	3.86
	Power density [W/m²]	413	253	196	129	71
70.0 m	Weibull A [m/s]	8.2	7.3	6.7	5.9	4.9
	Weibull k	2.03	2.24	2.18	2.12	2.05
	Mean speed [m/s]	7.25	6.49	5.94	5.19	4.31
	Power density [W/m²]	455	299	235	161	95
100.0 m	Weibull A [m/s]	8.4	8.0	7.4	6.5	5.5
	Weibull k	1.96	2.23	2.24	2.23	2.20
	Mean speed [m/s]	7.43	7.11	6.52	5.74	4.84
	Power density [W/m²]	507	393	303	207	126

Non-default parameters values: Air density [kg/m^3]: 1.27 (default is 1.225) Standard height #2 [m]: 30.00 (default is 25.00) Standard height #4 [m]: 70.00 (default is 100.00) Standard height #5 [m]: 100.00 (default is 200.00).

3.14 Suiling, Koumenzi (M08)

M08	127.64503°E	47.66755°N	327 m	E 398278 m	N 5280240 m	UTM 52

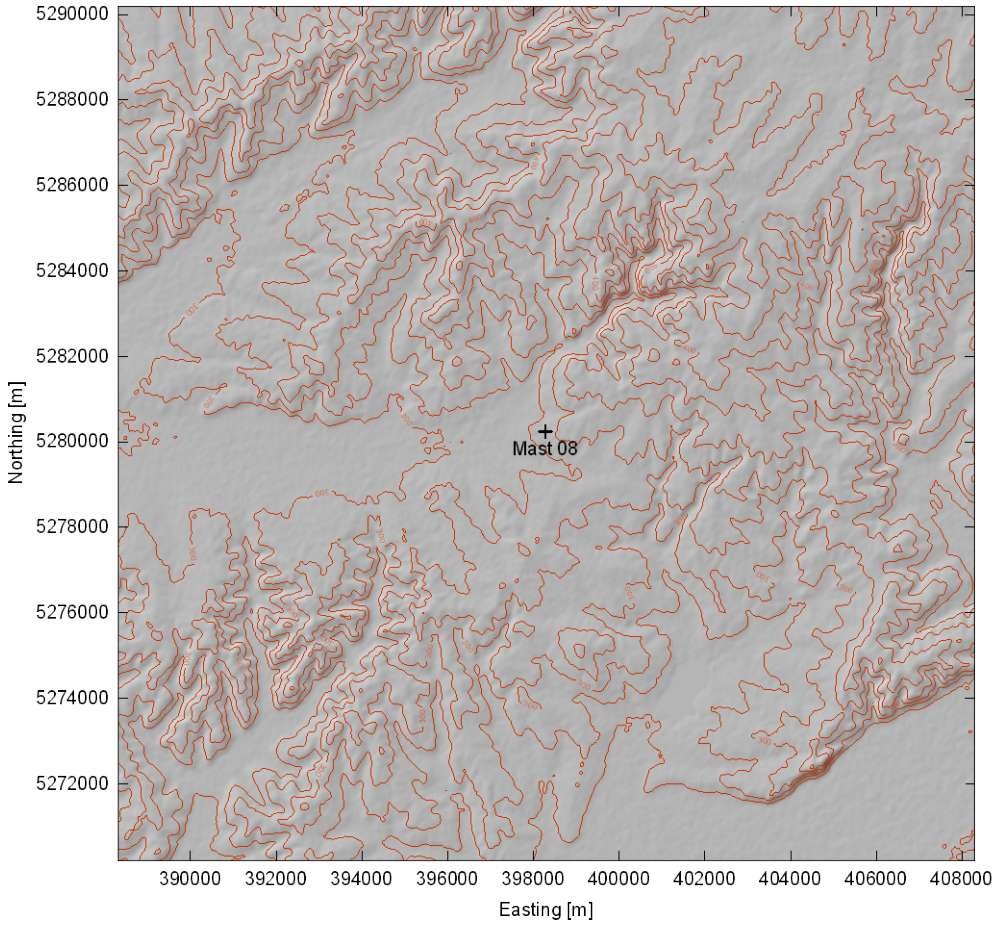

Figure 34. Elevation map from SRTM3 data, covering 20×20 km^2, with 20-m contours. The ruggedness index for the site is 0%.

3.14.1 Observed wind climate

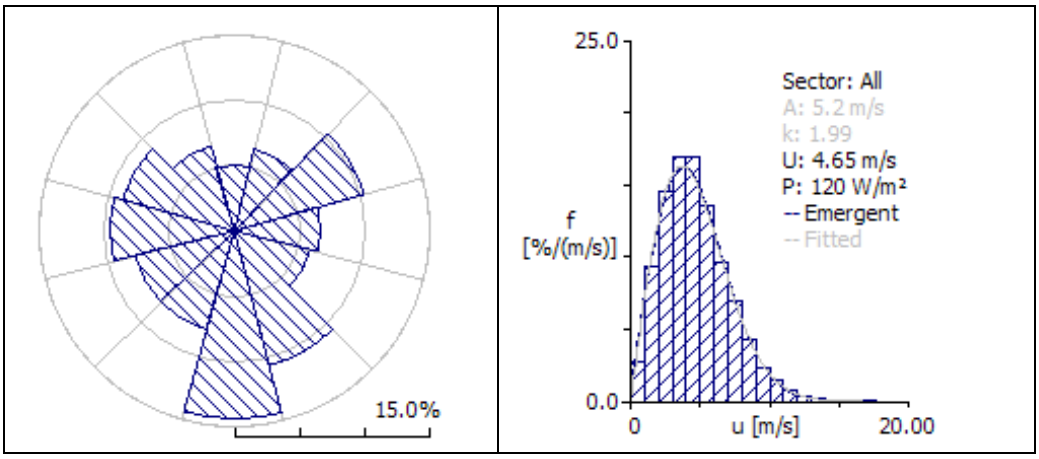

Figure 35. Wind rose and wind speed distribution for Suiling at 70 m a.g.l. The number of observations is 52560 and the recovery rate is 100%.

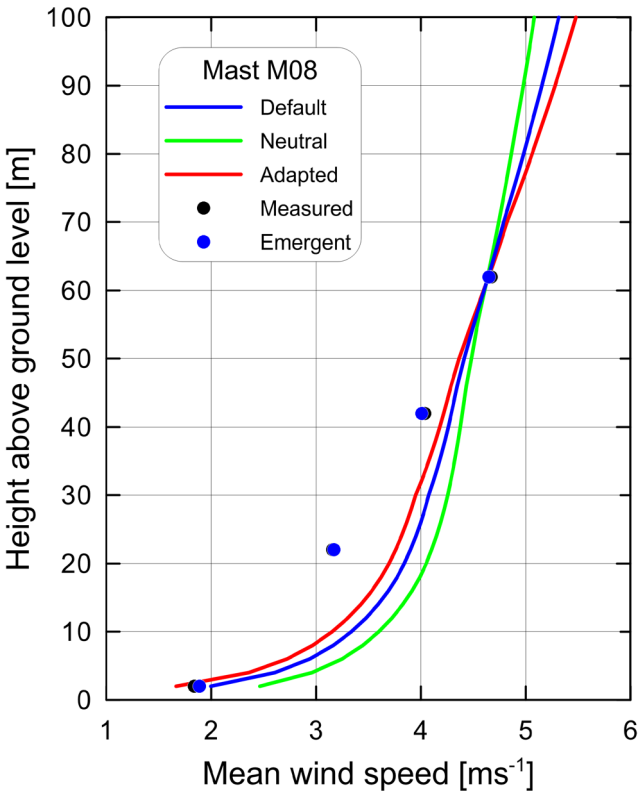

Figure 36. Measured and WAsP-modelled wind profiles for Suiling. The adapted wind profile corresponds to a mean heat flux over land of -80 Wm^{-2} (default -40 Wm^{-2}).

3.14.2 Generalised wind climate

Height	Parameter	0.00 m	0.03 m	0.10 m	0.40 m	1.50 m
10.0 m	Weibull A [m/s]	6.5	4.5	3.9	3.1	2.1
	Weibull k	1.84	1.60	1.60	1.62	1.60
	Mean speed [m/s]	5.74	4.06	3.53	2.79	1.86
	Power density [W/m²]	245	102	68	33	10
30.0 m	Weibull A [m/s]	7.1	5.6	5.1	4.3	3.4
	Weibull k	1.88	1.75	1.73	1.73	1.70
	Mean speed [m/s]	6.31	5.03	4.54	3.86	3.01
	Power density [W/m²]	317	175	130	80	39
50.0 m	Weibull A [m/s]	7.4	6.3	5.7	5.0	4.1
	Weibull k	1.88	1.89	1.86	1.83	1.79
	Mean speed [m/s]	6.57	5.60	5.10	4.43	3.60
	Power density [W/m²]	357	221	170	113	63
70.0 m	Weibull A [m/s]	7.6	6.8	6.2	5.5	4.5
	Weibull k	1.84	2.03	1.98	1.94	1.87
	Mean speed [m/s]	6.73	6.06	5.54	4.85	4.03
	Power density [W/m²]	394	259	203	140	83
100.0 m	Weibull A [m/s]	7.8	7.5	6.9	6.1	5.1
	Weibull k	1.78	2.01	2.02	2.04	2.00
	Mean speed [m/s]	6.90	6.64	6.08	5.37	4.53
	Power density [W/m²]	442	344	264	180	110

Non-default parameters values: Air density [kg/m^3]: 1.24 (default is 1.225) Standard height #2 [m]: 30.00 (default is 25.00) Standard height #4 [m]: 70.00 (default is 100.00) Standard height #5 [m]: 100.00 (default is 200.00).

3.15 Zhaozhou, Tianzhutang (M09)

M09	125.34413°E	45.74241°N	147 m	E 215611 m	N 5071930 m	UTM 52

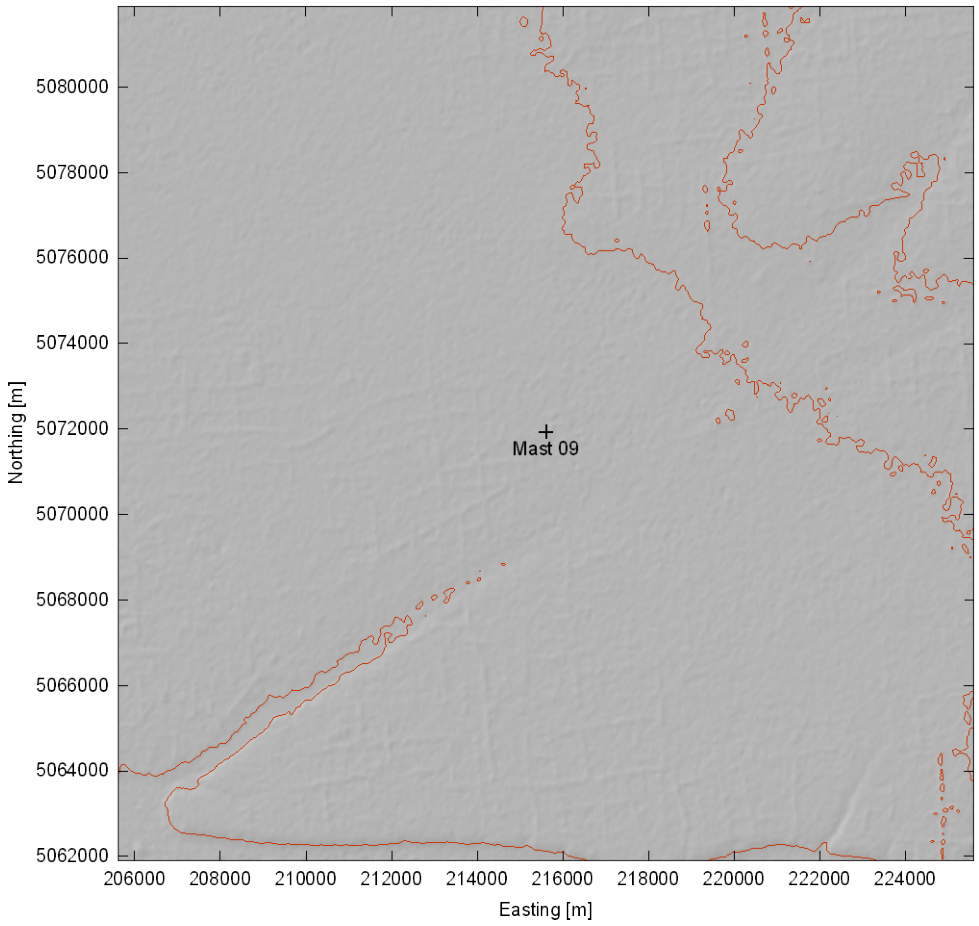

Figure 37. Elevation map from SRTM3 data, covering 20×20 km^2, with 20-m contours. The ruggedness index for the site is 0%.

3.15.1 Observed wind climate

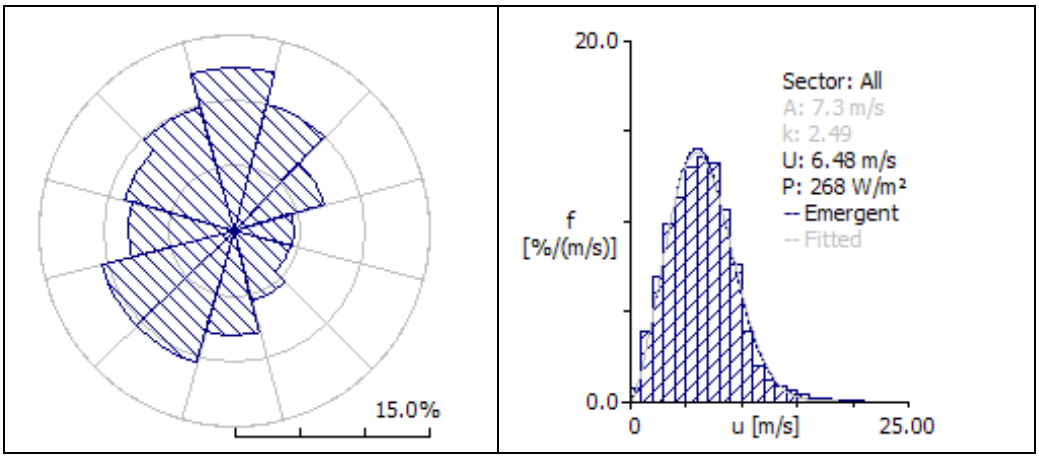

Figure 38. Wind rose and wind speed distribution for Zhaozhou at 70 m a.g.l. The number of observations is 52560 and the recovery rate is 100%.

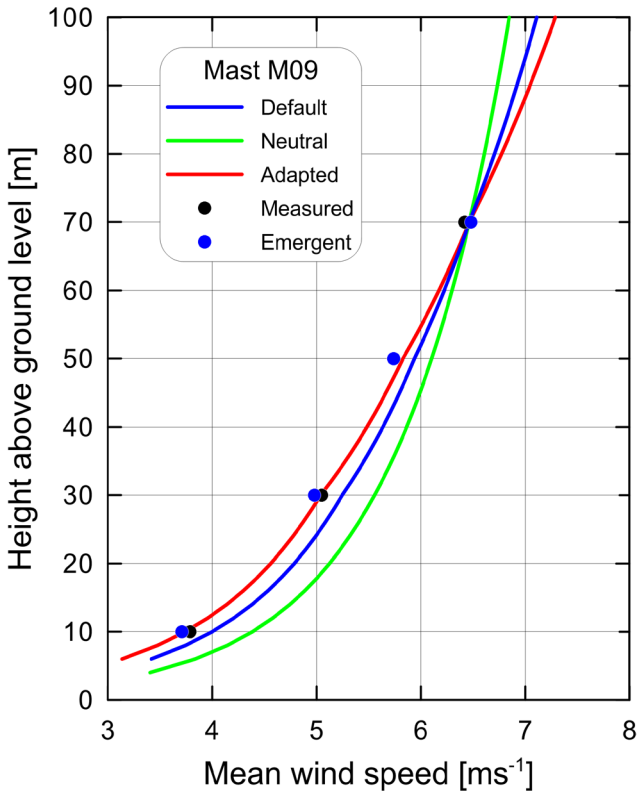

Figure 39. Measured and WAsP-modelled wind profiles for Zhaozhou. The adapted wind profile corresponds to a mean heat flux over land of -80 Wm^{-2} (default -40 Wm^{-2}).

3.15.2 Generalised wind climate

Height	Parameter	0.00 m	0.03 m	0.10 m	0.40 m	1.50 m
10.0 m	Weibull A [m/s]	8.0	5.6	4.9	3.8	2.5
	Weibull k	2.29	1.94	1.95	1.95	1.92
	Mean speed [m/s]	7.05	4.95	4.31	3.39	2.25
	Power density [W/m²]	367	148	97	47	14
30.0 m	Weibull A [m/s]	8.7	6.9	6.3	5.3	4.1
	Weibull k	2.34	2.14	2.12	2.10	2.05
	Mean speed [m/s]	7.75	6.14	5.54	4.69	3.65
	Power density [W/m²]	478	257	190	117	56
50.0 m	Weibull A [m/s]	9.1	7.7	7.0	6.1	4.9
	Weibull k	2.35	2.33	2.29	2.24	2.17
	Mean speed [m/s]	8.07	6.83	6.23	5.38	4.37
	Power density [W/m²]	538	329	253	167	91
70.0 m	Weibull A [m/s]	9.3	8.3	7.6	6.7	5.5
	Weibull k	2.29	2.52	2.46	2.38	2.28
	Mean speed [m/s]	8.27	7.39	6.76	5.90	4.88
	Power density [W/m²]	593	392	305	209	122
100.0 m	Weibull A [m/s]	9.6	9.1	8.4	7.4	6.2
	Weibull k	2.21	2.49	2.51	2.51	2.46
	Mean speed [m/s]	8.48	8.09	7.41	6.52	5.49
	Power density [W/m²]	657	519	397	270	164

Non-default parameters values: Air density [kg/m^3]: 1.24 (default is 1.225) Standard height #2 [m]: 30.00 (default is 25.00) Standard height #4 [m]: 70.00 (default is 100.00) Standard height #5 [m]: 100.00 (default is 200.00).

3.16 Jiamusi Tuanjiexishan (MH5)

MH5	130.33285°E	46.64002°N	312 m	E 602009 m	N 5166025 m	UTM 52

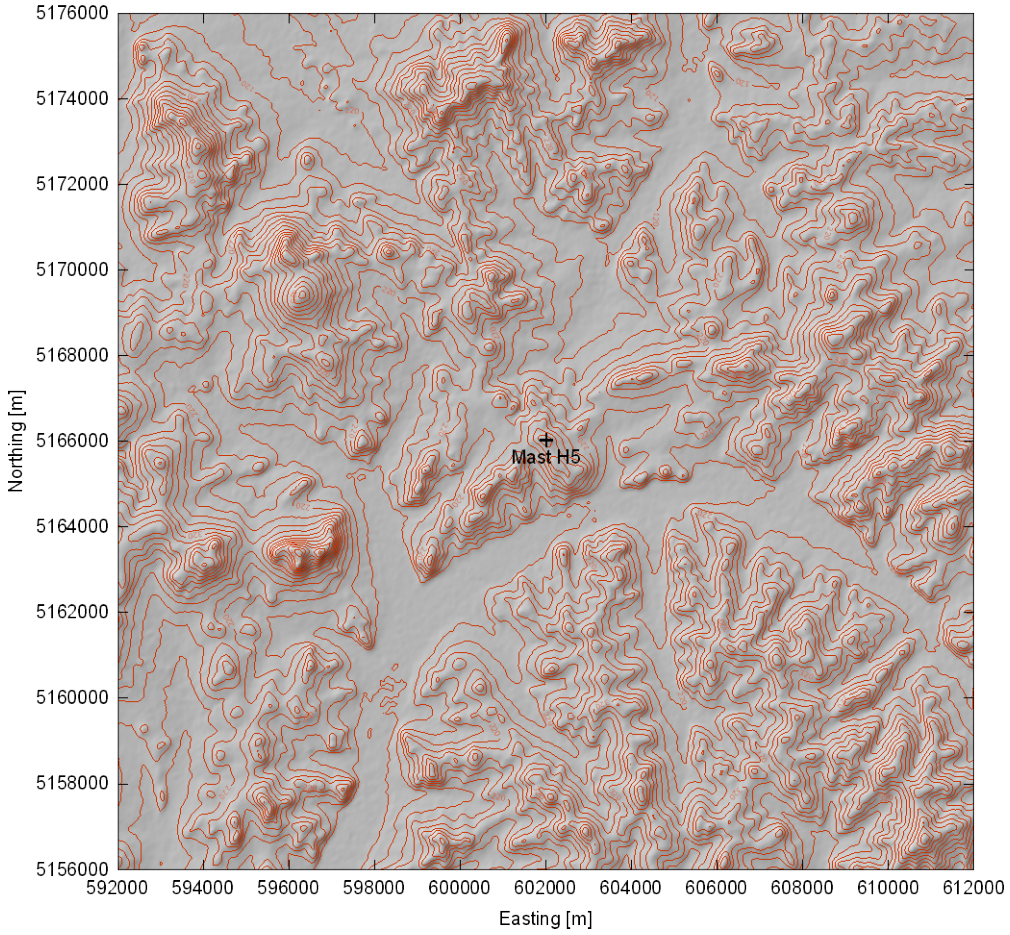

Figure 40. Elevation map from SRTM3 data, covering 20×20 km^2, with 20-m contours. The ruggedness index for the site is 0.2%.

3.16.1 Observed wind climate

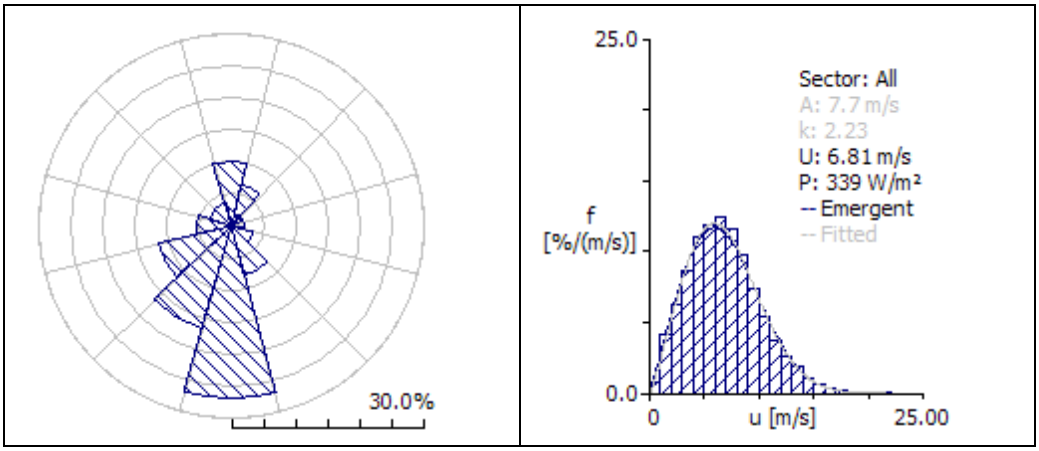

Figure 41. Wind rose and wind speed distribution for Jiamusi at 70 m a.g.l. Data period for mast MH5 is from 2008-11-01 to 2009-11-01. The number of observations is 52560 and the recovery rate is 100%.

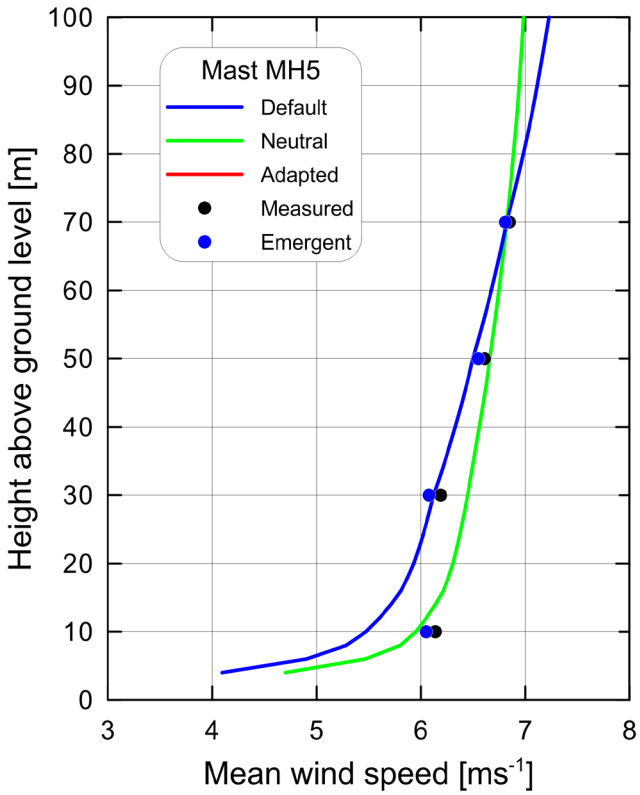

Figure 42. Measured and WAsP-modelled wind profiles for Jiamusi. No adapted wind profile is shown for this site. Note, that the data recovery for the 10-m level is 85% only.

3.16.2 Generalised wind climate

Height	Parameter	0.00 m	0.03 m	0.10 m	0.40 m	1.50 m
10.0 m	Weibull A [m/s]	7.4	5.2	4.5	3.6	2.4
	Weibull k	2.10	1.80	1.81	1.81	1.84
	Mean speed [m/s]	6.59	4.63	4.04	3.18	2.12
	Power density [W/m²]	319	130	86	42	12
30.0 m	Weibull A [m/s]	8.2	6.5	5.9	5.0	3.9
	Weibull k	2.15	1.98	1.97	1.95	1.96
	Mean speed [m/s]	7.24	5.75	5.19	4.40	3.45
	Power density [W/m²]	415	225	166	102	49
50.0 m	Weibull A [m/s]	8.5	7.2	6.6	5.7	4.7
	Weibull k	2.16	2.15	2.12	2.08	2.06
	Mean speed [m/s]	7.54	6.41	5.85	5.06	4.13
	Power density [W/m²]	467	287	221	146	80
70.0 m	Weibull A [m/s]	8.7	7.8	7.2	6.3	5.2
	Weibull k	2.10	2.32	2.28	2.21	2.17
	Mean speed [m/s]	7.73	6.94	6.35	5.55	4.62
	Power density [W/m²]	515	341	266	182	107
100.0 m	Weibull A [m/s]	8.9	8.6	7.9	6.9	5.9
	Weibull k	2.03	2.28	2.31	2.32	2.33
	Mean speed [m/s]	7.93	7.61	6.98	6.14	5.20
	Power density [W/m²]	574	457	350	237	143

Non-default parameters values: Standard height #2 [m]: 30.00 (default is 25.00) Standard height #4 [m]: 70.00 (default is 100.00) Standard height #5 [m]: 100.00 (default is 200.00).

3.17 Summary of Dongbei generalised wind climates

Table 10. Summary of the generalised wind climates at 70 m a.g.l. over roughness class 1 (roughness length z_0 = 0.03 m) at the meteorological stations: Data-collecting period, Weibull A- and k-parameters, mean wind speed (U), and mean power density (E).

Province Mast ID	**Year**	***A*** [ms^{-1}]	***k***	***U*** [ms^{-1}]	***E*** [Wm^{-2}]
Liaoning					
Mast 01	2009	5.7	2.10	5.08	141
Mast 02	2009	8.2	2.00	7.31	463
Mast 03	2009	6.9	2.45	6.10	203
Mast L5*	2009	8.7	2.28	7.67	462
Jilin					
Mast 04	2009	8.3	2.26	7.31	415
Mast 05	2009	8.2	2.18	7.31	426
Mast 06*	2009	8.2	2.26	7.25	403
Mast J5*	2009	7.6	2.22	6.72	325
Heilongjiang					
Mast 07	2009	7.3	2.24	6.49	299
Mast 08	2009	6.8	2.03	6.06	259
Mast 09	2009	8.3	2.52	7.39	392
Mast H5*	2009	7.8	2.32	6.94	341

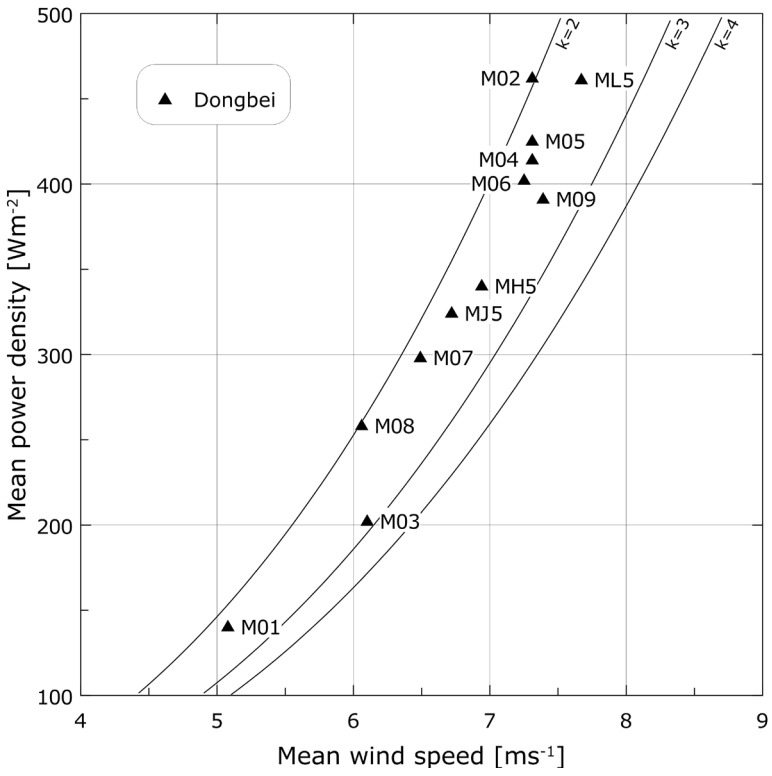

Figure 43. Summary of the generalised wind climates at 70 m a.g.l. over roughness class 1 (roughness length z_0 = 0.03 m) at the meteorological stations.

4 The Wind Atlas (WAsP) methodology

This chapter presents a brief survey of the physical and statistical models employed for the Atlas. A more thorough description of the different physical and statistical modelling tools, as well as the practical details related to data handling and the preparation of descriptions of anemometric conditions are given in the European Wind Atlas (Troen and Petersen, 1989). This volume also contains a general discussion of uncertainties and possible errors in the meteorological data and in the model.

4.1 The physical basis

As described in the introduction to this report, the Wind Atlas concept builds upon the use of a set of models for the correction of measured wind data and an analysis of the corrected data in terms of their frequency distributions. The integrated computer model used in the analysis is called the *Wind Atlas Analysis and Application Program* (WAsP). The sub-models are described briefly below – for more detailed information on the models and the WAsP-program, the reader is referred to the European Wind Atlas (Troen and Petersen, 1989) and the WAsP User's Guide (Mortensen *et al*. 2009), respectively.

4.1.1 Surface-layer similarity laws

The layer closest to the ground is called the atmospheric boundary layer. The layer extends up to about 100 m on clear nights with low wind speeds and up to more than 2 kilometres on a fine summer day. The lowest part of this layer is called the surface layer, which is sometimes defined as a fixed fraction; say 10% of the boundary layer depth. For the purpose of climatology relevant to wind power utilization, we can neglect the lowest wind speeds so only situations where the atmospheric boundary layer extends to approximately 1 km and surface-layer physics apply in the lowest 100 m of the layer are of concern.

At high wind speeds the wind profile over flat and reasonably homogeneous terrain is well modelled using the logarithmic law:

$$u(z) = \frac{u_*}{\kappa} \ln\left(\frac{z}{z_0}\right) \tag{3}$$

where $u(z)$ is the wind speed at height z above ground level, z_0 is the surface roughness length, κ is the von Kármán constant, taken here as 0.40, and u_* is the so-called friction velocity related to the surface stress τ through the definition:

$$|\tau| = \rho \cdot u_*^2 \tag{4}$$

where ρ is the air density. Even at moderate wind speeds, deviations from the logarithmic profile occur when z exceeds a few tens of metres. Deviations are caused by the effect of buoyancy forces in the turbulence dynamics; the surface roughness is no longer the only relevant surface characteristic but has to be supplemented by parameters describing the surface heat flux. With surface cooling at night-time, turbulence is lessened causing the wind profile to increase more rapidly with height; conversely, daytime heating causes increased turbulence and a wind profile more constant with height. Similarity expressions for these more general profiles are given by:

$$u(z) = \frac{u_*}{\kappa}\left(\ln\left(\frac{z}{z_0}\right) - \Psi\left(\frac{z}{L}\right)\right) \tag{5}$$

where Ψ is an empirical function (Businger, 1973; Dyer, 1974). The new parameter introduced in this expression is the so-called Monin-Obukhov length L:

$$L = -\frac{T_0}{\kappa g}\frac{\rho c_p u_*^3}{H_0} \tag{6}$$

where T_0 and H_0 are the surface absolute temperature and heat flux, respectively, c_p is the heat capacity of air at constant pressure, g the acceleration of gravity and the remaining quantities are defined above.

The stability modifications of the logarithmic wind profile are often neglected in connection with wind energy, the justification being the relative unimportance of the low wind speed range. The WAsP model treats stability modifications as small perturbations to a basic neutral state (Troen and Petersen, 1989). In order to take into account in an approximate manner the effects of varying the surface heat flux without the need for detailed modelling of each individual wind profile, a simplified procedure is adopted which only requires input in the form of the climatological average and root-mean-square of the surface heat flux.

4.1.2 The geostrophic drag law and the geostrophic wind

The winds in the atmospheric boundary layer can be considered to arise from pressure differences caused mainly by "synoptic" activity, i.e. the passing of high and low pressure systems. As the boundary layer structure has a rather rapid response to changes in pressure forcing, an approximate balance is found between the pressure gradient force and the frictional force at the surface of the earth. This balance can be theoretically derived under idealised conditions of stationarity, homogeneity and barotrophy (the pressure gradient being constant over the depth of the boundary layer). For conditions of neutral stability, the balance was already described by Rossby and Montgomery (1935). The result is usually expressed as a relation – called the geostrophic drag law – between the surface friction velocity u_* and the so-called geostrophic wind G:

$$G = \frac{u_*}{\kappa}\sqrt{\left(\ln\left(\frac{u_*}{fz_0}\right) - A\right)^2 + B^2} \tag{7}$$

$$\sin\alpha = -\frac{Bu_*}{\kappa G} \tag{8}$$

in which α is the angle between the near-surface winds and the geostrophic wind, f is the Coriolis parameter and A and B are empirical constants (here A = 1.8, B = 4.5). The geostrophic wind can be calculated from the surface pressure gradient and is often close to the wind speed observed by radiosondes above the boundary layer. The geostrophic drag law can be extended to conditions of non-neutral stability in which case the above constants A and B become functions of the stability parameter μ defined by:

$$\mu = \frac{\kappa u_*}{fL} \tag{9}$$

4.2 The roughness change model

The logarithmic wind profile applies only if the upwind terrain is reasonably homogeneous. If this is not the case, deviations will be observed and it is not possible to assign a unique roughness length to the terrain. Even though "effective"' roughness lengths can be assigned by different methods, these will depend on the height of observation. An exception to this is the effective roughness length implicitly defined by the geostrophic drag law.

The average surface stress and surface wind speed must depend on surface conditions only up to a certain upstream distance; distant obstacles are "forgotten"' by the tendency of the boundary layer to approach equilibrium between the pressure gradient force and friction. The distance scale involved is proportional to the Rossby radius G/f and is of the order of 10-100 km. For the wind frequency distribution it is assumed here that it is sufficient to consider surface conditions out to distances of the order of 10 km. From simple considerations pertaining to the surface layer, it is possible in the case of small-scale terrain inhomogeneities to model the change of surface stress which occurs when wind flows from a surface characterized by a roughness length z_{01} to another surface with a roughness of z_{02}. In this case an internal boundary layer (IBL) grows downwind from the roughness change; considering a point at a distance x downwind from the change, the IBL has grown to a height h given by (Panofsky, 1973):

$$\frac{h}{z_0'}\left(\ln\frac{h}{z_0'}-1\right)=\text{constant}\cdot\frac{x}{z_0'} \tag{10}$$

where $z_0' = \max(z_{01}, z_{02})$. Above h no change is felt whereas the wind profile has been perturbed in the layer below h. The value of the constant is here 0.9. It is empirically found that the change of surface friction velocity is well modelled using the following relation which can be derived from matching of neutral wind profiles at the height h:

$$\frac{u_{*2}}{u_{*1}}=\frac{\ln(h/z_{01})}{\ln(h/z_{02})} \tag{11}$$

where u_{*2} is the surface friction velocity at the point considered and u_{*1} the surface stress upwind from the change. The wind profile is perturbed in the IBL and the surface friction velocity cannot be calculated from observed wind speeds using the logarithmic profile. However, experimental evidence (Sempreviva *et al.*, 1990), as well as results from numerical models (Rao *et al.*, 1974), shows that the perturbed profile can be well modelled with three logarithmic parts:

$$u(z)=\begin{cases} u'\dfrac{\ln(z/z_{01})}{\ln(c_1h/z_{01})} & \text{for } z\ge c_1h \\ u''+(u'-u'')\dfrac{\ln(z/c_2h)}{\ln(c_1/c_2)} & \text{for } c_2h\le z\le c_1h \\ u''\dfrac{\ln(z/z_{02})}{\ln(c_2h/z_{02})} & \text{for } z\le c_2h \end{cases} \tag{12}$$

where $u'=(u_{*1}/\kappa)\ln(c_1h/z_{01})$, $u''=(u_{*2}/\kappa)\ln(c_2h/z_{02})$ and $c_1 = 0.3$, $c_2 = 0.09$.

From this equation and with the aid of Eq. (9) the surface friction velocity u_{*2} corresponding to a measured wind speed can be related to the friction velocity upstream of a change in surface roughness. For more roughness changes Eq. (9) can be applied in sequence, and thus a measured wind speed can be used for calculating the surface friction velocity far upstream. However, successive roughness changes must not occur too close to each other and therefore the following distance rule is applied. If x_n is the distance to the nth change in surface roughness, then the upstream roughness must be estimated as an average covering the area between the distance x_n and $2x_n$ in the azimuth sector considered. The factor 2 is somewhat arbitrary, and the rule may be deviated from in cases where clear roughness boundaries are found, e.g. at a coastline.

Moving further upstream, the roughness change model just described will give results deviating from reality because it does not incorporate the above-mentioned boundary layer approach to equilibrium. As was the case with stability corrections, the discrepancies are considered to be small perturbations and a simple model is constructed by considering the asymptotic behaviour. The far-upstream surface conditions must lose importance as x/D becomes large, where D is the chosen equilibrium distance (here taken to be 10 km) and also the above surface layer relations must apply for x much smaller than D. This behaviour is obtained by a simple weighting of the roughness changes by a factor W_n:

$$W_n = \exp\left(-\frac{x_n}{D}\right) \tag{13}$$

Instead of considering a change from z_{0n} to z_{0n+1} at distance x_n the value $\ln(z_{0n}) + W_n \ln(z_{0n+1}/ z_{0n})$ substitutes $\ln(z_{0n+1})$. By application of this weighting in sequence, a value of the surface friction velocity far upstream is obtained together with a value of the corresponding equilibrium surface roughness to which the geostrophic drag law applies.

4.3 The shelter model

The frictional effect of a land surface is caused by drag on surface-mounted obstacles ranging from individual sand grains, grass, leaves etc. to large trees and buildings. Their collective effect is modelled through the surface roughness length as described in the section above.

Close to an individual obstacle, at distances comparable to the height of the obstacle and at heights likewise comparable to the height of the obstacle, the wind profile is perturbed, particularly in the downstream wake, and the object must be treated separately. In the wake immediately behind a blunt object, such as a row of trees or a house (less than five object heights downstream and at heights less than twice the height of the object) the details of the object exert a critical influence on the effects. The wake behind a building depends for example on the detailed geometry of the roof and the incidence angle of the wind, to mention two parameters. In addition, wakes from other nearby objects may interfere, causing the problem to become very complicated.

The main reason for addressing the problem here is that some of the meteorological data sets used in previous studies come from meteorological stations at which the wind data are influenced by nearby obstacles. As far as the analyses of the four stations in the present study and the application of the Wind Atlas in siting are concerned, the problems are negligible.

The shelter model incorporated in WAsP should be seen as a tool for correcting data influenced by single obstacles that are sufficiently far away to make the perturbations small and to avoid the intricacies of the nearby wakes.

For simple two-dimensional semi-infinite obstacles such as long rows of trees, walls, or hedges, the expressions given by Perera (1981) obtained from wind-tunnel studies are used:

$$\frac{\Delta u}{u} = 9.8\left(\frac{z_a}{h}\right)^{0.14} \frac{x}{h}(1-p)\eta \exp(-0.67\eta^{1.5}) \tag{14}$$

where

$$\eta = \frac{z_a}{h}\left(\frac{0.32}{\ln(h/z_0)}\frac{x}{h}\right)^{-0.47} \tag{15}$$

and P is the porosity (open area/total area) of the obstacle, h is the height of the obstacle, z_a is the height considered (e.g. the anemometer height), and x is the downstream distance.

With finite obstacle lengths and skew incidence of the wind, the sheltering of an obstacle will in general be different. In the European Wind Atlas (Troen and Petersen, 1989) some simple guidelines are indicated; however, the model actually used in the analysis is slightly more refined.

For each of a number of radial lines or rays originating from the point considered, the distances to and heights of objects crossed by the ray are noted. If a single ray crosses several obstacles each of these crossings is initially treated as a single semi-infinite obstacle. Starting with the most distant one, the shelter on all downstream obstacles is calculated in sequence. If objects are so close to each other that their zones of separation join, the downstream sheltering is reduced by the relative area of the downstream obstacle which is embedded in the separation zone of the upstream obstacle. In this connection the separated zone upwind of a two-dimensional obstacle is considered to be limited by a straight line from the top of the obstacle down to the surface at a distance twice the height of the obstacle, and similarly downstream to a distance of five times the height.

Subsequent to this calculation of the shelter at the point considered from the sequence of objects, the sheltering for each ray is mixed with neighbouring values. This is done to model the actual mixing of momentum deficit at the edge of the wake. Finally, the average shelter is calculated over an azimuth sector by summing up the sheltering calculated on each ray in the azimuth sector. Here eight rays are used per 30° azimuth sector and an effective lateral spreading over an angle of 12°.

4.4 The orographic model

Like the change-of-roughness and shelter models, the orographic model is used to correct measured wind data for the effect of local terrain inhomogeneities; in the present case this means differences in terrain elevation around the meteorological stations. Emphasis is placed on the effects of terrain undulations with horizontal scales up to several tens of kilometres, and the model was especially developed to serve this purpose. It has strong similarities with the MS3DJH family of models based on the analysis of

flow over hills by Jackson and Hunt (1975). Readers who wish to become acquainted with these models should consult the papers by Walmsley *et al*. (1982), Troen and de Baas (1986). The model is different, however, in a number of respects, the most important being the high resolution and polar representation.

The first step in the model is the calculation of the potential flow perturbation induced by the terrain and corresponding to a unit wind vector in the undisturbed wind direction. This proceeds as follows: the velocity perturbation is related to the potential by:

$$\vec{u} = \nabla \chi \tag{16}$$

where χ is the potential and $\vec{u}$ the three-dimensional vector of velocity perturbations $\vec{u} = (u, v, w)$.

If vanishing potential is assumed at a given outer model radius R, a general solution to the potential flow problem in polar coordinates can be expressed as a sum in terms of the form:

$$\chi_j = K_{nj} J_n\left(c_j^n \frac{r}{R}\right) \exp(in\phi) \exp\left(-c_j^n \frac{z}{R}\right) \tag{17}$$

where K_{nj} are arbitrary coefficients, J_n the nth order Bessel function, r radius, ϕ azimuth, z height, and c_j^n are the ith zero of J_n. For a specific problem, the coefficients are determined by the boundary conditions, which are here the surface kinematic boundary condition:

$$w_0 = \frac{\partial}{\partial z} \chi\big|_{z=0} = \vec{u}_0 \cdot \nabla h(r, \phi) \tag{18}$$

where w_0 is the terrain-induced vertical velocity, $\vec{u}_0$ the basic state velocity vector and h the height of terrain. The functions $J_n\left(c_j^n \frac{r}{R}\right)$ form an orthogonal set of radial functions (Fourier-Bessel series) for each n, and the azimuth representation $\exp(in\phi)$ likewise forms an orthogonal set (Fourier series). The coefficients K_{nj} can therefore be calculated independently by projecting the right-hand side of Eq. (16) onto this basis of functions. The mathematical details of these transforms are described in Oberhettinger (1973).

The polar representation has important advantages over the more common Cartesian as used in the above-mentioned models, while maintaining the advantages of spectral decomposition. By defining the model centre to coincide with the point of interest, it is possible to concentrate the model resolution there and also to restrict the calculations to the perturbation at this point. For the centre point $r = 0$, the following solution is found:

$$\nabla \chi_j = \frac{1}{2}(1, i) K_{1_j} \frac{c_j^1}{R} \exp\left(-c_j^1 \frac{z}{R}\right) \tag{19}$$

The final result of the first step in the model is thus a series of coefficients k_{1_j} from which the solution of the potential flow perturbation is given as a sum of the terms stated

in Eq. (17). Each term has an associated horizontal scale $L_j = R/c_j^1$, which is also the characteristic depth to which the perturbation penetrates.

The second step in the model consists of a modification of the potential flow solution to accommodate in an approximate sense the effects of surface friction.

Potential flow implies a balance between the pressure gradient force and advection of momentum in the equations of momentum and vanishing turbulent momentum transfer. Near the surface the turbulent transfer cannot be neglected. The deviation from the potential flow behaviour is restricted to a layer whose depth is of the order ℓ_j with $\ell_j << L_j$. In the present model the value of ℓ_j is determined following Jensen *et al.* (1984) as:

$$\ell_j = 0.3 \cdot z_{0j} \left(\frac{L_j}{z_{0j}} \right)^{0.67} \tag{20}$$

where z_{0j} is the surface roughness length of the scale considered. For homogeneous conditions $z_{0j} = z_0$. For inhomogeneous sites the surface roughness length is taken as an exponentially weighted average from $r = 0$ to $r = 5\ L_j$ in the upwind direction (weighting $\ln(z_0)$).

For heights much smaller than ℓ_j, turbulent transfer forces a balance between stress and wind shear, leading to a logarithmic profile of the velocity perturbation. For heights comparable with ℓ_j maximum flow perturbation occurs, and this perturbation exceeds the value predicted from potential flow. In the present model the perturbation profile is modelled for each term in the above expansion by assigning a perturbation to the height z of magnitude Δu_j:

$$\frac{\Delta \vec{u}_j(z)}{|u_0(z)|} = \frac{|u_0(L_j)|^2}{|u_0(z_j')|^2} \nabla \chi_j \tag{21}$$

where $u_0(z)$ is the basic state velocity at height z and z_j' is equal to $\max(z, \ell_j)$.

The calculation of the coefficients k_{1_j} through the projection method involves numerical integrations over azimuth and radius. This is performed on a grid illustrated in Figure 44.

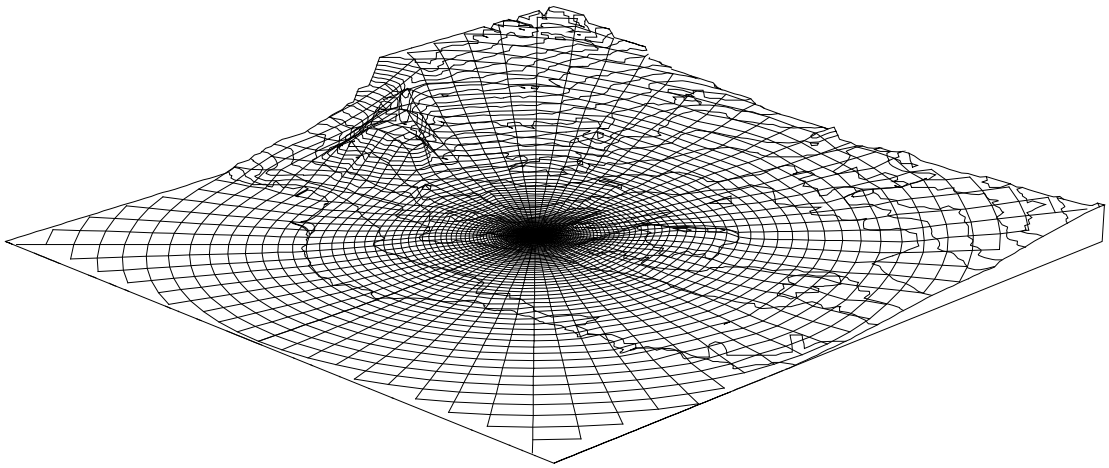

Figure 44. The polar zooming grid employed by the model for the calculation of flow in complex terrain. The grid is superimposed here on the terrain and centered on the meteorological station. The side length is 20 km.

The radial grid size is smallest at the centre and is increased by a constant factor (=1.06) outwards for each grid cell. In principle, the necessary input is the height of terrain at each grid point, but a much more convenient representation of the terrain height is the contour lines (lines of constant height) as given on standard topographical maps. The model was designed, therefore, to directly accept arbitrarily chosen contour lines as input and integrates the estimation of grid-point values and the numerical integrations in one process. The grid consists of 100 radial stations and the resulting resolution near the centre is approximately 2 m for a model with R = 10 km, and approximately 10 m for R = 50 km, etc. Therefore resolution is limited in practice only by the accuracy and density of the contour data from the topographical maps.

4.5 The statistical basis

The presentation of wind data makes use of the Weibull distribution (Weibull, 1951) as a tool to represent the frequency distribution of wind speed in a compact form. The two-parameter Weibull distribution is expressed mathematically as:

$$f(u) = \frac{k}{A}\left(\frac{u}{A}\right)^{k-1} \exp\left(-\left(\frac{u}{A}\right)^{k}\right) \qquad (22)$$

where $f(u)$ is the frequency of occurrence of wind speed u (as elsewhere in the Atlas the indication of mean value $\langle u \rangle$ is not shown explicitly). The two Weibull parameters thus defined are usually referred to as the scale parameter A and the shape parameter k. The influence on the shape of $f(u)$ for different values of the shape parameter is illustrated in Figure 45. For $k > 1$ the maximum (modal value) lies at values $u > 0$, while the function decreases monotonically for $0 < k \leq 1$.

The Weibull distribution can degenerate into two special distributions, namely for $k = 1$ the exponential distribution and for $k = 2$ the Rayleigh distribution. Since observed wind data, especially in the Westerlies, exhibit frequency distributions which are often well described by the Rayleigh distribution, this one-parameter distribution is sometimes used to represent wind data; here, however, the more general two-parameter Weibull distribution is used throughout. Inspection of the k-parameter for individual stations in

the Atlas shows that the values cover the range from two to four; the two-parameter distribution will therefore provide much better fits to the data than the Rayleigh distribution.

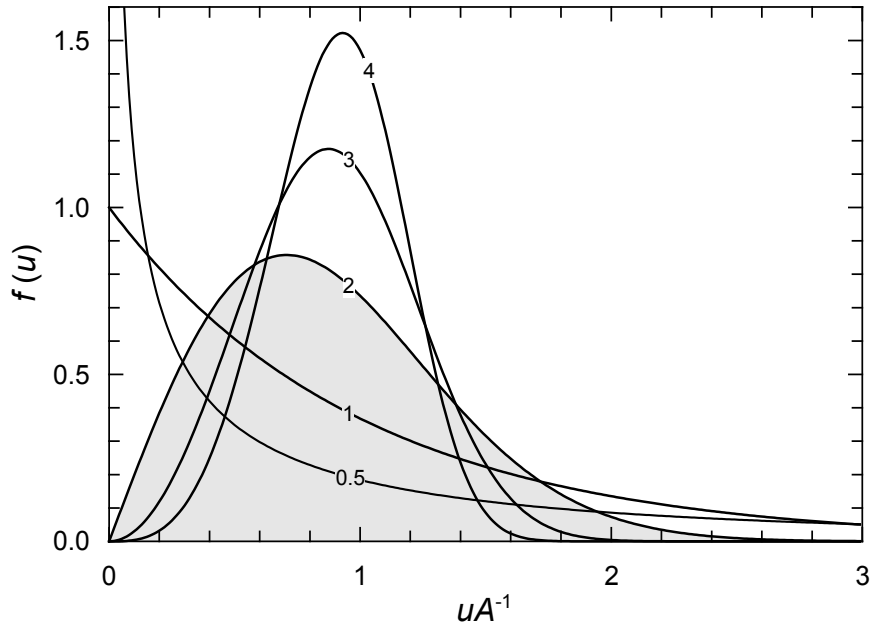

Figure 45. The shape of the Weibull distribution function for different values of the shape parameter: k = 0.5, 1, 2, 3, 4.

The cumulative Weibull distribution $F(u)$ gives the probability of the wind speed exceeding the value u and is given by the simple expression:

$$F(u) = \exp\left(-\left(\frac{u}{A}\right)^k\right) \tag{23}$$

The Weibull distribution generates Weibull-distributed higher powers: if u is Weibull-distributed with parameters A and k, then u^m is Weibull-distributed with the parameters A^m and k/m.

Moments and other important characteristics of Weibull distributions are easy to derive; a list of the more common characteristics is given here for reference:

$$\begin{aligned}
&\text{mean value}: A\Gamma(1+1/k)\\
&\text{mean square}: A^2\Gamma(1+2/k)\\
&\text{mean cube}: A^3\Gamma(1+3/k)\\
&\text{mean } m\text{th power}: A^m\Gamma(1+m/k)\\
&\text{variance}: A^2\left[\Gamma(1+2/k)-\Gamma^2(1+1/k)\right]\\
&\text{modal value}: A\left(\frac{k-1}{k}\right)^{1/k}\\
&\text{median}: A(\ln 2)^{1/k}
\end{aligned} \tag{24}$$

where $\Gamma(x)$ is the gamma function. The available wind power density is proportional to the mean cube of the wind speed:

$$E = \frac{1}{2}\rho A^3 \Gamma\left(1+\frac{3}{k}\right) \tag{25}$$

where E is power density (Wm^{-2}), ρ is air density (1.225 kg m^{-3} for a temperature of 15°C and a standard pressure of 1013.25 hPa).

The wind speeds at which the highest power density is available is given by:

$$u_m = A\left(\frac{k+2}{k}\right)^{1/k} \tag{26}$$

Thus, for a Rayleigh distribution, the wind speed which contains the highest energy on the average is twice the most frequent speed (modal value).

Many different methods can be used for the fitting of the two Weibull parameters to a histogram giving the frequency of occurrence of wind speed in a number of intervals (bins). If the observed data are well represented by the Weibull distribution over the whole range of speeds, then the fitting procedure can be chosen at will. In general, however, observed histograms will show deviations due to a number of causes, and a fitting procedure must be selected which focuses on the wind speed range relevant to the application. Here the emphasis is on the higher wind speeds and a moment fitting method is used which focuses on the higher but not the extreme wind speeds.

For each azimuthal sector, the two Weibull parameters are determined by the requirements that: 1) the total wind power in the fitted Weibull distribution and the observed distribution are equal, and 2) the frequencies of occurrence of wind speeds higher than the observed average speed are the same for both distributions. The combination of these two requirements leads to an equation in k only, which is solved by a standard root-finding algorithm.

Most difficulties in fitting to observed data are related to the treatment of very low and very high wind speeds. The highest wind speeds, say the uppermost percentile of observations, are statistically very uncertain and special methods (i.e. Gumbel, 1958) must be employed in extreme wind analysis. This analysis is not included in the WAsP program, and the Weibull distributions given here should not be used for the estimation of frequencies of occurrence much below 0.01.

At low wind speeds, limitations in instrument response, reporting practices and data truncation can in general lead to substantial errors in the frequency of occurrence. Sometimes such errors give rise to an abnormally high frequency of recorded calms. For wind power applications, the precise form of the frequency curve for wind speeds lower than the average is of little concern and the present fitting method is designed with this in mind. It should be noted, however, that for meteorological stations with mean speeds of ~3 ms^{-1} or lower, located in a reasonably windy climate, but locally heavily sheltered, the calculated regional wind climate from such stations becomes inaccurate because of these difficulties. In addition, the physical models used in the analysis are deficient at low wind speeds. Fortunately, none of the stations reported in the present atlas are of this type.

The fitting method described above is used to estimate the Weibull parameters for each of the observed azimuth sectors and for the sector-wise fitting of model-derived (or transformed) frequency distributions. The parameters pertaining to the associated total or

azimuth-independent wind distributions are obtained from the sector-wise distributions fitting to the sums of the first and third moments.

4.6 The Wind Atlas analysis model

The model is composed of the submodels described in the preceding sections. By means of measured wind data, descriptions of local terrain roughness, sheltering obstacles and topographical height data, a regional wind climatology is calculated in the form of Weibull parameters pertaining to standard conditions. For each of the meteorological stations used in the Atlas, the input to the model is summarized on the three first pages and the model output is given on the last page in the station statistics in Chapter 7. A schematic representation of the analysis model is shown in Figure 46.

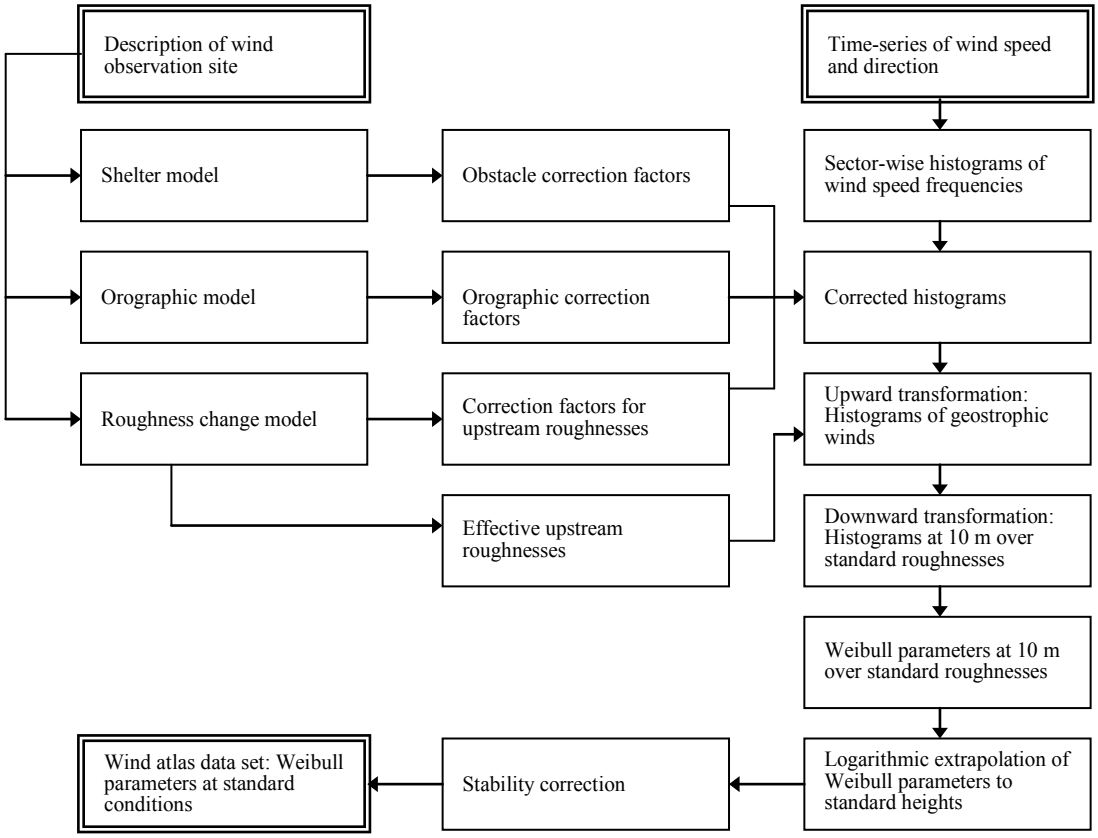

Figure 46. A schematic representation of the Wind Atlas analysis model.

The calculation procedure can be summarized as follows: input data are in the form of histograms for each of 12 azimuth sectors, giving the frequency of occurrence of wind speeds in bins of 1 ms^{-1} width.

First, wind speed-independent correction factors are calculated for each azimuth sector. Three sets of factors are considered:

- The obstacle correction factors, calculated using the shelter model, here denoted C^j_{obs} for the *j*th azimuth sector.
- The roughness change factors C^j_{rou} .The roughness change model relates the velocity at the station to the velocity upstream of the specified roughness

changes. In addition, the area weighting of surface roughness gives an effective upstream surface roughness z_{0e}^{j}.

- The orography correction factors, calculated by application of the orographic model. The model is applied using as input a wind profile with direction in the centre of each sector. As described in Section 4.4 the actual surface roughnesses are taken into account as parameters in the orographic model. From this C_{oro}^{j} and D_{oro}^{j} are obtained, where D_{oro}^{j} is degrees of turning of the wind vector calculated by the orographic model.

Secondly, each combined azimuth and wind-speed bin is transformed using these factors. Considering the *j*th sector and the wind-speed bin from $u^{(k)}$ to $u^{(k+1)}$, application of the obstacle correction factor C_{obs}^{j} gives the corresponding values which would pertain if the obstacles were removed. Similarly, the orographic corrections and the roughness change corrections are applied to transform the bin boundaries to values for upstream conditions. For the turning of the azimuthal boundaries, the orographic turning angles are applied using the average of the two values nearest the boundary considered.

The effective surface roughness z_0^j is used with each of the new bin boundaries in the geostrophic drag law, Eq. (5), to calculate the corresponding boundaries $G^{k,j}$ and $G^{k+1,j}$ with associated directions D_{low}^{kj} and D_{high}^{kj} from the low and high side of the original azimuth bin. In this transformation process the frequency of occurrence in the bin is conserved. The geostrophic wind could be used as a means of representation of the regional climatology, but the transformation process is instead continued to obtain the wind distributions over the standard values of surface roughness. Again using the geostrophic drag law, u_*-values for the standard surface roughness are obtained from the above $G^{k,j}$, $G^{k+1,j}$ and wind directions from the D-values above. From the logarithmic profile (Eq. 1) the corresponding values for the wind speeds at the lowest standard level (10 m) are obtained. At this stage the contributions to each of the "standard" azimuth (30°) and speed (1 ms^{-1}) bins are calculated.

This procedure is repeated for each azimuth/speed bin in the input data and the result is four sets of histograms of the same form as the input histograms, but pertaining to the lowest standard level of 10 metres and to each of the four roughness classes. For each azimuth sector, the corresponding frequency of occurrence is extracted and the Weibull parameters are determined using the fitting procedure described in Section 4.5. The Weibull parameters corresponding to the higher standard levels z_n are then calculated as described in Section 4.1, using a modification of the logarithmic profile which takes into account the effects of the variation of surface heat flux. The average and root-mean-square heat fluxes are specified independently for over-land and over-sea conditions. The following standard values from the European Wind Atlas (Troen and Petersen, 1989) are adopted for all the analysed stations:

Average heat flux over land	-40 Wm^{-2}
Average heat flux over sea	15 Wm^{-2}
Root-mean-square heat flux over land	100 Wm^{-2}
Root-mean-square heat flux over sea	30 Wm^{-2}

The European Wind Atlas (Troen and Petersen, 1989) further gives factors of "contamination" by the stability effects on mean values and standard deviations, respectively. These expressions are evaluated for contamination in the input data using the anemometer height, distance to the coast, and upstream equilibrium surface roughness in each azimuth sector. Similarly, the contamination is calculated for the different standard heights, and the ratios of these values to those on input are used to correct the Weibull parameters calculated using a logarithmic profile. The corresponding means and standard deviations are calculated using the expressions given in Eq. (22), the corrections are applied, and an inverse calculation is performed to determine the Weibull parameters corresponding to corrected values for means and variances. In this calculation, roughness class 0 refers to conditions over water and the three other roughness classes are corrected to conditions well inland beyond any coastal influence.

4.7 The Wind Atlas application model

For the construction of the Atlas itself, the analysis model described in the preceding section is complete. Equally important, however, is the model built to enable an inverse calculation of site-specific wind speed distributions from the regional climatology. The model is shown schematically in Figure 47. Such a model can be used to check the calculated regional statistics and can also be offered as a siting tool to the Wind Atlas user.

The model incorporated in WAsP is designed to be as close as possible to the inverse of the analysis model. The correction factors for local shelter, orography, and roughness changes are calculated exactly as in the analysis model, now of course using the obstacle list, roughness description, and orographic data pertaining to the site where the Atlas data are to be applied.

For the height considered, the Wind Atlas table is referenced and the appropriate Weibull parameters A_j and k_j for each azimuth sector are extracted in addition to the sector frequency f_j. For heights different from the standard heights and for surface roughnesses different from the standard values, a logarithmic interpolation is used. The surface roughness values used for each sector are the values calculated in the roughness change model z_{0e} (Section 4.2). The correction factors are applied to the A-parameter for each sector while keeping the k-parameter values at the table values. Finally, the stability correction is performed in the manner described above.

For a given height above the terrain and from a specification of terrain roughnesses, sheltering obstacles, and orographic details, the model therefore calculates values for the sector-wise Weibull parameters, and sector frequencies for a chosen regional climatology. Internal consistency is checked by calculating the station climatology using the regional climatology derived from the same station via the analysis model.

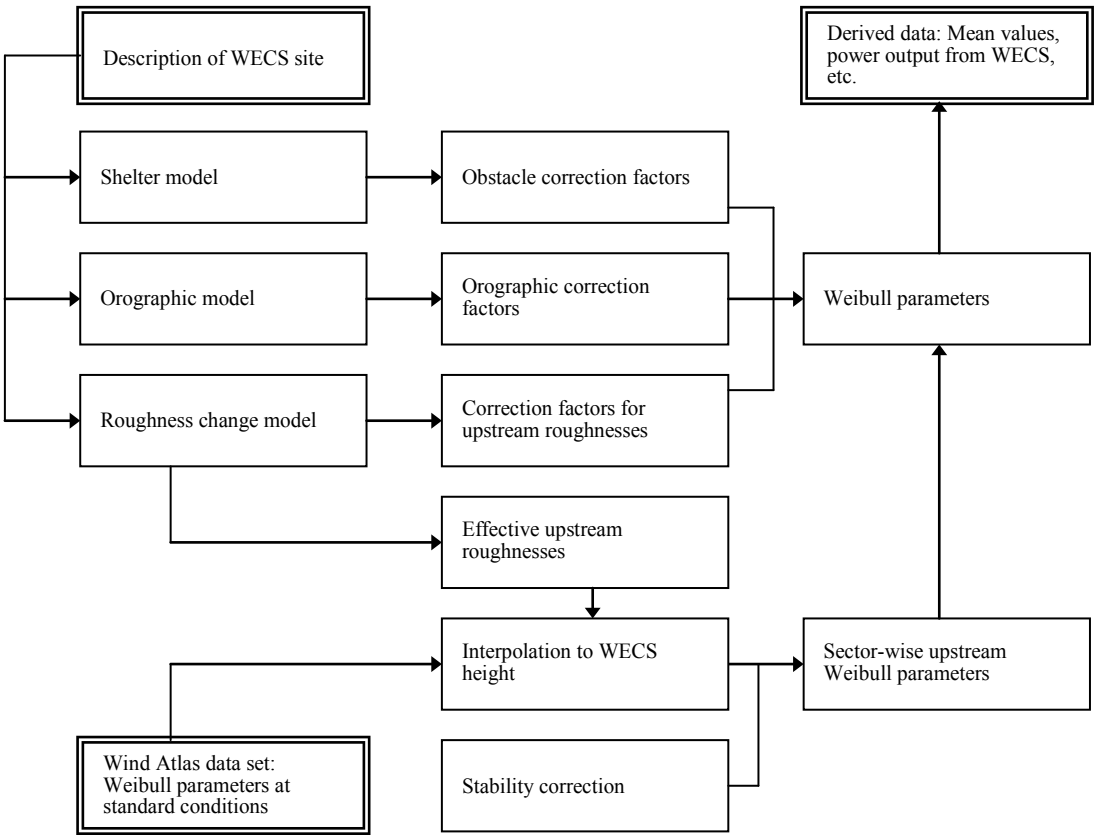

Figure 47. A schematic representation of the Wind Atlas application model.

5 Concluding remarks

With this report, an observational wind atlas for Dongbei has been established, based on the data and analyses from 12 meteorological masts in Liaoning, Jilin and Heilongjiang. The main results of the wind atlas analysis are reported in Chapter 3, but much more data and information are available in the Climate Analyst projects and WAsP workspaces that accompany this report. Based on this work, it will be relatively effortless to update the observational wind atlas if and when more data becomes available. It should be borne in mind that the present atlas is based on one year only and that long-term data from near-by meteorological stations are not included here.

The generalised wind climates determined in the wind atlas analysis can be used for verification of the mesoscale modelling close to the met. station sites; this verification is described by Badger *et al*. (2010).

The observed wind climates established during the wind atlas analysis can be used for verification of the microscale modelling, in particular how well the vertical wind profile can be modelled from 0-70 metres above the terrain. The main results of this comparison are shown in Chapter 3. The verification also includes study of modelling sensitivities and uncertainties, and possible adaptations of the methodology and models to Dongbei.

The general impression is that WAsP works well in Dongbei – within its operational envelope. The default modelling parameters work well for most sites, but it is found that the modelling can be improved by changing the standard wind atlas heights to reflect the

project-specific heights, i.e. anemometer and prediction heights. Hilly (M08) and very steep (M03) sites with forest are less well modelled; this is not surprising and is the case in many parts of the world. Ongoing research at Risø DTU addresses exactly these two issues: steep terrain and sites close to forestry.

The wind profile analysis suggests that the modelling of the vertical wind profile can be improved slightly by adjusting the heat flux settings in WAsP. It has not been possible to develop an objective way of selecting the proper heat flux values for any given site, but it is demonstrated that this parameter can be used to tweak the modelled wind profile to better fit the wind profile observed. Evidently, this requires accurate and reliable wind profile measurements at the site.

The measured mean wind profiles at sites in Liaoning seem to be slightly more unstable than the wind profiles modelled with the default stability settings in WAsP. The mean absolute deviation between measured and default modelled wind profiles is 1% at M02 and ML5, which cannot be readily improved. However, at mast M01 the mean absolute deviation can be decreased from 3% to 1% by selecting a slightly more unstable wind profile.

The measured mean wind profiles at sites in Jilin seem to be slightly more stable than the wind profiles modelled with the default stability settings in WAsP. At mast M05 and MJ5 the mean absolute deviation can be decreased from 2% to 1% by selecting a somewhat more stable wind profile in WAsP. At M04 and M06 the deviations can be decreased from 3% to 1% and from 6% to 2%, respectively, by selecting significantly more stable profiles in WAsP. These heat flux values are not realistic and are used here to simply demonstrate the effect on the modelled wind profiles.

The measured mean wind profiles at sites in Heilongjiang also seem to be slightly more stable than the wind profiles modelled with the default stability settings in WAsP. The mean absolute deviations at M08 and MH5 cannot be readily improved, but at M07 and M09 the deviations can be decreased from 5% to 2% and from 4% to 1%, respectively, by selecting significantly more stable profiles in WAsP. Again, these heat flux values are not realistic and are used here to simply demonstrate the effect on the modelled wind profiles.

The sensitivity of the WAsP modelling to 11 different input parameters was investigated in Chapter 2 and it was found that the modelling is rather robust to changes in input data and parameters, when using the 70-m level anemometer as predictor. Site-specific air density (and power curve) and calibrated anemometers are confirmed to be prerequisites for reliable wind power predictions; and project-specific wind atlas heights seem to decrease the modelling uncertainty.

Based on the work reported here, it is strongly recommended to follow the general *WAsP Best Practices* closely when applying WAsP in Dongbei and elsewhere; the current version of these is given in the Appendix. One significant improvement to the current measurement setup at the 12 sites would be the use of a top-mounted anemometer in order to minimise mast flow distortion. The use of two instrumentations at each level with boom-mounted anemometers can also be used to minimise the mast effects on the observed wind climate as was shown in Section 2.7.5, but this requires careful design of the mounting hardware and very high data recovery rates from the two anemometers.

6 Acknowledgements

The support of staff members from China Meteorological Administration (CMA) in Beijing and the Provincial Meteorological Administrations of Heilongjiang, Jilin and Liaoning is gratefully acknowledged.

At Risø DTU, we would like to thank Ib Troen and Erik L. Petersen for permission to publish excerpts from the European Wind Atlas.

The Danish contribution to "Mesoscale and Microscale Modelling in China" is funded by the Danish Ministry of Foreign Affairs (Danida) through the Sino-Danish Wind Energy Development Programme (WED).

7 References

Badger, J., N.G. Mortensen and J.C. Hansen (2006). The KAMM/WAsP Numerical Wind Atlas – A powerful ingredient for wind energy planning. In: Proceedings CD-ROM. *Great Wall World Renewable Energy Forum and Exhibition*, Beijing, 23-27 October 2006.

Badger, J., X.G. Larsén, A. Hahmann, R. Zhu, C. Yuan (2010). Mesoscale modelling in China: Risø DTU numerical wind atlas calculation for NE China (Dongbei). Risø-I-3070(EN). 68 pp.

Businger, J. (1973). Turbulent transfer in the atmospheric surface layer. In: Workshop on Micrometeorology. Ed. by D.A. Haugen. American Meteor. Soc., Boston, Mass. 67-100.

Dyer, A.J. (1974). A review of flux-profile relationships. Boundary-Layer Meteorol. 7, 363-372.

Frank, H.P., O. Rathmann, N.G. Mortensen and L. Landberg (2001). The numerical wind atlas – the KAMM/WAsP method. Risø-R-1252(EN). 60 pp.

Gumbel, E. J. (1958). Statistics of extremes. Columbia University Press, New York. 375 pp.

Hansen, J.C., N.G. Mortensen, J. Badger, N.-E. Clausen and P. Hummelshøj (2007). Opportunities for wind resource assessment using both numerical and observational wind atlases – modelling, verification and application. In Proceedings of *Wind Power Shanghai* 2007, Shanghai (CN), 1-3 Nov 2007. (Chinese Renewable Energy Industry Association, Shanghai, 2007) p. 320-330.

Hansen, J.C., N.G. Mortensen, J. Badger and O. Rathmann (2010). Meso- and Micro-scale Modelling in China: Application of Wind Atlas. Risø-I-3073(EN). 58 pp.

Jackson, P.S. and J.C.R. Hunt (1975). Turbulent wind flow over a low hill. Quart. J. Roy. Meteor. Soc. 101, 929-955.

Jensen, N.O, E.L. Petersen and I. Troen (1984). Extrapolation of mean wind statistics with special regard to wind energy applications. World Meteorological Organization, WCP-86. 85 pp.

Lindelöw-Marsden, P. and Enevoldsen, K. (2010). Meso- and Micro-scale Modelling in China: Wind measurements at 12 meteorological stations in NE China (Dongbei). Risø-I-3071(EN). 65 pp.

Mortensen, N.G., D.N. Heathfield, O. Rathmann and Morten Nielsen (2009). Wind Atlas Analysis and Application Program: WAsP 10 Help Facility. Risø National Laboratory for Sustainable Energy, Technical University of Denmark, Roskilde, Denmark. 356 topics.

Mortensen, N.G., J.C. Hansen, Z. Yang and Y. Luo (2008). Mesoscale and microscale modeling in NE China. In Proceedings of Global Wind Power 2008, Beijing (CN), 29-31 Oct 2008.

Mortensen, N.G., J.C. Hansen, Z. Yang, H. Yu, J. Xie and G. Yuan (2010). Meso- and Micro-scale Modelling in China: Site inspection trip to NE China (Dongbei). Risø-I-2900(EN). 61 pp.

Oberhettinger, F. (1973). Fourier expansions. A collection of formulas. Academic Press, New York and London. 64 pp.

Panofsky, H.A. (1973). Tower micrometeorology. In: Workshop on micrometeorology. Ed. D.A. Haugen, American Meteorological Society, Boston, Mass., 151-176.

Perera, M.D. (1981). Shelter behind two-dimensional solid and porous fences. J. Wind Engin. and Industrial Aerodyn. 8, 93-104.

Rao, K.S., J.C. Wyngaard and D.R. Coté (1974). The structure of the two-dimensional internal boundary layer over a sudden change of surface roughness. J. Atmos. Sci. 26, 432-440.

Rossby C.-G. and R.B. Montgomery (1935). The layer of frictional influence in wind and ocean currents. Papers in Phys. Oceanogr. Meteor., MIT and Woods Hole Oceanogr. Inst., III no. 3. 101 pp.

Sempreviva, A.M., S.E. Larsen, N.G. Mortensen and I. Troen (1990). Response of neutral boundary layers to changes of roughness. Boundary-Layer Meteorology 50: 205-225.

Troen, I. and A.F. de Baas (1986). A spectral diagnostic model for wind flow simulation in complex terrain. Proceedings of the European Wind Energy Association Conference and Exhibition, Rome, October 7-9, 1986, 243-249.

Troen, I. and E.L. Petersen (1989). European Wind Atlas. Risø National Laboratory, Roskilde. 656 pp. ISBN 87-550-1482-8.

Walmsley, J.L., J.R. Salmon and P.A. Taylor (1982). On the application of a model of boundary-layer flow over low hills to real terrain. Boundary-Layer Meteorol. 23, 17-46.

Weibull, W. (1951). A statistical distribution function of wide applicability. J. Appl. Mech. 18, 293-297.

Appendices

Availability of wind measurements

Figure 48 shows the status of the meteorological measurements conducted with Risø DTU equipment at the time of writing.

CMA Component of WED: Status of Risø DTU measurements and data by 2010-06-15.

Station	Installed	Position	Data start	Data end	Raw data	CA project	Team site	In operation	Risø Rodeo	CMA
Liaoning							availability	% of 2009	database	database
Mast 01	Yes	Verified	2008-10-07	2010-01-31	Team site	Revision 1	481 d	100%	Yes	
Mast 02	Yes	Verified	2008-08-29	2010-02-10	Team site	Revision 1	541 d	100%	Yes	
Mast 03	Yes	Verified	2008-09-25	2010-01-31	Team site	Revision 1	491 d	100%	Yes	
Mast 10	No	Verified	n/a	n/a	n/a	n/a	n/a	n/a	n/a	n/a
Mast L5	n/a	Verified	n/a	n/a	n/a	n/a	n/a	n/a	n/a	n/a
Jilin										
Mast 04	Yes	Verified	2008-10-14	2010-03-24	Team site	Revision 1	526 d	100%	Yes	
Mast 05	Yes	Verified	2008-10-15	2010-03-25	Team site	Revision 1	526 d	100%	Yes	
Mast 06	Yes	Verified	2009-06-10	2010-03-26	Team site	Revision 1	289 d	56%	Yes	
Mast 11	No	Verified	n/a	n/a	n/a	n/a	n/a	n/a	n/a	n/a
Mast J5	n/a	Verified	n/a	n/a	n/a	n/a	n/a	n/a	n/a	n/a
Heilongjiang										
Mast 07	Yes	Verified	2008-09-04	2010-01-31	Team site	Revision 1	515 d	100%	Yes	
Mast 08	Yes	Verified	2008-10-12	2010-01-31	Team site	Revision 1	476 d	100%	Yes	
Mast 09	Yes	Verified	2008-10-10	2010-01-31	Team site	Revision 1	479 d	100%	Yes	
Mast 12	No	Verified	n/a	n/a	n/a	n/a	n/a	n/a	n/a	n/a
Mast H5	n/a	Preliminary	n/a	n/a	n/a	n/a	n/a	n/a	n/a	n/a
Total								**95%**		

Figure 48. Status of Risø DTU measurements as of 15 June 2010. The "% of 2009" column shows the potential availability of data rather than the actual data recovery rate.

Figure 49 shows the status of the meteorological measurements conducted with CMA equipment at the time of writing.

CMA Component of WED: Status of CMA measurements and data by 2010-06-15.

Station	Installed	Position	Data start	Data end	Raw data	CA project	Team site	In operation	Risø Rodeo	CMA
Liaoning							availability	% of 2009	database	database
Mast 01	Yes	Verified					0 d	0%		
Mast 02	Yes	Verified	2008-10-16	2009-11-10	Team site	Revision 1	390 d	63%	In progress	
Mast 03	Yes	Verified	2008-11-08	2009-10-16	Team site	Revision 1	342 d	74%	In progress	
Mast 10	Yes	Verified	n/a	n/a	n/a	n/a	n/a	n/a	n/a	n/a
Mast L5	Yes	Verified	2008-11-12	2009-12-31	Team site	Final draft	414 d	100%	In progress	
Jilin										
Mast 04	Yes	Verified	2008-10-14	2010-03-24	Team site	Revision 1	526 d	100%	In progress	
Mast 05	Yes	Verified	2008-10-15	2009-06-23	Team site	Revision 1	251 d	48%	In progress	
Mast 06	Yes	Verified	2008-10-11	2010-03-26	Team site	Revision 1	531 d	100%	In progress	
Mast 11	Yes	Verified	n/a	n/a	n/a	n/a	n/a	n/a	n/a	n/a
Mast J5	Yes	Verified	2008-10-10	2010-03-25	Team site	Revision 1	512 d	100%	In progress	
Heilongjiang										
Mast 07	Yes	Verified	2008-10-15	2009-11-04	Team site	Revision 1	385 d	84%	In progress	
Mast 08	Yes	Verified	2008-10-12	2009-11-06	Team site	Revision 1	390 d	85%	In progress	
Mast 09	Yes	Verified	2008-10-09	2009-07-13	Team site	Revision 1	277 d	53%	In progress	
Mast 12	Yes	Verified	n/a	n/a	n/a	n/a	n/a	n/a	n/a	n/a
Mast H5	Yes	Preliminary	2008-10-14	2009-11-03	Team site	Revision 1	385 d	84%	In progress	
Total								**74%**		

Figure 49. Status of CMA measurements as of 15 June 2010. The "% of 2009" column shows the potential availability of data rather than the actual data recovery rate.

Liaoning observed wind climates

Table 11. Summary of wind observations for the year 2009 at the meteorological stations in the province of Liaoning: height of anemometer (h), data recovery rate (R), Weibull A- and k-parameters, Weibull-derived mean wind speed (U) and mean power density (E). Mast L5 features CMA instrumentation only.

	h	***R***	***A***	***k***	***U***	***E***
Mast ID	[m]	[%]	[ms^{-1}]		[ms^{-1}]	[Wm^{-2}]
Mast 01	70	100.0	5.9	2.10	5.22	156
	50	100.0	5.7	2.05	4.98	144
	30	100.0	5.3	1.97	4.67	122
	10	100.0	4.2	1.69	3.84	77
Mast 02	70	100.0	8.8	1.96	7.78	566
	50	100.0	8.2	2.00	7.24	445
	30	100.0	7.6	1.72	6.89	430
	10	100.0	6.2	1.51	5.73	281
Mast 03	70	91.1	8.3	2.11	7.49	406
	50	91.7	7.9	2.22	7.08	359
	30	97.3	7.6	2.22	6.81	321
	10	92.2	3.8	1.61	3.57	61
Mast L5	70	100.0	8.3	2.18	7.42	426
	50	100.0	7.8	2.11	7.01	372
	30	100.0	7.2	2.01	6.43	299
	10	100.0	5.8	1.87	5.21	168

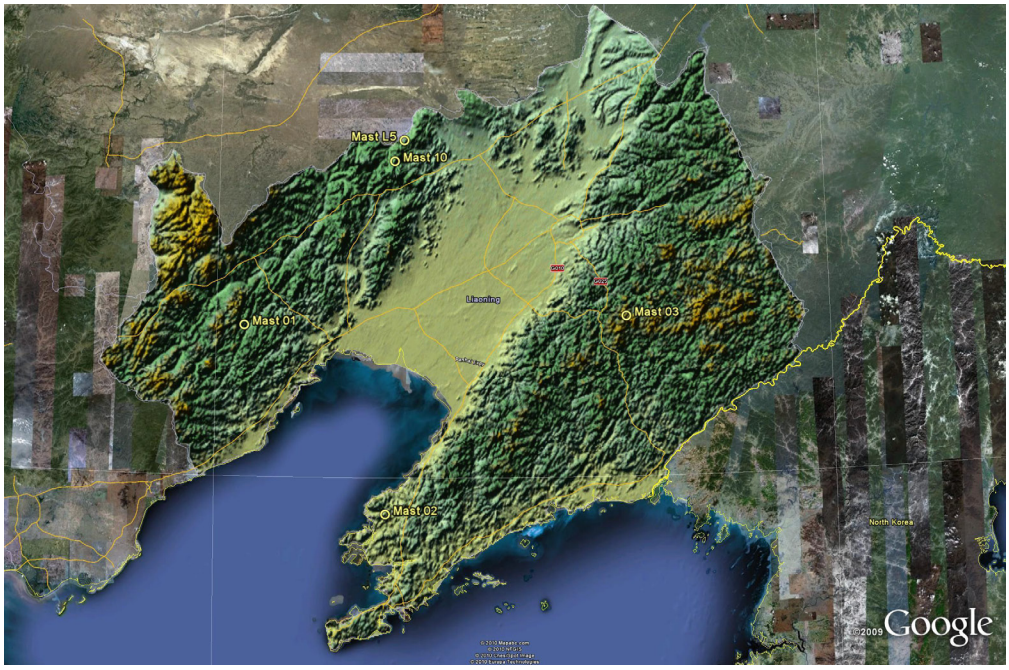

Jilin observed wind climates

Table 12. Summary of wind observations for the year 2009 at the meteorological stations in the province of Jilin: height of anemometer (h), data recovery rate (R), Weibull A- and k-parameters, Weibull-derived mean wind speed (U) and mean power density (E). Mast J5 features CMA instrumentation only. M06 combines Risø DTU and CMA wind measurements in order to get one full year of data.

	h	***R***	***A***	***k***	***U***	***E***
Mast ID	[m]	[%]	[ms^{-1}]		[ms^{-1}]	[Wm^{-2}]
Mast 04	70	100.0	8.0	2.22	7.07	376
	50	100.0	7.3	2.13	6.51	299
	30	100.0	6.3	1.91	5.62	215
	10	100.0	4.8	1.61	4.33	121
Mast 05	70	100.0	7.9	2.18	7.03	378
	50	100.0	7.2	2.07	6.39	299
	30	100.0	6.3	1.84	5.63	228
	10	100.0	5.1	1.54	4.60	152
Mast 06	70	100.0	7.5	2.17	6.69	323
	50	100.0	6.6	1.99	5.86	232
	30	100.0	5.8	1.70	5.21	195
	10	100.0	4.4	1.46	4.04	110
Mast J5	70	53.9	—	—	—	—
	50	53.9	—	—	—	—
	30	100.0	5.8	1.88	5.18	176
	10	100.0	4.9	1.66	4.44	123

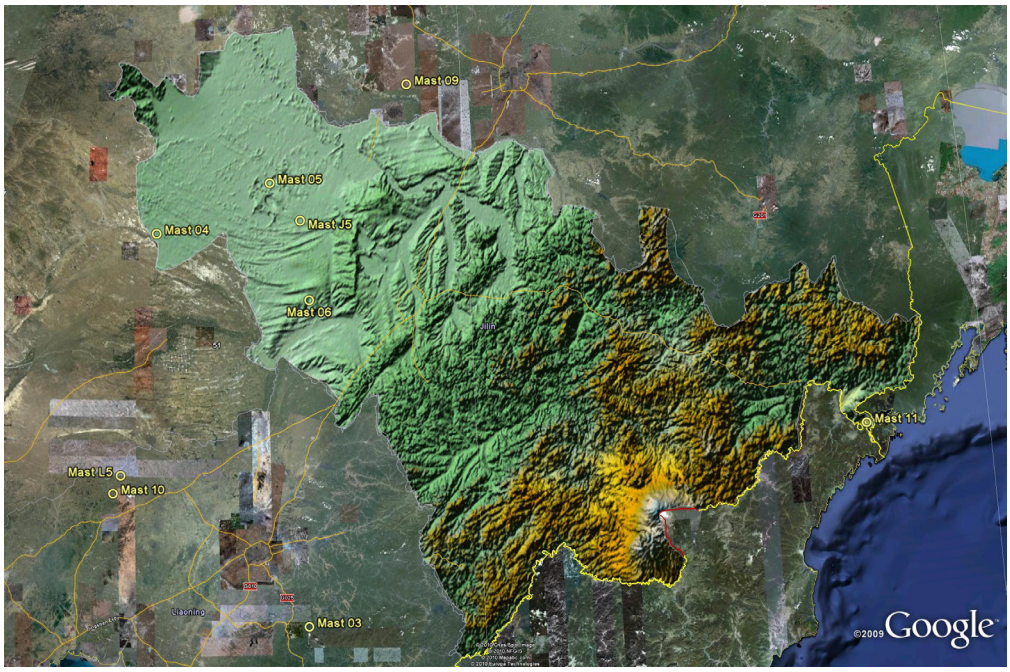

Heilongjiang observed wind climates

Table 13. Summary of wind observations for the year 2009 at the meteorological stations in the province of Heilongjiang: height of anemometer (h), data recovery rate (R), Weibull A- and k-parameters, Weibull-derived mean wind speed (U) and mean power density (E). Mast H5 features CMA instrumentation only and data are given for the one-year period from 2008-11-01 to 2009-11-01.

	h	***R***	***A***	***k***	***U***	***E***
Mast ID	[m]	[%]	[ms^{-1}]		[ms^{-1}]	[Wm^{-2}]
Mast 07	70	100.0	7.5	2.30	6.66	319
	50	100.0	6.9	2.24	6.05	237
	30	100.0	5.8	1.96	5.18	165
	10	100.0	4.4	1.62	4.02	93
Mast 08	70	100.0	5.2	1.99	4.65	120
	50	100.0	4.5	1.89	4.01	80
	30	100.0	3.5	1.78	3.17	41
	10	100.0	2.1	1.55	1.89	10
Mast 09	70	100.0	7.3	2.49	6.48	268
	50	100.0	6.5	2.30	5.74	196
	30	100.0	5.6	1.95	4.98	147
	10	100.0	4.1	1.59	3.71	78
Mast H5	70	100.0	7.7	2.23	6.81	344
	50	100.0	7.4	2.19	6.55	307
	30	100.0	6.9	1.97	6.08	271
	10	85.0	—	—	—	—

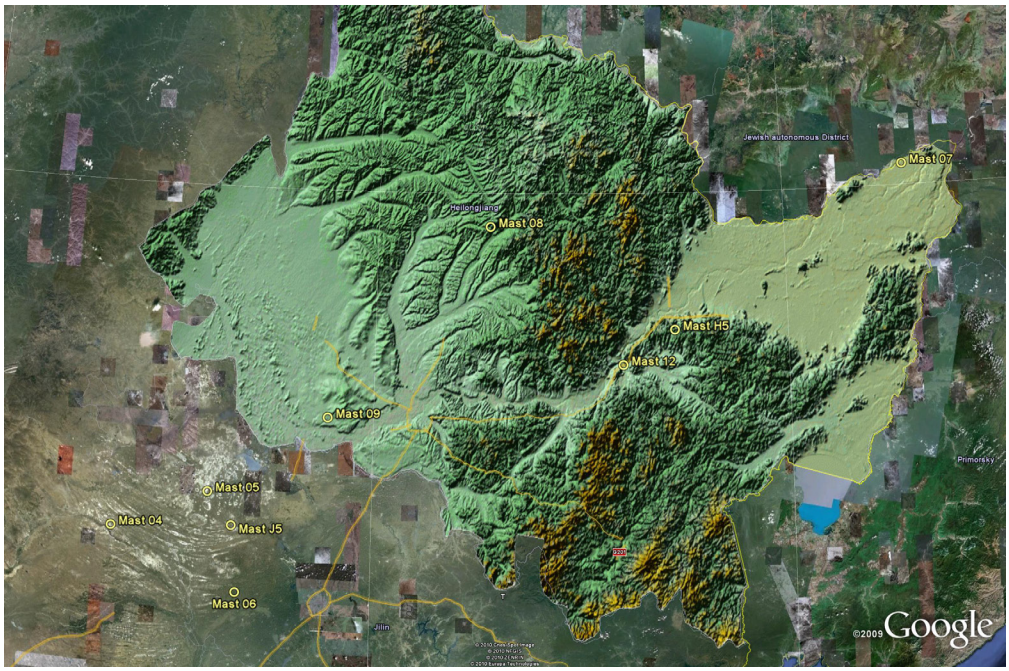

WAsP best practices and checklist

The list below of requirements, best practices and recommendations is not exhaustive, but is meant to provide a brief summary of some important considerations regarding WAsP modelling. More information is available in the WAsP help system and at www.wasp.dk.

Measurement programme

- Design measurement programme based on preliminary WAsP analysis
    - Use SRTM elevation data and land-use from Google Earth
- Follow similarity principle as much as possible when siting the mast(s)
- Height of reference anemometer(s) similar to hub height (preferably > 2/3 h_{hub})
- Optimum boom direction is @ 90° (lattice) or @ 45° (tubular) to prevailing wind. Deploy one top-mounted anemometer if at all possible.
- Deploy 2 or more masts for horizontal extrapolation analyses
- Deploy 2 or more masts if RIX and ΔRIX analyses are required
- Deploy 2 or more levels on masts for vertical wind profile analyses
- Deploy 2 or more levels on masts for redundancy in instrumentation
- Measure temperature and pressure for air density calculations

Wind data analysis

- Collect required information, e.g. by filling out the Data Description Form
- All fields in Climate Analyst protocol editor should correspond to data spec's
- Plot and inspect time traces of all meteorological measurements
- Visual inspection of time-series – in particular reference wind speed and direction
- Visual inspection of polar scatter plot – any patterns or gaps?

Observed wind climate

- Use an integer number of whole years when calculating the OWC
- Check Weibull fit: is power density discrepancy < 1%?
- Check Weibull fit: is mean wind speed discrepancy < a few per cent?
- Check within context of long-term wind climate (MCP)

Elevation map(s)

- Size of map: should extend at least max(100×h, 10 km) from any site – meteorological mast, reference site, turbine site or resource grid point.
- Coordinates and elevations must be in meters
- Set projection and datum for map in the Map Editor
- Add spot heights within wind farm site
- Check range of elevations in map

Roughness/Land-use map(s)

- Size: map should extend at least max(100×h, 10 km) from any site – meteorological mast, reference site, turbine site or resource grid point.
- Coordinates and elevations must be in meters
- Set projection and datum for map in the Map Editor
- Set roughness length of water surfaces to 0.0 m!
- Check range of roughness values in map
- Map date should correspond to modelling scenario (met. mast or wind farm)
- Check for dead ends and cross points – and edit map as needed
- Check consistency of roughness values – there must be no LFR-errors!

Sheltering obstacles

- Is site closer to obstacle than 50 obstacle heights, and is height lower than about 3 obstacle heights?
- If yes to both, treat as sheltering obstacle; if no, then treat as roughness element

WAsP modelling – site visit

- Go on a site visit! Use e.g. the WAsP Site/Station Inspection Checklist
- Print and bring the WAsP forms for recording the necessary information
- Bring GPS and note projection and datum settings – change if required
- Determine coordinates of masts, landmarks and other characteristic points
- Take photos of station and surroundings (12 × 30°-sector panorama)
- Download GPS data and photographs to PC as soon as possible (daily)

WAsP modelling – parameters

- Wind atlas structure: standard roughness classes should span site conditions
- Wind atlas structure: standard heights should represent project
- Adjust off- & on-shore mean- and RMS-heat flux values to site conditions (caution!)
- Ambient climate: Set air density to site-specific value (WAsP 10 and later)

WAsP modelling – analysis and application

- Get site-specific wind turbine generator data from manufacturer
- Within forest: effective height = nominal height minus displacement length
- Complex or steep terrain is when the ruggedness index RIX > 0 for one or more sites (terrain slope angles > 17°)
- Make RIX and ΔRIX analyses if RIX > 0 for any site

WAsP modelling – offshore

- Roughness length of sea (and other water) surfaces: set = 0.0 m in WAsP!
- Add combined elevation/roughness change line around wind farm site
- Change wake decay constant to offshore conditions

WAsP modelling and sensitivity analyses

- Identify and try to estimate uncertainties
- Sensitivity of results to background roughness value and other important parameters

WAsP version and configuration

The WAsP modelling results reported in this atlas were obtained using the most recent version of the Wind Atlas Analysis and Application Program, WAsP version 10.00.0192 (2010). This program, as well as the underlying wind atlas methodology, is described in some detail by Troen and Petersen (1989). Details of setting up and running the software are given by Mortensen *et al*. (2009). The standard configuration of the WAsP program has been used throughout the report unless stated otherwise.

In addition, the WAsP Climate Analyst version 1.01.0112, the WAsP Map Editor version 10.0.0.306 and the WAsP Utility Programs version 3.1 have been used. Surfer 9.9 was used to generate the height contour maps from SRTM 3 data.

Risø DTU is the National Laboratory for Sustainable Energy. Our research focuses on development of energy technologies and systems with minimal effect on climate, and contributes to innovation, education and policy. Risø has large experimental facilities and interdisciplinary research environments, and includes the national centre for nuclear technologies.

Risø DTU
National Laboratory for Sustainable Energy
Technical University of Denmark

Frederiksborgvej 399
P.O. Box 49
DK-4000 Roskilde
Denmark
Phone +45 4677 4677
Fax +45 4677 5688

www.risoe.dtu.dk